Dissecting the Mechanisms of Direct Activation for Proapoptotic BAK and BAX

Dissecting the Mechanisms of Direct Activation for Proapoptotic BAK and BAX

A dissertation presented

by

Elizaveta Sergeyevna Leshchiner

to

The Department of Chemistry and Chemical Biology

in partial fulfillment of the requirements

for the degree of

Doctor of Philosophy

in the subject of

Chemistry

Harvard University

Cambridge, Massachusetts

April 2013

Dr. Loren David Walensky Elizaveta Sergeyevna Leshchiner

Dissecting the Mechanisms of Direct Activation for Proapoptotic BAK and BAX

Abstract

Pro-apoptotic BAK and BAX form toxic mitochondrial pores in response to cellular stress. Whereas BAX predominantly resides in the cytosol, BAK is constitutively localized to the outer mitochondrial membrane. Select BH3 domain helices directly activate BAX by engaging an α1/α6 trigger site. The inability to express full-length BAK has hampered full dissection of its activation mechanism. Here, I report the production of full-length, monomeric BAK by mutagenesis-based solubilization of its C-terminal α-helical surface. Recombinant BAK auto-translocates to mitochondria, but only releases cytochrome *c* upon BH3 triggering. A direct activation mechanism was explicitly demonstrated using a liposomal system that recapitulates BAK-mediated release upon addition of BH3 ligands alone. Photoreactive BH3 helices mapped both triggering and auto- interactions to the canonical BH3-binding pocket of BAK, whereas the same ligands crosslinked to the α1/α6 site of BAX. Thus, BAK and BAX activation are initiated by direct BH3 interaction, but at distinct trigger sites. These structural and biochemical insights provide new opportunities for developing pro-apoptotic agents that activate the death pathway through direct but differential engagement of BAK and BAX.

Table of Contents

Acknowledgements

I am delighted to acknowledge those who made this work possible.

I would like to thank Professor Michael Eck and Professor Stuart Schreiber for joining my Graduate Advisory Committee, and for their commitment and guidance throughout my years of graduate research.

I would like to express my most sincere gratitude to my thesis advisor Dr. Loren Walensky, who has enormously contributed to my scientific development, who has taught me not only full dedication to science and lab, but also showed me the fulfillment of accomplished work and the excitement of presenting your work to other people. Thank you for creating such a bright environment for all of us to thrive. I am and always will be thankful for your personal support through some difficult times for me.

I would like to thank all the members of the Walensky lab, past and present – it has been a great joy to have worked with you, and to learn from you. I would like to especially thank Craig Braun for being a wonderful collaborator and a great friend. Amanda Edwards, Michelle Stewart, Silvia Escudero and Lauren Barclay have always been a source of great support. Sam Katz, Evris Gavathiotis have been great mentors and friends, and I thoroughly enjoyed our discussions. I am very thankful for Greg Bird's help throughout my thesis work, including his wise words of advice. Fed Bernal, James LaBelle, Greg Bird, Nicole Cohen, Meg Davis, Kojo Opoku-Nsiah, Jo Bellairs, Denis Reyna-Ruiz, David Whitehead, Jared Tepper, Marina Godes, Sharon Gittens, Regina Valeriano, Cat Gallagher, Susan Lee, Becca Goldstein, Annie Huhn – thank you for making the lab such an enjoyable place to be in. Joe Lavin and Stephen Steinecke from Harvard University also helped me along the way of graduate school. I would like to thank

Dr. Daniel Anderson from MIT, who has sparked the greatest interest in science for me, and has since been a source I could always turn to.

None of my accomplishments would have ever been possible without the strongest support from my family whom I have always relied on. My parents have been my ultimate mentors and the best supporters through all times. I am endlessly thankful for all of their efforts and sacrifices. Without you, I would have never come to where I am now. My brother Pavel; my parents; my grandparents Tatiana and Kirill, Anna and Piotr; Vadim; Alexander and the rest of my dear family – thank you for everything.

I have been extremely lucky to have the friends that I do. Maslov, Kozlov, Kruk, and Ivkov families have been the biggest part of my life outside of the lab. Liudmila Dzhekieva, Alexander Korotkov and Alexander Reznichenko, thank you for everything.

My wonderful children Andrey and Darya have been a great source of inspiration and joy at all times. My husband Ignat Leshchiner – thank you for all that we have done together. Had it not been for you, I wouldn't have started my graduate studies at Harvard. Thank you for all of your help along the way.

For my parents Liliya and Sergey

For Piotr and Anna, Kirill and Tatiana

Chapter 1

Introduction

Introduction to the BCL-2 family

Introduction to apoptosis

Apoptosis, or programmed cell death, is an essential biochemical pathway that allows organisms to control the function of cells and tissues in a concerted and defined manner. Apoptosis is critical during mammalian development, as well as for the maintenance of cellular homeostasis later in life. In accordance with the importance of this pathway, apoptosis is tightly regulated in order to properly balance proliferation and cell death. The disruption of either process can lead to disease: too little cell death leads to unregulated cell survival in diseases such as cancer and autoimmunity, while too much cell death can cause neurodegeneration, immunodeficiency, and infertility. Evasion of apoptosis is one of the hallmarks of cancer[1]. Two distinct but interconnected pathways are responsible for initiating apoptosis following signals of cellular stress. Extracellular signals stimulate the extrinsic apoptotic pathway, whereas intracellular stress initiates the intrinsic, or mitochondrial, pathway.

The BCL-2 family-regulated intrinsic apoptotic pathway is initiated by intracellular processes of cellular stress, such as viral infection, DNA damage, growth-factor deprivation, or transcriptional cues[2,3]. This pathway is tightly controlled by the balance between the pro-death (proapoptotic) and pro-survival (antiapoptotic) members of the BCL-2 protein family and the protein-protein interactions among them. Apoptotic signals are ultimately relayed through this pathway, causing BCL-2-family-mediated destabilization of the outer mitochondrial membrane and release of cytochrome *c* and other apoptogenic factors from the mitochondrial intermembrane space[4]. This release triggers the formation of a protein complex known as the apoptosome, which consists of cytochrome *c* molecules, cytosolic protein APAF-1, and

procaspase-9 that is subsequently processed within the apoptosome complex into active caspase 9, which is formed by cleavage[5-7].

The extrinsic pathway is triggered when the cell receives an external signal, such as tumor necrosis factor (TNF) family receptor trimerization upon binding to its cognate ligands at the cell surface[8,9]. These receptors contain an intracellular domain that is responsible for the recruitment and activation of caspase-8 (cysteine aspartyl protease) via its binding to the adaptor protein FADD (Fas-associated death domain) and for its subsequent cleavage into its active form. This results in the activation of the downstream effector caspases, caspase-3, -6 and -7 – an irreversible caspase cascade[10]. Alternatively, capase-8 can trigger the activation of BCL-2 family member BID by cleaving it into an active truncated form, tBID, thus funneling the extrinsic death signal to the BCL-2 family-mediated mitochondrial apoptotic pathway[11].

Both apoptotic pathways converge at the activation of multiple caspases, which execute the dismantling and clearance of the cell destined to die. This caspase cascade is responsible for the physiologic features associated with apoptosis, including DNA condensation and plasma membrane blebbing.

The BCL-2 protein family

The founding member of the BCL-2 family was identified as a gene partner of immunoglobulin heavy chain translocation t(14;18) in follicular lymphoma, which leads to the pathologic upregulation of its gene product[12,13]. The gene was named *Bcl-2*, which represents the *B-cell lymphoma 2* oncogene. It was later found that rather than promoting cellular proliferation, the BCL-2 protein inhibits cell death[14], constituting the first of many examples in which aberrant

apoptosis contributes to a cancerous phenotype. Since then, more than 20 human BCL-2 family members have been discovered, all of which are involved in the precise control of apoptosis.

All BCL-2 family proteins possess very high sequence and structural homology within several different evolutionarily conserved BCL-2 family homology regions (or domains), known as BH domains[15]. BCL-2 family protein sequences contain up to four of BH (**B**CL-2 **h**omology) domains: BH1, BH2, BH3 and BH4, of which the most conserved and unifying is the BH3 domain (Figure 1.1). The BH3 domain represents a conserved alpha helix that mediates protein-protein interactions between BCL-2 family members. Interestingly, despite this very high homology and structural similarity, BCL-2 family proteins can have opposing functions and are thus functionally subdivided into three classes of proteins: antiapoptotic, multidomain proapoptotic, and BH3-only proteins (Figure 1.2).

The primary function of pro-apoptotic BCL-2 family member proteins (such as BAK and BAX) is to execute mitochondrial induced apoptosis in response to stress stimuli[16-18]. Upon culmination of the apoptotic signal, activated BAX and BAK self-associate to form pores in the outer mitochondrial membrane[19,20], resulting in the propagation and execution of the cell death cascade by releasing critical signaling factors, such as cytochrome *c*[21,22] and Smac/Diablo[23], which drive the apoptotic process.

Antiapoptotic proteins counteract the function of pro-apoptotic members of the BCL-2 family[24,25]. They inhibit BAK and BAX, by binding to and sequestering their BH3 domains – also called "death domains" – via a conserved BH3 binding groove[26]. This effective sequestration leads to a complete inhibition of apoptosis, both in homeostatic conditions and in disease [27].

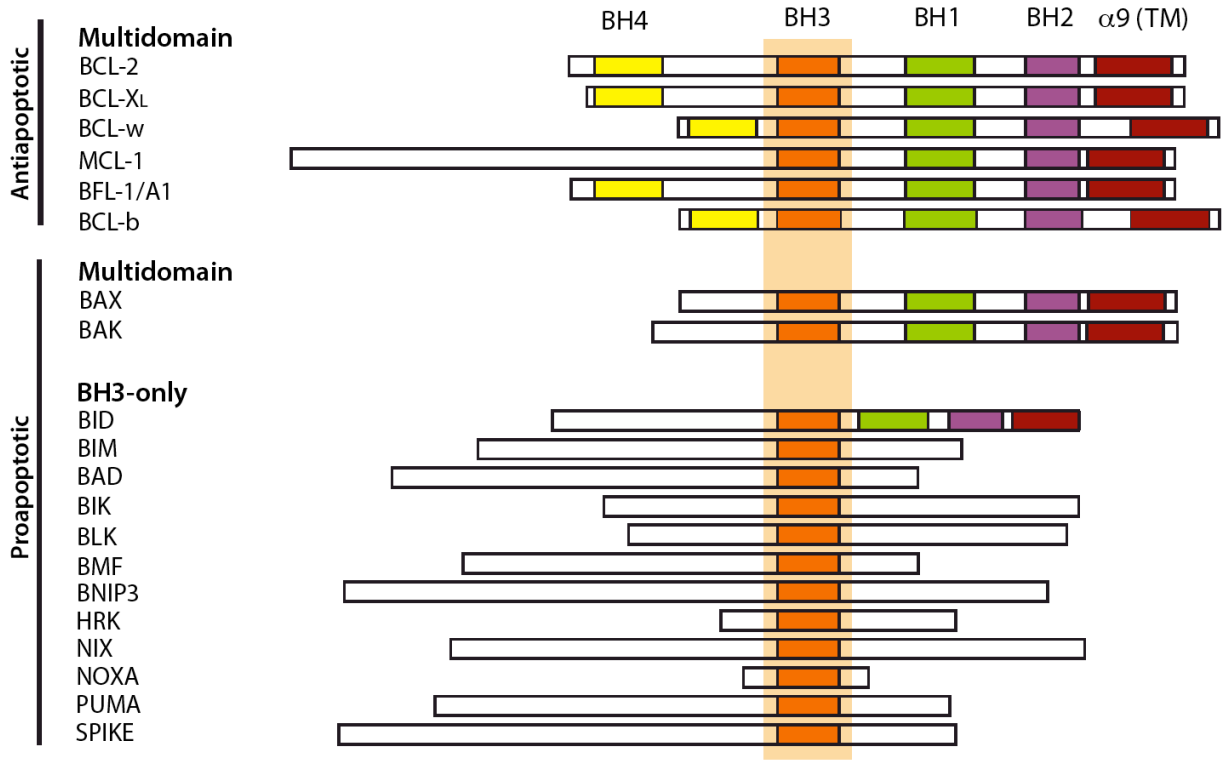

Figure 1.1. The BCL-2 family of proteins. BCL-2 family proteins consist of multidomain proapoptotic, antiapoptotic, and BH3-only members. BCL-2 family proteins share a high degree of sequence similarity within the BH (BCL-2 homology) domains. BH3 domains mediate the protein-protein interactions within the BCL-2 family.

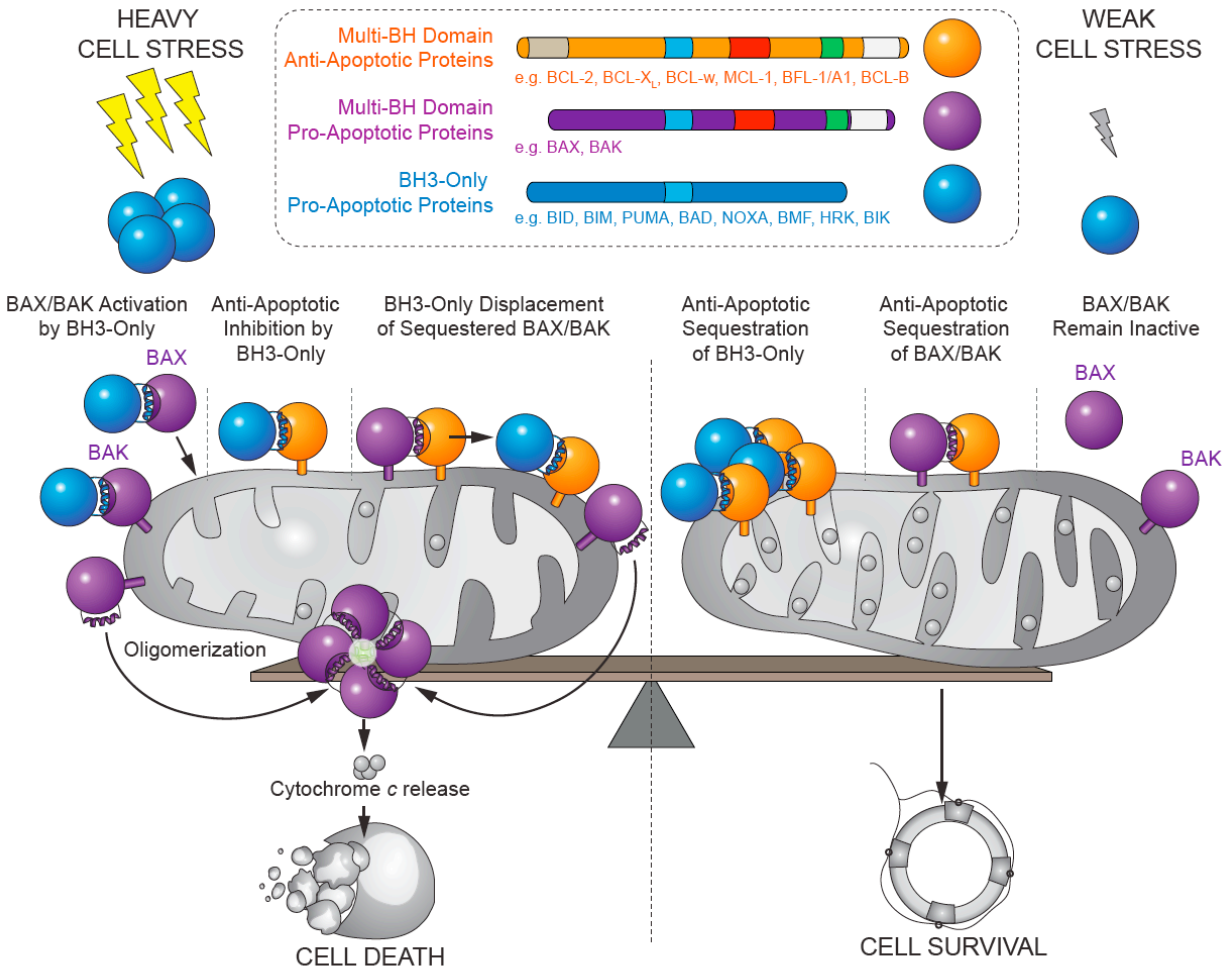

Figure 1.2. Mitochondrial apoptosis is regulated by the BCL-2 family protein interaction network. In response to stress stimuli, BH3-only proteins promote activation of BAX and BAK through direct and indirect mechanisms, leading to the transformation of monomeric BAX/BAK into oligomeric pores that pierce the mitochondrial outer membrane and release apoptogenic factors. BH3-only proteins can activate BAX/BAK through direct binding interactions and/or by targeting the BH3-binding pocket of antiapoptotic proteins, releasing BH3-only proteins and conformationally active forms of BAX/BAK sequestered in heterodimeric complex (**left**). Conversely, antiapoptotic proteins prevent BAX/BAK-mediated mitochondrial apoptosis by impounding the BH3 domains of BH3-only proteins and BAX/BAK in a surface groove,

Figure 1.2 (Continued).

effectively suppressing proapoptotic signaling (**right**). The life-or-death decision for the cell is ultimately dictated by the relative abundance and functional activity of pro- and antiapoptotic BCL-2 family proteins.

The third class of BCL-2 family members, BH3-only proteins, transmits the signals of cellular stress to the apoptotic machinery, and is also proapoptotic in nature. Diverse conditions, such as DNA damage[28-30], growth factor deprivation[31], and endoplasmic reticulum stress[32], lead to the activation of BH3-only proteins. The exact mechanism of activation varies for different BH3-only proteins, ranging from transcriptional upregulation[33], to phoshorylation[34,35], protease cleavage[11,36,37], and myirstoylation[38]. Once activated, BH3-only proteins "inhibit the inhibitors" by binding to the anti-apoptotic proteins and essentially neutralizing them, thus liberating BAX and BAK and allowing BAX/BAK-dependent apoptosis to be ensue[39]. Thus, the equilibrium between the antiapoptotic and BAK/BAX/BH3-only members of the BCL-2 family determines the cell's susceptibility to apoptosis[40]. Specific interactions between all three classes of BCL-2 proteins govern cell fate by tightly controlling the balance between the pro- and antiapoptotic stimuli.

Structural aspects of the BCL-2 family

The structures of multidomain BCL-2 proteins, i.e. antiapoptotic proteins and proapoptotic BAK and BAX, are strikingly similar, despite their opposing functions. All of these proteins have a globular structure with two core hydrophobic helices (α5 and α6) surrounded by several amphipathic α-helices[15]. The hydrophobic C-terminal α-helix is a transmembrane domain responsible for mitochondrial targeting. The standard approach of structural determination for these proteins has been through the truncation of the transmembrane region[41-43], a consequence of which is the omission of the C-terminal helix from all determined structures, with the only exception being an NMR structure of full-length BAX[44]. The majority of BH3-only proteins are intrinsically unstructured, except for BID (BH3-interacting domain death

agonist)[45,46], which is so structurally similar to multidomain BCL-2 proteins that it was suspected to have an autonomous oligomerization capability[47,48].

Interactions between BCL-2 family proteins are mediated by the binding of the BH3 domains of proapoptotic BAK, BAX or BH3-only proteins to the hydrophobic C-terminal binding pocket, or groove, on antiapoptotic proteins such as MCL-1, BCL-2, and BCL-X_L. This interaction is stable, stoichiometric, and mutually neutralizing: once the BH3 binding pocket is occupied, no other allosteric site or modification on the antiapoptotic protein is available for an additional interaction. Accordingly, once their BH3 domains are bound and buried in the antiapoptotic hydrophobic binding groove, neither BAK/BAX, nor BH3-only proteins can exert their proapoptotic action. This binding interface is so ubiquitous for BCL-2 family heterodimerizations, that the term 'canonical pocket' was coined to describe this particular class of interactions. Structures of antipoptotic proteins complexed with peptides corresponding to the BH3 domains of other BCL-2 family members abound and all follow this described structural pattern[26,43,49,50] (Figure 1.3, *A*). Despite homology within the canonical groove between anti-apototic BCL-2 family members, the profile of BH3-only binding partners for each of these proteins is distinct. For example, MCL-1 binds NOXA and BAK BH3 helices, but does not interact with BAD BH3, while BCL-2 binds BAD, but not NOXA or BAK BH3. All antitapoptotic proteins readily bind BH3-only proteins BIM and PUMA, and potentially BID.

Notably, BH3 domains of BAK and BAX are not exposed in the inactive conformations[44,51], but rather represent an internal part of the globular fold. It is thus necessary for BAK and BAX to undergo a conformational change to become activated, or primed, in order to allow for hetero-, homodimerization and oligomerization. In fact, the result of this

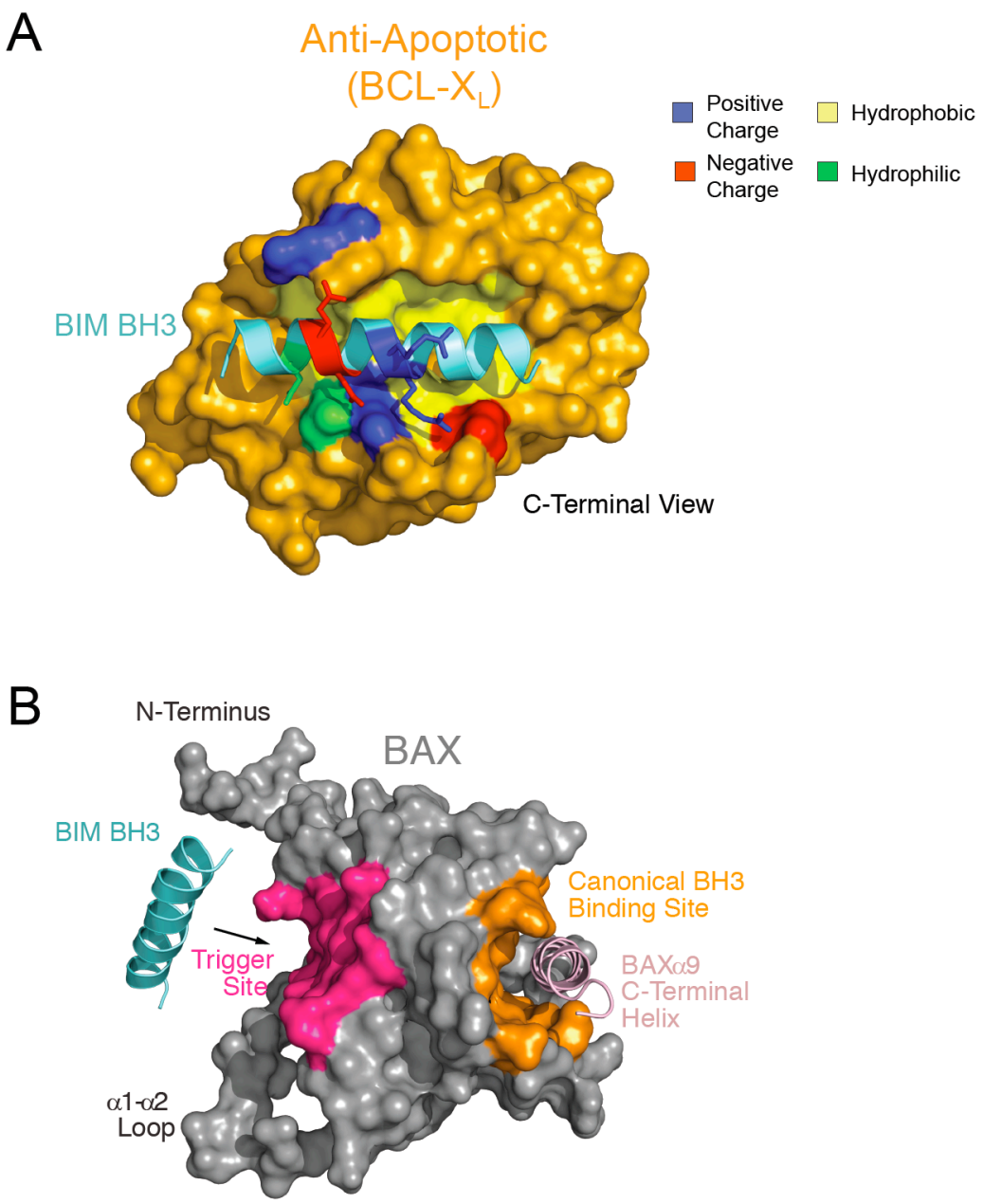

Figure 1.3. Two sites of BH3 domain interaction on apoptotic proteins. The stable and inhibitory BIM BH3 interaction site on anti-apoptotic BCL-X_L (*A*) and the dynamic and activating BIM BH3 interaction site on pro-apoptotic BAX (*B*) are geographically distinct. (*A*) The bulk of the BIM BH3 binding interface with BCL-X_L comprises extensive contacts between the hydrophobic face of the a-helix and the hydrophobic cleft formed at the protein surface by a

Figure 1.3 (Continued).

confluence of residues from BCL-X_L a-helices 2, 4, 5, 7, and 8. (B) In the inactive, monomeric form of BAX, the canonical BH3 binding pocket is occupied by BAX's C-terminal a9 helix. By contrast, the surface groove of the BAX activation site, located on the opposite side of the protein at the confluence of BAX a-helices 1 and 6, is accessible for BH3 triggering.

conformational change – the N-terminal exposure of BAK and BAX – is an early marker of apoptosis, and as such is widely used in studies characterizing the onset of cell death[52-54].

Whether the canonical hydrophobic binding pocket also exists on BAK and BAX is still uncertain. The NMR structure of BAX is the only BCL-2 family protein structure that contains the full-length C-terminal domain, and strikingly, this very domain occupies the canonical pocket, thus occluding and rendering it unavailable for interactions, at least in the inactive state of the protein. The full-length structure is not available for BAK, and interestingly, both C-terminally truncated structures of BAK reveal a severely collapsed canonical pocket[51,55]. With the overall fold similar to that of BAX, the canonical pocket in BAK is dramatically occluded. This either suggests that the C-terminal helix may play a role in shaping the canonical pocket binding surface, enforcing a structural difference compared to antiapoptotic proteins structures, or it could simply represent a difference in its native fold from that of BAX, which is likely due to the membrane localization of BAK and, presumably, its membrane-embedded C-terminus.

BCL-2 proteins in health and disease

The critical role of BCL-2 family proteins in apoptosis translates into dependency on BCL-2 proteins during normal tissue homeostasis, with deregulation contributing to disease.

Mice deficient in *Bcl-2* or *Bcl-X_L* are embryonic lethal[56,57]. This highlights the importance of maintaining cellular survival by counteracting apoptosis at the developmental stage. Some cells, however, have to die during embryonic development to allow tissue remodeling and organ formation. Accordingly, maintaining the ability to apoptose is crucial and the majority of mice that lack both BAK and BAX (*Bax*$^{-/-}$*Bak*$^{-/-}$) die during embryonic development due to severe neurological defects[58]. Mice with deletions of either only BAK or only BAX, however, have

relatively few defects[58,59], providing insight into some degree of redundancy in the functions of BAK and BAX.

Deletion of single BH3-only protein genes results in few developmental defects in mice (with the exception of BIM[60]), probably due to an even greater redundancy within this subgroup of the family. When several of the BH3-only proteins are concomitantly deleted, a defective phenotype becomes much more apparent: the triply negative Bim Bid Puma KO mice recapitulate many of the features of *Bax*$^{-/-}$*Bak*$^{-/-}$ mice[61]. Collectively, these studies highlight a critical role for BCL-2 family during development, as well as the complex nature of unique and redundant functions within the family.

Inhibition of apoptosis is a hallmark of cancer[1]. The discovery of the BCL-2 protein at the t(14;18) translocation proved that it was causally linked with follicular B-cell lymphoma[12,13]. Since then, many more examples of antiapoptotic upregulation leading to cancer have been observed, including chronic lymphocytic leukaemias[62], breast carcinomas[63], non-Hodgkin's lymphoma[64] and glioblastomas[65]. Hijacking the apoptotic machinery seems to be an effective means for malignant cells to promote cell survival. High levels of antiapoptotic proteins are often prognostic of disease aggressiveness and diminished therapeutic response[66].

Proapoptotic BAK and BAX deletions in cancers are relatively rare, likely due to the fact that both copies of both genes would have to be deleted for an observable advantage – due to their functional redundancy and significant expression of both BAK and BAX in most tissues. Still, low levels of BAK and BAX, as well as a low ratio of proapoptotic to antiapoptotic proteins, have been linked to poor prognosis and chemotherapeutic resistance[66-68]. Based on these findings, the determination of the ratio of pro- to antiapoptotic BCL-2 proteins by 'BH3

profiling' has been proposed as a clinical predictive tool to estimate potential chemotherapeutic reponses[69-71].

Pro-apoptotic BCL-2 family members BAK and BAX

BAK is a pro-apoptotic BCL-2 family member that resides in the mitochondrial outer membrane as a quiescent monomer until stimulated by cellular stress to undergo conformational activation and oligomerization[19,20]. First discovered in 1995[17,18,72], BAK was found to share functional homology with BAX, each containing an essential BH3 domain required for oligomerization-based killing activity[73]. The solution structure of the BAK BH3 domain complexed to a surface groove on anti-apoptotic BCL-X_L defined a protein interaction paradigm that contributes to BCL-2 family regulation of mitochondrial apoptosis[49]. Indeed, anti-apoptotic suppression of BAK and BAX through sequestration of BH3 helices is such an effective means of blocking apoptosis that cancer cells hijack and amplify this natural regulatory mechanism to enforce pathologic cell survival.

In the inactive state, BAX is a soluble, cytosolic, and monomeric protein[74,75] whose hydrophobic surfaces are buried within its core, including its C-terminal membrane insertion helix that is entrapped in the canonical surface groove[44]. In order to perform its function, BAX must be translocated from the cytosol, where it resides under homeostatic conditions, to the mitochondria. In contrast, monomeric BAK is a membrane-resident protein[39] whose C-terminus is presumably dislodged from the canonical binding groove and inserted into the outer mitochondrial membrane, potentially rendering BAK more vulnerable to activation in the absence of additional "security" mechanisms. Although a matter of ongoing debate, the homeostatic suppression of BAK may involve structural stabilization of the inactive monomer as

a result of conformationally restricted access to the canonical binding groove[51,55], and/or constitutive interactions with anti-apoptotic proteins[76], voltage-dependent anion channel 2[77], and/or perhaps other unknown proteins.

Mechanism of BAK and BAX activation

Although BAK and BAX are an essential gateway to apoptosis[78], and when deleted give rise to severe developmental defects[58], a host of questions persist regarding the physiologic mechanisms that govern their inhibition, activation, and self-association. Owing to a wealth of structural and biochemical studies that elucidated the mechanistic basis for anti-apoptotic suppression of the conformationally-activated, BH3-exposed forms of BAX and BAK[25,43,49,76,79], this aspect of BAX/BAK regulation is widely accepted and has formed the basis for major efforts to pharmacologically disrupt such interactions to reactivate apoptosis in human cancer[80-82]. However, the mechanisms by which BAK and BAX are activated have been the focus of much debate. Two models have been proposed: a direct activation model and an indirect activation model[83,84]. The indirect activation model proposes that BAK and BAX homeostatically exist in primed form and as soon as antiapoptotic inhibition is relieved, BAX and BAK proceed to form oligomers[39,76]. However, this model does not explain the stimulus responsible for the initial BAX and BAK activation event, and fails to account for the fact that only a small fraction of BAX and BAK is bound to antiapoptotic proteins in healthy, non-apoptotic cells[85].

The direct activation model posits that in addition to inhibiting the anti-apoptotic proteins, a direct triggering interaction is necessary to activate BAK and BAX[86], most likely by the BH3-only proteins.The hypothesis that BH3-only proteins could activate multidomain pro-apoptotics through direct and transient engagement dates back to the very discovery of the BH3-

only protein BID, based on its interaction with BCL-2 and BAX[87]. However, likely due to the transient nature of the proposed direct interaction, binding of activator BH3-only proteins to BAX and BAK was controversial and difficult to detect. Subsequent studies documented the capacity of select BH3-only proteins and BH3 peptides to induce recombinant BAX-mediated pore formation in liposomal and mitochondrial systems[88,89], with hydrocarbon-stapled peptide helices corresponding to the BID and BIM BH3 domains employed to explicitly detect and quantitate direct binding interactions with BAX[90]. Structural and biochemical analyses of the interaction between full-length recombinant BAX and a stapled BIM BH3 helix revealed a non-canonical BH3 interaction site at the confluence of BAX α-helices 1 and 6, a trigger site for BH3-mediated direct BAX activation (Figure 1.3, *B*)[91]. Upon engagement by a triggering BH3 ligand, BAX undergoes a major conformational change that includes allosteric release of its C-terminal helix for mitochondrial translocation and exposure of its BH3 domain, which both propagates BAX activation and induces functional oligomerization within the mitochondrial outer membrane[92].

While there is a substantial amount of research devoted to BAX[91,93], little is known about the direct activation mechanism for BAK, an equally important mediator of the cell death process. BAK was shown to co-immunoprecipitate with the activated form of BID, *t*BID, in whole cell lysates[19], but the overall evidence for such direct interactions of BAK in cells and *in vivo* is very limited. In contrast to BAX, full-length BAK has been refractory to protein expression and purification[76], precluding the corresponding structural and biochemical studies to dissect its interactions and activation mechanisms using fully intact recombinant protein. Instead, truncated forms of BAK have been generated and employed in a series of studies that documented (1) dimeric structures of BAK truncates 23-185 and 16-186[51,55], (2) binding of select

BH3 domains to the exposed canonical pocket of BAKΔC[94] and N- and C-terminal calpain-cleaved BAK (cBAK)[51], (3) auto-active and ligand-stimulated pore-forming functionality of an artificially membrane-tethered form of BAKΔC[95], and (4) BH3 ligand-induced activation of BAK truncates in liposomal and mitochondrial release assays[94,96,97]. The application of select BH3 peptides to native BAK-containing mouse liver mitochondria[98] and of IVTT (in vitro transcribed and translated) BH3-only proteins to mitochondria isolated from wild-type and mutant BAK-reconstituted DKO MEFs may also implicate a direct activation mechanism for BAK-mediated mitochondrial apoptosis[99,100].

Despite significant efforts to define the mechanism of BAK and BAX oligomerization, how these proteins self-associate to form pores remains elusive. An insertional cysteine mutagenesis and disulfide crosslinking approach implicated the involvement of two binding interfaces, BAK BH3 domain in canonical groove and α6/α6 interactions, in propelling BAK poration via an oligomerization of dimers mechanism[101,102], a model also supported by EPR (electron paramegnetic resonance) analysis[95]. More recently, a similar mode of oligomerization was proposed for BAX[103]. In the absence of definitive structural support for this model, it remains unknown just how an oligomer of dimers would integrate into a membrane bilayer using its once buried hydrophobic surfaces. Crystallization of α2-α5 of BAX, a dramatically truncated BAX form, also hinted at the possibility of dimeric oligomer structure and provided some insight into the possible structure of the dimeric unit, yet it is still unclear how the pore is assembled in the presence of a lipidic bilayer[104]. Interestingly, cryo-EM studies of BAX-permeabilized liposomes documented that BAX oligomeric pores are non-uniform in nature and grow in size over time[91], presumably as a chain reaction with each oligomeric complex recruiting more and more BAX molecules to participate and eventually lead to strikingly large openings in

membranes. These studies are corroborated by *in vivo* studies of the size of BAK and BAX oligomers, with estimates ranging from 25 to 1340 kDa as detected by chemical crosslinking[105,106] and size-exclusion fractionation[107]. So far, the maximal BAX or BAK pore size has not been determined, and it is in fact unclear whether there are any constraints on the growth of the oligomeric pore or if there are other protein subcomponents.

Lipids play an important role in BAK and BAX oligomerizaion. Mitochondrial outer membrane permeabilization requires a tight cooperation between BAK/BAX, their activators, and the lipidic membrane[85]. Not only is the hydrophobic lipid bilayer the medium in which BAK and BAX oligomerization takes place[93], certain lipids can actively contribute to BAX and BAK conformational change and pore-forming activities. Some lipids have been shown to aid in the recruitment of BAX to the mitochondrial membrane, with the notable example of cardiolipin[108-110]. Lipids can also be components of the lipidic/proteinaceous apoptotic pore[89,111,112]. Recently, it was shown that sphingolipid metabolism cooperates with BAK and BAX activation, with specific byproducts necessary to sensitize mitochondria to permeabilization by BAX and BAK. Interestingly, sphingosine-1-phosphate was found to specifically promote BAK pore-forming activity, whereas another sphingolipid metabolite, hexadecenal, plays a role in BAX function[113].

Taken together, these studies highlight the importance of studying BAK and BAX activity in the lipidic membrane context, and also reveal the complexity of factors involved in BAK and BAX regulation and activation.

Challenges of studying BCL-2 family members

Some of the intrinsic properties of BCL-2 family proteins make them difficult to study, both in an *in vitro* and *in vivo* context. *In vivo*, genetic knockout studies have proven to be

extremely useful to elucidate the importance of several BCL-2 family members, such as BCL-2, BCL-X_L, MCL-1, BAK/BAX, and BIM[56,57,114]. Genetic studies also provided insight into a mechanistic understanding of apoptosis[61,76], however the functional redundancy among family members renders interpretation of such experiments difficult.

Co-immunoprecipitation has been employed to study the interactions among BCL-2 family members, but this approach may not be as suitable for detecting transient binding interactions[90]. Moreover, some detergents that are commonly used for studies in cellular lysates, such as Triton X-100, have been shown to artificially activate BAK and BAX[8], which imposes great restrictions on interpretation of data obtained by these techniques.

Several other features of BCL-2 family members complicated discerning between the proposed direct vs. indirect activation mechanisms of mitochondrial permeabilization. Some BCL-2 family proteins, such as BAK, are hydrophobic and localized to membranes; other members of the BCL-2 family, such as BAX, shuttle from the cytosol to the mitochondrial membrane, complicating biochemical expression and purification, structural determination, and even mass-spectrometry analysis.

Conformational alterations associated with BCL-2 family function are also difficult to pinpoint due to the transient nature of these changes. The N-terminal exposure in BAK and BAX detected by conformation-specific antibodies[52] and protease susceptibility[115] dramatically change over the course of BAX and BAK activation. The conformational change associated with BAK and BAX membrane embedding that is necessary to promote the oligomeric structure is reminiscent of near full protein unfolding, according to some models[116]. Moreover, even when oligomerized, BAK and BAX are elusive as it is impossible to pinpoint the precise species of the oligomer[66], due to the increase in pore size over time. Clearly, this family represents a unique

challenge for structural determination, yet its central role in apoptosis regulation has marshaled tremendous research attention.

With the lack of definitive structural knowledge, biochemical techniques have been employed to gain indirect insight into the mechanistic structural biology of BAX and BAK. Chemical crosslinking has shown some promise for answering several pressing questions about BAK and BAX activation[101-103]. However, routinely employed disulfide crosslinking may be biased because of the selective installation of non-native cysteine residues into the protein sequence, which introduces uncertainly in interpreting these data. The fairly low temporal resolution of crosslinking techniques is another limiting factor[117].

Given the shortcomings of disulfide crosslinking approaches, alternative biochemical experiments have allowed more definitive dissection of BAX/BAK interactions[93]. Indeed, generating full-length forms of BCL-2 family proteins is crucial for definitive elucidation of their physiologic mechanisms.

Hydrophobic proteins: associated challenges

Most BCL-2 family proteins are associated with intracellular membranes at least at some point in the signaling cascade. Indeed, properties intrinsic to all membrane proteins significantly hinder their mechanistic and biochemical dissection *in vitro*. Structural determination and biochemical analysis of membrane proteins has generally lagged in comparison to their cytosolic counterparts. A striking illustration of this is the fact that only 2% of the structures deposited in the protein data bank are membrane proteins, whereas membrane proteins constitute 30% of the mammalian proteome[118]. In addition, membrane proteins account for 60% of all drug targets[119]. This disparity often derives from difficulties in expressing membrane proteins, which are

usually expressed at low levels in cells. Despite the introduction of many new expression systems in recent years, low yields, often due to toxicity, is still a recurring problem with recombinant expression and biochemical purification of membrane proteins.

As membrane proteins are unstable in aqueous solution, detergents often have to be used at concentrations higher than their CMC (critical micelle concentration). Unfortunately, BCL-2 family proteins are extremely sensitive to these environments[85], which greatly limits the options to unfold and refold them *in vitro* during isolation. In addition to expression and purification issues, X-ray crystallography, NMR protein spectroscopy and even mass spectrometry have limitations for membrane protein analysis. These challenges highlight the need for new tools and techniques to gain a better understanding of how membrane proteins, and in particular, BCL-2 family members, function in their native setting.

Summary

The BCL-2 family plays a crucial role in apoptosis. It consists of three sub-classes: multidomain proapoptotic, antiapoptotic, and BH3-only proteins. Proapoptotic proteins BAK and BAX, when not inhibited by antiapoptotic BCL-2 family proteins, oligomerize in the outer mitochondrial membrane to form toxic pores that release apoptogenic factors from the mitochondrial intermembrane space, triggering the caspase cascade and dismantling the cell. Whether BAK and BAX need to be activated by a specific trigger to oligomerize has been the focus of intense debate. Recent studies with recombinant full-length BAX revealed the crucial dependency of its activation on the interaction with BH3-only proteins. The interaction site has been structurally defined at the confluence of α-helices 1 and 6 at the N-terminal face of the protein, which lies on the opposite side of protein from the canonical BH3 groove of BAX.

Thus far, recombinant full-length BAK had been refractory to expression and isolation in a pure monomeric form, precluding definitive biochemical studies of its activation behavior.

Stapled peptides as research tools and prototype therapeutics

Alpha-helices mediate protein-protein interactions

The spatial structure of proteins and their binding compatibilities play a crucial role in mediating protein-protein interactions. Specific substructures, such as α-helices, β-sheets, β-turns, and coiled coils, all participate in determining the binding affinity between two proteins. As such, protein-protein interaction surfaces tend to be large in their surface area and encompass many amino acid residues. While the resultant complexity of such large surfaces creates a versatile medium for distinguishing between homologous targets, it simultaneously renders prediction of the important specificity determinants of the interface quite difficult. Studying and recapitulating these protein-protein interactions *in vitro* and *in vivo* can therefore be challenging. Generating chemical inhibitors of such interactions has also proven to be difficult due to the absence of small and well-circumscribed binding pockets.

The peptide α-helix represent the single largest class of protein secondary structures[120,121] and mediates an abundance of of physiologic protein interactions. α-Helices as protein subcomponents tend to be rather small and span 2 to 3 helical turns[122,123]. With this in mind, it is theoretically conceivable to design an α-helix as a protein mimetic, serving both as a discovery tool and a prototype therapeutic. However, once excised from the protein sequence and overall tertiary fold, secondary structures rarely preserve their conformation and shape. In the case of α-helices, unstabilized peptides lose their helical shape, becoming essentially a mixture of different conformers, and as such, fail to mediate protein interaction as effectively as when in the context

of the original full-length protein[124]. Additionally, proteolytic instability of unstructured peptides, as well as their cellular impermeability, makes them unsuitable for mechanistic dissection in cells and *in vivo*.

The ability to preserve the helical shape of an isolated peptide would address many of the shortcomings of peptides. By restoring the peptide's original shape, the original interaction specificities may be restored[125], and as most proteolytic enzymes rely on extended peptide chains for cleavage, α-helical conformation could also remedy the proteolytic instability of short peptides[126]. Some stabilized helices have also been shown to be effectively taken up by cells, most likely due to the reduced exposure of the polar amide backbone as a result of helical stabilization[124].

Strategies for stabilization of α-helical peptide conformation

Several approaches have been successful used to stabilize the α-helical structure of short peptides. Three general strategies exist: (1) stabilization of the native-alpha-helical sequence by side-chain crosslinking or hydrogen bond surrogates[127]; (2) creating 'foldamers', which are peptide analogs employing β- or γ-amino acids and are capable of adopting conformations resembling an alpha helix[128]; (3) helical surface mimetics that are chemically unrelated to the original peptidic backbone but are designed to mimic the pattern of positioning of the side functional groups on a peptide helix[129]. The latter may include conformationally restricted scaffolds (such as rigid terphenyls). Out of this list of different approaches, only the first strategy involves the use of α-amino acids as building blocks and produces native α-helical shapes, thus most fully recapitulating the structural pattern of an α-helical interaction domain.

The α-helix contains 3.6 residues per turn, which positions *i, i+4, i+7, i+11* residues on the same side along a folded helix. It is thus conceivable to stabilize the α-helical fold by crosslinking the residues between *i* and *i+4* or *i* and *i+7* positions. Lactam[130], disulfide[131], and metal chelating bonds[132] have all been used in this capacity to create α-helicity in a given peptide sequence. Hydrocarbon stapling derived from olefinic metathesis reaction of the side functional groups of the peptide has also been employed with great success (Figure 1.4). Compared to lactam and disulfide bonds that are susceptible to protease digestion or a reducing intracellular environment, respectively, all-hydrocarbon stapling provides resistance to proteolysis[80]. Depending on a combination of factors, including hydrophobicity, amphipathicity, and overall charge, all-hydrocarbon stapled peptides can also demonstrate increased propensity for cellular uptake.

In addition, several studies reported using hydrogen bond surrogates as a method to stabilize or nucleate α-helicity. In this approach, a covalent bond is substituted for a hydrogen bond between a carbonyl group at *i* and an N-H group at *i+4* residues in the neighboring helical turns. A hydrazone bond[133] or a carbon-carbon double bond obtained by olefinic metathesis were both proposed and used successfully to recapitulate the native α-helical shape, although only when applied to short (7-15 residues) peptides[134,135].

Several studies examined the influence of linker rigidity on helix stability. A rigid, aromatic staple that spanned *i, i+11* has provided much greater stability than a flexible linker of comparable length[136]. Analysis of various flexible and rigid linkers, as well as their positioning along the peptide helix and the distance between the crosslinked residues, confirmed that the rigidity of the linkers can lead to improved α-helical stabilization[137]. Another interesting approach involved the application of "click" chemistry to generate a triazole-containing staple by

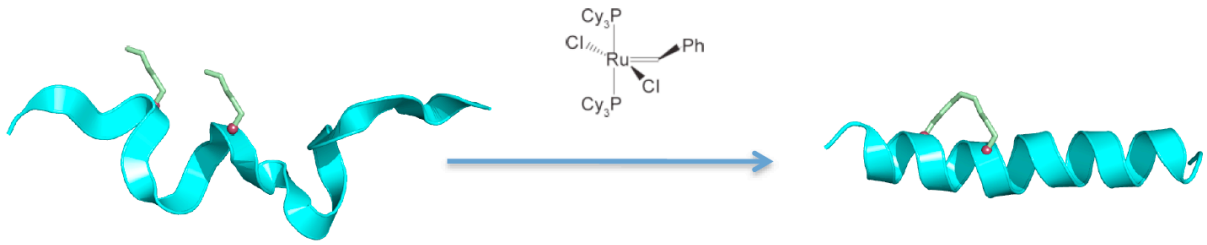

Figure 1.4. All-hydrocarbon peptide stapling. Insertion of non-natural amino acids bearing olefin tethers at *i, i+4* positions within the peptide sequence followed by ruthenium-catalyzed olefin metathesis generates stabilized α-helical domains.

the use of the Huisgen 1,3-dipolar cycloaddition reaction[138]. High efficiency and mild conditions contributed to the attractiveness of this approach. Because this crosslink is generated from asymmetrical building blocks (side chains in the peptide sequence), it allowed for easier generation of a doubly stapled BCL9 peptide with markedly increased helicity, stability, and binding affinity towards β-catenin, although cell uptake was not achieved.

Hydrocarbon stapling

All-hydrocarbon stapling of peptides is perhaps the best characterized approach for stabilizing alpha-helical structures. Initial attempts to generate an all-hydrocarbon stapled peptide were made by Grubbs and co-workers who employed O-allyl modified serine derivatives in the peptide sequence. Ring-closing metathesis generated a covalent linkage spanning one helical turn[139]. Unexpectedly, these peptides did not display increased helicity. In another study, Schafmeister et al. carefully investigated the stereochemistry and linker length to successfully obtain hydrocarbon-bridged peptides with increased helical stabilization[140]. The key advance was the use of α,α-disubstituted amino acids for the crosslinkable side chains, which provided additional methyl groups at the α-carbon position and limited peptide backbone rotation by restricting the φ and ψ angles, and therefore promoted α-helicity.

Interestingly, while some configurations provided significant helical stabilization, others destabilized the helix. Even small changes in crosslinked ring size or configuration lead to dramatic changes in outcome: as one of several examples, the 31-membered macrocycle – corresponding to *R, S* crosslinking at *i, i+7* positions with 9 carbons in the metathesized crosslink – formed successfully, while shortening the crosslink by one carbon under the same exact conditions completely abrogated the macrocycle formation. This suggested that

'templating' of the ring-closing metathesis reaction was achieved by short-lived, dynamic helix induction. Schafmeister et al. found that optimal crosslink length led to effective α-helical stabilization, whereas crosslinks that were too short or too long led to suboptimal or even decreased α-helicity by hindering the formation of a proper α-helix by the former, or not providing enough restraint and stabilization by the latter. Once the intended helical stabilization was achieved, the binding affinity of the peptide to its target was greatly increased[80,141-143] by alleviating the entropic cost of binding[144].

Select all-hydrocarbon stapled peptides penetrate the cells effectively, as assessed by flow cytometry, confocal microscopy and intracellular fluorescence detection,[80,141,143] and are thus capable of targeting intracellular protein targets. Stapled peptide uptake was inhibited when the active (energy-dependent) forms of cellular uptake were blocked. However, stapled peptides did not co-localize with transferrin-labeled endosomes[80] and instead tracked with dextrans, consistent with a pincytotic mechanism of cellular uptake.

As cleavage by proteases is a key pathway for peptide elimination in biological systems, examining the protease susceptibility of stabilized peptides is an important measure of translational potential. All-hydrocarbon stapled peptides are significantly resistant to protease digestion compared to non-crosslinked analogs[80,140,143,145]. Overall structural reinforcement minimizes the presence of unfolded conformations of the peptide and thus leads to decreased susceptibility to proteolytic cleavage at any residue along the peptide sequence. Additionally, proteomic studies showed that the sites directly adjacent to the staple are virtually spared of proteolytic degradation, most likely due to the complete inability to unfold at the covalently restrained region. Importantly, the increased proteolytic stability *in vitro* was predictive of enhanced performance of stapled peptides *in vivo*[80,145], at least in part due to the optimized

pharmacokinetic properties and sustained plasma concentration. In the case of the HIV derived T649v peptide, incorporation of two hydrocarbon staples led to the development of a double-stapled construct that even exhibited oral bioavailability in mice, which contrasts to the twice daily subcutaneous mode of administration for the FDA-approved HIV fusion inhibitor peptide Enfuvirtide[145].

These diverse examples confirm that chemical stabilization of α-helical peptide conformation is a viable strategy to confer the desired shape to an otherwise unstructured peptide, and clearly indicate the benefits of the use of a proteolytically-resistant, cell-permeable stapled peptide, afforded by installing an all-hydrocarbon crosslink.

Stapled peptides as prototype therapeutics

As α-helices are frequent motifs in protein-protein interactions, stabilized peptides hold great promise to selectively disrupt or, conversely, stabilize protein-protein interactions and thus serve as prototype therapeutics for the manipulation of physiologic or aberrant pathways in disease. Because protein-protein interactions tend to employ large interaction surfaces, frequently lacking defined deep binding pockets[146] required for small molecule targeting, they represent a formidable pharmacologic challenge. When properly leveraged, the distinctive characteristics of stabilized peptides offer a unique opportunity and an extremely attractive niche for therapeutic design. One major limitation for peptide therapeutics is their diminished efficacy in vivo, mostly due to their proteolytic instability, cellular impermeability and compromised structural fold when taken out of the three-dimensional protein context. As peptide stapling has been shown to redress these liabilities, stapled peptides are being developed as promising next generation peptide therapeutics for targets that have been refractory to small molecule inhibition.

Several successful examples of the development and application of stabilized peptides as potential therapeutics are discussed below.

Among several oncologic pathways that drive cancer, evasion of BCL-2-family-mediated apoptosis has emerged as a significant barrier to treatment. Sequestration of the BH3 domains of BAK, BAX and BH3-only proteins by the canonical pockets of overexpressed antiapoptotic BCL-2 proteins represents the key mechanism by which apoptosis is blocked in human cancers. The critical BH3 interaction domain is a conserved α-helix and is thus an attractive substrate for the development of pharmacologic agents to overcome antiapoptotic inhibition. Indeed, stapled peptides modeled after the BH3 domains of BH3-only proteins BIM and BID (proapoptotic activators) have been shown to directly bind to antiapoptotic proteins such as BCL-X_L, BCL-2 and BFL-1 with low nanomolar affinity[141], and have demonstrated the capacity to induce apoptosis at low micromolar concentrations in leukemia cells. Moreover, both BID and BIM stapled peptides, as single agents or in combination with ABT-263, halted tumor growth in mouse models of aggressive leukemia and often produced a dramatic decrease in tumor burden, while sparing normal tissues.

Transcription factors are another class of proteins that are notoriously difficult to target. With the exception of nuclear hormone receptors that contain binding pockets for their respective ligands, transcription factors usually lack a defined hydrophobic pocket, and instead possess extended protein-protein interfaces. Thus far, potent and specific small molecule inhibitors are not available, despite the overwhelming importance of master transcription factors, such as myc and ras, in development and disease. Two examples of stapled peptides provided proof-of-concept that transcription factor targeting can be successful both in vitro and in vivo. NOTCH signaling is directly implicated in several diseases, most notably NOTCH-dependent

cancers[147,148] that are causally linked to NOTCH-activating mutations. An opportunity for direct inhibition of the NOTCH transcription factor complex emerged from the discovery of the dominant negative fragment of mastermind (MAML1) protein that interferes with the NOTCH transactivation complex[149,150]. Specifically, a stapled peptide modeled after the 16-amino acid stretch of the dominant negative MAML1 sequence was capable of disrupting the transactivation complex of NOTCH intracellular domain (ICN) with its DNA transcription factor partner CSL by competitively displacing MAML1[151], whereas a point mutant construct served as a specificity control. After binding, the active stapled peptide, but not the control peptide, repressed NOTCH target gene expression and thus halted the proliferation of NOTCH-sensitive acute T-lymphoblastic leukemia (T-ALL) both in culture and *in vivo*.

Another elegant example of transcription factor targeting is inhibition of Wnt signaling by the stapled peptide derived from the sequence of the Wnt downstream transcriptional factor coactivator, BCL9[152]. This peptide was designed to competitively inhibit formation of the BCL9/β-catenin activating complex, and was shown to reduce the proliferation of colorectal cancer and multiple myeloma cell lines. In mouse models of Wnt-driven cancer, the stapled peptide, in a sequence-dependent manner, suppressed tumor growth, angiogenesis, and metastasis with little observed toxicity to normal tissues.

Several other studies have been successful in applying the stapled peptide approach to notoriously difficult targets. A stapled peptide derived from a helical region of p53 was shown to competitively bind to the p53 inactivators MDM2 and MDMX, resulting in a surge in native p53 protein and reactivation of the death pathway[143]. This p53-derived stapled peptide inhibited tumor cell proliferation as a single agent, and was shown to synergize with nutlin-3, an MDM2 inhibitor, in vitro and in a mouse model of MDMX-driven choriocarcinoma. Additional

examples include the use of stapled peptides to inhibit the proliferation in HIV, where mimetics of HIV gp41[145] or the C-terminal domain of HIV-1 capsid[153,154] led to blockade of viral fusion or viral assembly, respectively.

Stapled peptides as research tools for structural elucidation

As biological discovery tools, stapled peptides have been especially fruitful in the dissection of BCL-2 family protein functions and mechanisms. One of the important advancements relates to dissecting the BAX activation mechanism. Whether BAX oligomerization and mitochondrial poration are active processes that require direct triggering by another protein partner, or whether oligomerization is the default BAX state, executed once antiapoptotic inhibition is relieved, has been the subject of active discourse in the cell death field. The debate overdirect vs. indirect models of BAX activation was successfully addressed by use of stapled peptides corresponding to the proposed BAX activators – BH3-only proteins – allowing for functional and structural studies of direct BAX binding. By stapling the BH3 domain of BID, Walensky et al. showed BID SAHB (**s**tabilized **a**lpha-**h**elix of **B**CL-2 domain), directly interacted with BAX, which led to its activation, pore formation in a liposomal assay, and cytochrome *c* release from mitochondria, in BAX- and SAHB-dependent fashion[90]. Gavathiotis et al. subsequently showed that the stapled peptide corresponding to the BH3 domain of another BH3-only protein, BIM (BIM SAHB), interacted with BAX at a novel trigger site[91] on the opposite side of the protein from the canonical hydrophobic pocket, that correspondsto the location of the antiapoptotic binding groove. This structural information was obtained by protein NMR spectroscopy using chemically modified BIM SAHBs to determine the orientation of the BH3 domain. BIM SAHBs modified with a paramagnetic label, TEMPO, at N- or C-termini,

resulted in peak intensity changes in select subgroups of residues of BAX, providing key distance information that enabled successful docking of the peptide at the novel binding site (PDB ID 2K7W). Indeed, the versatility of SAHBs, in terms of their potential to be readily modified chemically to suit a variety of needs, provides fresh opportunities to dissect the structural and functional features of protein interactions.

Interestingly, the canonical pocket in BAX in its monomeric state is occupied with its own C-terminal hydrophobic α-helix, thus precluding BH3 domain binding to that region. However, as soon as BH3 binding occurs at the recently discovered allosteric trigger site, BAX undergoes a major conformational change that includes the displacement of the loop located between helices 1 and 2, exposure of the BH3 domain of BAX, and allosteric release of the C-terminal α-helix from the canonical pocket, all of which culminate in BAX membrane insertion and permeabilization[92]. Importantly, the self-propagation mechanism of BAX activation was analyzed by employing BAX SAHB, corresponding to the BH3 domain of BAX. Just like BIM SAHB, BAX SAHB was able to activate BAX in the context of mitochondrial apoptosis, and triggered BAX auto-activation at the same novel trigger site. These studies highlighted the capacity of stapled peptides to generate new insight into dynamic protein mechanisms and conformational changes, particularly when conventional NMR or X-ray crystallographic studies are not achievable.

Recently, another chemical modification was employed to expand the utility of stapled peptides into proteomic and interactome research. Photoreactive stapled BH3 peptides were engineered to contain a benzophenone moiety (4-benzophenylalanine, Bpa) in the form of an amino acid side chain through conservative aromatic substitution[155]. This moiety is capable of covalently crosslinking to protein targets upon UV irradiation and can covalently trap both static

and dynamic protein binding partners, such as BCL-X_L and BAX, respectively. These photoreactive SAHBs, or pSAHBs, were able to precisely localize the binding site on the target protein following crosslinking and nano-LC-MS/MS analysis, which identified the pSAHB-crosslinked fragments of the interaction site. Attaching a biotin affinity tag to the photoreactive peptide enabled enrichment for the crosslinked species, making the LC-MS/MS analysis possible. The versatility of peptides and their chemistries make them invaluable, sophisticated chemical biology tools that can be applied to biologically relevant questions spanning protein interactomes, molecular biology, biochemistry, and structure-function mechanistic analyses.

Chemical cross-linking and proteomics for structural discovery

Biochemical and mechanistic studies of protein complexes rely heavily on structural information. Sophisticated X-ray crystallographic techniques, including recent advances for membrane proteins, have contributed enormously to the progress in our understanding of biological mechanisms[156,157]. A complementary approach for crystallographic studies is protein NMR spectroscopy, which provides invaluable information about protein behavior in solution and dynamic changes associated with conformational alteration. Unfortunately this technique is limited by the maximum size of the protein under investigation[158].

Both of these structural methods usually require large quantities of protein, and significant optimization of expression and purification: there is often a multiyear gap between the understanding of a protein's biological importance and the availability of its refined structure. This reality has spurred significant interest in techniques that would expedite the delivery of structural information on proteins and their complexes in a relatively short time frame, even if the resolution is partially compromised. Chemical crosslinking for mass spectrometry-based

identification of protein interactions and binding sites has been one of the most important alternativetechnologies in this arena, especially considering the speed and sensitivity of MS analyses (theoretically up to femtomolar scale). If protein reactive groups are in close proximity, they can undergo covalent linkage. Trypsinolysis and LC-MS/MS of the peptidic mixture allows the identification of specific crosslinking residues on protein complex surfaces. The identified crosslinked peptides provide a dataset of distance constraints, much like NOEs in protein NMR, ultimately yielding information on binding surface topologies.

Key advances in this area lie in the ability to identify by mass spectrometry the low-abundant crosslinked peptides in the presence of the significantly more abundant native peptides that represent the "background." Availability of sophisticated instrumentation (e.g., Orbitrap instruments[159]) and analytical software enabled significant technological improvements. However, a seminal issue is the choice of an optimal chemical crosslinker that is reactive under mild and native conditions to allow for good yields, yet selective enough to avoid artifacts. Most chemical crosslinkers are limited by the intrinsic protein chemistry that reacts with a limited number of amino acid side chains, limiting the breadth of crosslinking opportunities in the protein target.

The two most common protein reactive groups employed for crosslinking are the amine group of lysine and the thiol group of cysteine. By using activated esters for lysines, (such as DSS[160]), or Michael addition reactions for cysteine crosslinking (e.g., with maleimides[161]), one can obtain sufficiently high yields of crosslinked species. The major drawback of this approach is that proteins typically contain relatively few lysine and cysteine functionalities, dramatically decreasing the resolution of the binding site information obtained; covalent modifications of lysine prevent efficient digestion by common proteases, such as trypsin. Another approach

involves carboxyl functionalities of protein side chains (aspartic and glutamic acids) that can be activated by incubation with carbodiimide and crosslinked by a diamine crosslinker[162]. Using this approach, typical yields are low due to hydrolysis of the activated ester in the aqueous media.

Introducing non-natural amino acid functionalities into the protein or peptide sequence, either by synthesis or by genetic mutation, allows for highly specific crosslinking reactions and even potential *in vivo* use. Azido- and alkynyl functional groups have been used for Huisgen 1,3-dipolar cycloaddition to form 1,2,3-triazole links[163,164]. Ketogroups have been introduced with subsequent crosslinking by hydrazides[165]. Finally, photoreactive crosslinkers that intercalate into local C-H bonds irrespective of side chain composition have also been employed. For example, benzophenone, diazirine and aryl azide side groups have all been used for photoaffinity labeling. Among these groups, only benzophenone has the important advantage of its UV- induced radical being reversible in the presence of water, which allows the UV-sensitive moiety to undergo sequential rounds of photoactivation until successful carbon-carbon crosslinking is achieved[166].

In addition to increasing the chemical yield of crosslinking reactions, several additional strategies have been employed to enrich for low-abundant crosslinked peptides, such as incorporation of affinity tags[155] or bio-orthogonal chemical "handles"[167]. Other approaches include introducing a cleavable ion reporter tag[168] or using isotopic labeling for high-confidence mass spectrometry identification of crosslinked peptides.

Summary

α-Helices are a common structural motif that mediates protein-protein interactions. Reconstituted short α-helical peptides corresponding to key interaction domains are useful

research tools, as well as promising prototype therapeutics. Several common strategies exist to stabilize the α-helical shape of peptides once taken out of context from the full-length protein and unfolded in solution. One of the most successful approaches has been all-hydrocarbon stapling of installed olefinic peptide side chains that are one or two helical turns apart. Stapled peptides serve as *in vivo* agents that target previously intractable pathways, including NOTCH, p53, Wnt, and BCL-2 family signaling networkss. As versatile research tools, stapled peptides can be chemically modified to incorporate affinity tags, fluorescent probes, and photoreactive crosslinker side chains, all of which facilitate their use as research tools to uncover the structures and biochemical functions of medically-relevant protein-protein interactions.

References

1. Hanahan, D. & Weinberg, R.A. The hallmarks of cancer. *Cell* **100**, 57-70 (2000).

2. Strasser, A., Cory, S. & Adams, J.M. Deciphering the rules of programmed cell death to improve therapy of cancer and other diseases. *EMBO J* **30**, 3667-83 (2011).

3. Danial, N.N. BCL-2 family proteins: critical checkpoints of apoptotic cell death. *Clin Cancer Res* **13**, 7254-63 (2007).

4. Vaux, D.L. Apoptogenic factors released from mitochondria. *Biochim Biophys Acta* **1813**, 546-50 (2011).

5. Li, P. et al. Cytochrome c and dATP-dependent formation of Apaf-1/caspase-9 complex initiates an apoptotic protease cascade. *Cell* **91**, 479-89 (1997).

6. Riedl, S.J. & Salvesen, G.S. The apoptosome: signalling platform of cell death. *Nat Rev Mol Cell Biol* **8**, 405-13 (2007).

7. Hakem, R. et al. Differential requirement for caspase 9 in apoptotic pathways in vivo. *Cell* **94**, 339-52 (1998).

8. Youle, R.J. & Strasser, A. The BCL-2 protein family: opposing activities that mediate cell death. *Nat Rev Mol Cell Biol* **9**, 47-59 (2008).

9. Ashkenazi, A. & Dixit, V.M. Death receptors: signaling and modulation. *Science* **281**, 1305-8 (1998).

10. Porter, A.G. & Janicke, R.U. Emerging roles of caspase-3 in apoptosis. *Cell Death Differ* **6**, 99-104 (1999).

11. Li, H., Zhu, H., Xu, C.J. & Yuan, J. Cleavage of BID by caspase 8 mediates the mitochondrial damage in the Fas pathway of apoptosis. *Cell* **94**, 491-501 (1998).

12. Tsujimoto, Y., Ikegaki, N. & Croce, C.M. Characterization of the protein product of bcl-2, the gene involved in human follicular lymphoma. *Oncogene* **2**, 3-7 (1987).

13. Tsujimoto, Y., Cossman, J., Jaffe, E. & Croce, C.M. Involvement of the bcl-2 gene in human follicular lymphoma. *Science* **228**, 1440-3 (1985).

14. Vaux, D.L., Cory, S. & Adams, J.M. Bcl-2 gene promotes haemopoietic cell survival and cooperates with c-myc to immortalize pre-B cells. *Nature* **335**, 440-2 (1988).

15. Petros, A.M., Olejniczak, E.T. & Fesik, S.W. Structural biology of the Bcl-2 family of proteins. *Biochim Biophys Acta* **1644**, 83-94 (2004).

16. Annis, M.G. et al. Bax forms multispanning monomers that oligomerize to permeabilize membranes during apoptosis. *EMBO J* **24**, 2096-103 (2005).

17. Kiefer, M.C. et al. Modulation of apoptosis by the widely distributed Bcl-2 homologue Bak. *Nature* **374**, 736-9 (1995).

18. Chittenden, T. et al. Induction of apoptosis by the Bcl-2 homologue Bak. *Nature* **374**, 733-6 (1995).

19. Wei, M.C. et al. tBID, a membrane-targeted death ligand, oligomerizes BAK to release cytochrome c. *Genes & Development* **14**, 2060-2071 (2000).

20. Wei, M.C. et al. Proapoptotic BAX and BAK: A Requisite Gateway to Mitochondrial Dysfunction and Death. *Science* **292**, 727-730 (2001).

21. Jurgensmeier, J.M. et al. Bax directly induces release of cytochrome c from isolated mitochondria. *Proc Natl Acad Sci U S A* **95**, 4997-5002 (1998).

22. Yang, J. et al. Prevention of apoptosis by Bcl-2: release of cytochrome c from mitochondria blocked. *Science* **275**, 1129-32 (1997).

23. Du, C., Fang, M., Li, Y., Li, L. & Wang, X. Smac, a mitochondrial protein that promotes cytochrome c-dependent caspase activation by eliminating IAP inhibition. *Cell* **102**, 33-42 (2000).

24. Zhai, D., Jin, C., Huang, Z., Satterthwait, A.C. & Reed, J.C. Differential regulation of Bax and Bak by anti-apoptotic Bcl-2 family proteins Bcl-B and Mcl-1. *J Biol Chem* **283**, 9580-6 (2008).

25. Chen, L. et al. Differential targeting of prosurvival Bcl-2 proteins by their BH3-only ligands allows complementary apoptotic function. *Mol Cell* **17**, 393-403 (2005).

26. Liu, X., Dai, S., Zhu, Y., Marrack, P. & Kappler, J.W. The structure of a Bcl-xL/Bim fragment complex: implications for Bim function. *Immunity* **19**, 341-52 (2003).

27. Adams, J.M. & Cory, S. The Bcl-2 apoptotic switch in cancer development and therapy. *Oncogene* **26**, 1324-37 (2007).

28. Oda, E. et al. Noxa, a BH3-only member of the Bcl-2 family and candidate mediator of p53-induced apoptosis. *Science* **288**, 1053-8 (2000).

29. Nakano, K. & Vousden, K.H. PUMA, a novel proapoptotic gene, is induced by p53. *Mol Cell* **7**, 683-94 (2001).

30. Yu, J., Zhang, L., Hwang, P.M., Kinzler, K.W. & Vogelstein, B. PUMA induces the rapid apoptosis of colorectal cancer cells. *Mol Cell* **7**, 673-82 (2001).

31. Dijkers, P.F., Medema, R.H., Lammers, J.W., Koenderman, L. & Coffer, P.J. Expression of the pro-apoptotic Bcl-2 family member Bim is regulated by the forkhead transcription factor FKHR-L1. *Curr Biol* **10**, 1201-4 (2000).

32. Puthalakath, H. et al. ER stress triggers apoptosis by activating BH3-only protein Bim. *Cell* **129**, 1337-49 (2007).

33. Villunger, A. et al. p53- and drug-induced apoptotic responses mediated by BH3-only proteins puma and noxa. *Science* **302**, 1036-8 (2003).

34. Puthalakath, H., Huang, D.C., O'Reilly, L.A., King, S.M. & Strasser, A. The proapoptotic activity of the Bcl-2 family member Bim is regulated by interaction with the dynein motor complex. *Mol Cell* **3**, 287-96 (1999).

35. Zha, J., Harada, H., Yang, E., Jockel, J. & Korsmeyer, S.J. Serine phosphorylation of death agonist BAD in response to survival factor results in binding to 14-3-3 not BCL-X(L). *Cell* **87**, 619-28 (1996).

36. Akiyama, T. et al. Regulation of osteoclast apoptosis by ubiquitylation of proapoptotic BH3-only Bcl-2 family member Bim. *EMBO J* **22**, 6653-64 (2003).

37. Ley, R., Ewings, K.E., Hadfield, K. & Cook, S.J. Regulatory phosphorylation of Bim: sorting out the ERK from the JNK. *Cell Death Differ* **12**, 1008-14 (2005).

38. Zha, J., Weiler, S., Oh, K.J., Wei, M.C. & Korsmeyer, S.J. Posttranslational N-myristoylation of BID as a molecular switch for targeting mitochondria and apoptosis. *Science* **290**, 1761-5 (2000).

39. Willis, S.N. et al. Proapoptotic Bak is sequestered by Mcl-1 and Bcl-xL, but not Bcl-2, until displaced by BH3-only proteins. *Genes Dev* **19**, 1294-305 (2005).

40. Chipuk, J.E., Moldoveanu, T., Llambi, F., Parsons, M.J. & Green, D.R. The BCL-2 family reunion. *Mol Cell* **37**, 299-310 (2010).

41. Muchmore, S.W. et al. X-ray and NMR structure of human Bcl-xL, an inhibitor of programmed cell death. *Nature* **381**, 335-41 (1996).

42. Petros, A.M. et al. Solution structure of the antiapoptotic protein bcl-2. *Proc Natl Acad Sci U S A* **98**, 3012-7 (2001).

43. Day, C.L. et al. Solution structure of prosurvival Mcl-1 and characterization of its binding by proapoptotic BH3-only ligands. *J Biol Chem* **280**, 4738-44 (2005).

44. Suzuki, M., Youle, R.J. & Tjandra, N. Structure of Bax: Coregulation of Dimer Formation and Intracellular Localization. *Cell* **103**, 645-654 (2000).

45. Chou, J.J., Li, H., Salvesen, G.S., Yuan, J. & Wagner, G. Solution structure of BID, an intracellular amplifier of apoptotic signaling. *Cell* **96**, 615-24 (1999).

46. McDonnell, J.M., Fushman, D., Milliman, C.L., Korsmeyer, S.J. & Cowburn, D. Solution structure of the proapoptotic molecule BID: a structural basis for apoptotic agonists and antagonists. *Cell* **96**, 625-34 (1999).

47. Grinberg, M. et al. tBID Homooligomerizes in the mitochondrial membrane to induce apoptosis. *J Biol Chem* **277**, 12237-45 (2002).

48. Billen, L.P., Shamas-Din, A. & Andrews, D.W. Bid: a Bax-like BH3 protein. *Oncogene* **27 Suppl 1**, S93-104 (2008).

49. Sattler, M. et al. Structure of Bcl-xL-Bak Peptide Complex: Recognition Between Regulators of Apoptosis. *Science* **275**, 983-986 (1997).

50. Petros, A.M. et al. Rationale for Bcl-xL/Bad peptide complex formation from structure, mutagenesis, and biophysical studies. *Protein Sci* **9**, 2528-34 (2000).

51. Moldoveanu, T. et al. The X-ray structure of a BAK homodimer reveals an inhibitory zinc binding site. *Mol Cell* **24**, 677-88 (2006).

52. Hsu, Y.T. & Youle, R.J. Nonionic detergents induce dimerization among members of the Bcl-2 family. *J Biol Chem* **272**, 13829-34 (1997).

53. Griffiths, G.J. et al. Cellular damage signals promote sequential changes at the N-terminus and BH-1 domain of the pro-apoptotic protein Bak. *Oncogene* **20**, 7668-76 (2001).

54. Bleicken, S. et al. Molecular details of Bax activation, oligomerization, and membrane insertion. *J Biol Chem* **285**, 6636-47 (2010).

55. Wang, H. et al. Novel dimerization mode of the human Bcl-2 family protein Bak, a mitochondrial apoptosis regulator. *J Struct Biol* **166**, 32-7 (2009).

56. Veis, D.J., Sorenson, C.M., Shutter, J.R. & Korsmeyer, S.J. Bcl-2-deficient mice demonstrate fulminant lymphoid apoptosis, polycystic kidneys, and hypopigmented hair. *Cell* **75**, 229-40 (1993).

57. Motoyama, N. et al. Massive cell death of immature hematopoietic cells and neurons in Bcl-x-deficient mice. *Science* **267**, 1506-10 (1995).

58. Lindsten, T. et al. The Combined Functions of Proapoptotic Bcl-2 Family Members Bak and Bax Are Essential for Normal Development of Multiple Tissues. *Molecular Cell* **6**, 1389-1399 (2000).

59. Knudson, C.M., Tung, K.S., Tourtellotte, W.G., Brown, G.A. & Korsmeyer, S.J. Bax-deficient mice with lymphoid hyperplasia and male germ cell death. *Science* **270**, 96-9 (1995).

60. Bouillet, P. et al. Proapoptotic Bcl-2 relative Bim required for certain apoptotic responses, leukocyte homeostasis, and to preclude autoimmunity. *Science* **286**, 1735-8 (1999).

61. Ren, D. et al. BID, BIM, and PUMA are essential for activation of the BAX- and BAK-dependent cell death program. *Science* **330**, 1390-3 (2010).

62. Hanada, M., Delia, D., Aiello, A., Stadtmauer, E. & Reed, J.C. bcl-2 gene hypomethylation and high-level expression in B-cell chronic lymphocytic leukemia. *Blood* **82**, 1820-8 (1993).

63. Rochaix, P. et al. In vivo patterns of Bcl-2 family protein expression in breast carcinomas in relation to apoptosis. *J Pathol* **187**, 410-5 (1999).

64. Monni, O. et al. BCL2 overexpression associated with chromosomal amplification in diffuse large B-cell lymphoma. *Blood* **90**, 1168-74 (1997).

65. Strik, H. et al. BCL-2 family protein expression in initial and recurrent glioblastomas: modulation by radiochemotherapy. *J Neurol Neurosurg Psychiatry* **67**, 763-8 (1999).

66. Fecker, L.F. et al. Loss of proapoptotic Bcl-2-related multidomain proteins in primary melanomas is associated with poor prognosis. *J Invest Dermatol* **126**, 1366-71 (2006).

67. Pepper, C., Hoy, T. & Bentley, D.P. Bcl-2/Bax ratios in chronic lymphocytic leukaemia and their correlation with in vitro apoptosis and clinical resistance. *Br J Cancer* **76**, 935-8 (1997).

68. Jansson, A. & Sun, X.F. Bax expression decreases significantly from primary tumor to metastasis in colorectal cancer. *J Clin Oncol* **20**, 811-6 (2002).

69. Ni Chonghaile, T. et al. Pretreatment mitochondrial priming correlates with clinical response to cytotoxic chemotherapy. *Science* **334**, 1129-33 (2011).

70. Vo, T.T. et al. Relative mitochondrial priming of myeloblasts and normal HSCs determines chemotherapeutic success in AML. *Cell* **151**, 344-55 (2012).

71. Davids, M.S. et al. Decreased mitochondrial apoptotic priming underlies stroma-mediated treatment resistance in chronic lymphocytic leukemia. *Blood* **120**, 3501-9 (2012).

72. Farrow, S.N. et al. Cloning of a bcl-2 homologue by interaction with adenovirus E1B 19K. *Nature* **374**, 731-3 (1995).

73. Chittenden, T. et al. A conserved domain in Bak, distinct from BH1 and BH2, mediates cell death and protein binding functions. *EMBO J* **14**, 5589-96 (1995).

74. Hsu, Y.T., Wolter, K.G. & Youle, R.J. Cytosol-to-membrane redistribution of Bax and Bcl-X(L) during apoptosis. *Proc Natl Acad Sci U S A* **94**, 3668-72 (1997).

75. Hsu, Y.T. & Youle, R.J. Bax in murine thymus is a soluble monomeric protein that displays differential detergent-induced conformations. *J Biol Chem* **273**, 10777-83 (1998).

76. Willis, S.N. et al. Apoptosis initiated when BH3 ligands engage multiple Bcl-2 homologs, not Bax or Bak. *Science* **315**, 856-9 (2007).

77. Cheng, E.H., Sheiko, T.V., Fisher, J.K., Craigen, W.J. & Korsmeyer, S.J. VDAC2 inhibits BAK activation and mitochondrial apoptosis. *Science* **301**, 513-7 (2003).

78. Wei, M.C. et al. Proapoptotic BAX and BAK: a requisite gateway to mitochondrial dysfunction and death. *Science* **292**, 727-30 (2001).

79. Cheng, E.H. et al. BCL-2, BCL-X(L) sequester BH3 domain-only molecules preventing BAX- and BAK-mediated mitochondrial apoptosis. *Mol Cell* **8**, 705-11 (2001).

80. Walensky, L.D. et al. Activation of apoptosis in vivo by a hydrocarbon-stapled BH3 helix. *Science* **305**, 1466-70 (2004).

81. Oltersdorf, T. et al. An inhibitor of Bcl-2 family proteins induces regression of solid tumours. *Nature* **435**, 677-81 (2005).

82. Nguyen, M. et al. Small molecule obatoclax (GX15-070) antagonizes MCL-1 and overcomes MCL-1-mediated resistance to apoptosis. *Proc Natl Acad Sci U S A* **104**, 19512-7 (2007).

83. Chipuk, J.E. & Green, D.R. How do BCL-2 proteins induce mitochondrial outer membrane permeabilization? *Trends Cell Biol* **18**, 157-64 (2008).

84. Dewson, G. & Kluck, R.M. Mechanisms by which Bak and Bax permeabilise mitochondria during apoptosis. *J Cell Sci* **122**, 2801-8 (2009).

85. Leber, B., Lin, J. & Andrews, D.W. Embedded together: the life and death consequences of interaction of the Bcl-2 family with membranes. *Apoptosis* **12**, 897-911 (2007).

86. Letai, A. et al. Distinct BH3 domains either sensitize or activate mitochondrial apoptosis, serving as prototype cancer therapeutics. *Cancer Cell* **2**, 183-192 (2002).

87. Wang, K., Yin, X.M., Chao, D.T., Milliman, C.L. & Korsmeyer, S.J. BID: a novel BH3 domain-only death agonist. *Genes Dev* **10**, 2859-69 (1996).

88. Kuwana, T. et al. BH3 Domains of BH3-Only Proteins Differentially Regulate Bax-Mediated Mitochondrial Membrane Permeabilization Both Directly and Indirectly. *Molecular Cell* **17**, 525-535 (2005).

89. Kuwana, T. et al. Bid, Bax, and Lipids Cooperate to Form Supramolecular Openings in the Outer Mitochondrial Membrane. *Cell* **111**, 331-342 (2002).

90. Walensky, L.D. et al. A stapled BID BH3 helix directly binds and activates BAX. *Mol Cell* **24**, 199-210 (2006).

91. Gavathiotis, E. et al. BAX activation is initiated at a novel interaction site. *Nature* **455**, 1076-81 (2008).

92. Gavathiotis, E., Reyna, D.E., Davis, M.L., Bird, G.H. & Walensky, L.D. BH3-triggered structural reorganization drives the activation of proapoptotic BAX. *Mol Cell* **40**, 481-92 (2010).

93. Lovell, J.F. et al. Membrane Binding by tBid Initiates an Ordered Series of Events Culminating in Membrane Permeabilization by Bax. *Cell* **135**, 1074-1084 (2008).

94. Dai, H. et al. Transient binding of an activator BH3 domain to the Bak BH3-binding groove initiates Bak oligomerization. *J Cell Biol* **194**, 39-48 (2011).

95. Oh, K.J. et al. Conformational Changes in BAK, a Pore-forming Proapoptotic Bcl-2 Family Member, upon Membrane Insertion and Direct Evidence for the Existence of BH3-BH3 Contact Interface in BAK Homo-oligomers. *Journal of Biological Chemistry* **285**, 28924-28937 (2010).

96. Landeta, O. et al. Reconstitution of Proapoptotic BAK Function in Liposomes Reveals a Dual Role for Mitochondrial Lipids in the BAK-driven Membrane Permeabilization Process. *Journal of Biological Chemistry* **286**, 8213-8230 (2011).

97. Du, H. et al. BH3 domains other than Bim and Bid can directly activate Bax/Bak. *J Biol Chem* **286**, 491-501 (2011).

98. Letai, A. et al. Distinct BH3 domains either sensitize or activate mitochondrial apoptosis, serving as prototype cancer therapeutics. *Cancer Cell* **2**, 183-92 (2002).

99. Kim, H. et al. Hierarchical regulation of mitochondrion-dependent apoptosis by BCL-2 subfamilies. *Nat Cell Biol* **8**, 1348-1358 (2006).

100. Kim, H. et al. Stepwise Activation of BAX and BAK by tBID, BIM, and PUMA Initiates Mitochondrial Apoptosis. *Molecular Cell* **36**, 487-499 (2009).

101. Dewson, G. et al. Bak activation for apoptosis involves oligomerization of dimers via their alpha6 helices. *Mol Cell* **36**, 696-703 (2009).

102. Dewson, G. et al. To trigger apoptosis, Bak exposes its BH3 domain and homodimerizes via BH3:groove interactions. *Mol Cell* **30**, 369-80 (2008).

103. Dewson, G. et al. Bax dimerizes via a symmetric BH3:groove interface during apoptosis. *Cell Death Differ* **19**, 661-70 (2012).

104. Czabotar, P.E. et al. Bax Crystal Structures Reveal How BH3 Domains Activate Bax and Nucleate Its Oligomerization to Induce Apoptosis. *Cell* **152**, 519-31 (2013).

105. Mikhailov, V. et al. Association of Bax and Bak homo-oligomers in mitochondria. Bax requirement for Bak reorganization and cytochrome c release. *J Biol Chem* **278**, 5367-76 (2003).

106. Mikhailov, V. et al. Bcl-2 prevents Bax oligomerization in the mitochondrial outer membrane. *J Biol Chem* **276**, 18361-74 (2001).

107. Antonsson, B., Montessuit, S., Sanchez, B. & Martinou, J.C. Bax is present as a high molecular weight oligomer/complex in the mitochondrial membrane of apoptotic cells. *J Biol Chem* **276**, 11615-23 (2001).

108. Lucken-Ardjomande, S., Montessuit, S. & Martinou, J.C. Contributions to Bax insertion and oligomerization of lipids of the mitochondrial outer membrane. *Cell Death Differ* **15**, 929-37 (2008).

109. Lutter, M. et al. Cardiolipin provides specificity for targeting of tBid to mitochondria. *Nat Cell Biol* **2**, 754-61 (2000).

110. Kim, T.H. et al. Bid-cardiolipin interaction at mitochondrial contact site contributes to mitochondrial cristae reorganization and cytochrome C release. *Mol Biol Cell* **15**, 3061-72 (2004).

111. Basanez, G. et al. Bax-type apoptotic proteins porate pure lipid bilayers through a mechanism sensitive to intrinsic monolayer curvature. *J Biol Chem* **277**, 49360-5 (2002).

112. Terrones, O. et al. Lipidic pore formation by the concerted action of proapoptotic BAX and tBID. *J Biol Chem* **279**, 30081-91 (2004).

113. Chipuk, J.E. et al. Sphingolipid metabolism cooperates with BAK and BAX to promote the mitochondrial pathway of apoptosis. *Cell* **148**, 988-1000 (2012).

114. Opferman, J.T. et al. Development and maintenance of B and T lymphocytes requires antiapoptotic MCL-1. *Nature* **426**, 671-6 (2003).

115. Llambi, F. et al. A unified model of mammalian BCL-2 protein family interactions at the mitochondria. *Mol Cell* **44**, 517-31 (2011).

116. Antignani, A. & Youle, R.J. How do Bax and Bak lead to permeabilization of the outer mitochondrial membrane? *Curr Opin Cell Biol* **18**, 685-9 (2006).

117. Billen, L.P., Kokoski, C.L., Lovell, J.F., Leber, B. & Andrews, D.W. Bcl-XL inhibits membrane permeabilization by competing with Bax. *PLoS Biol* **6**, e147 (2008).

118. Krogh, A., Larsson, B., von Heijne, G. & Sonnhammer, E.L. Predicting transmembrane protein topology with a hidden Markov model: application to complete genomes. *J Mol Biol* **305**, 567-80 (2001).

119. Overington, J.P., Al-Lazikani, B. & Hopkins, A.L. How many drug targets are there? *Nat Rev Drug Discov* **5**, 993-6 (2006).

120. Guharoy, M. & Chakrabarti, P. Secondary structure based analysis and classification of biological interfaces: identification of binding motifs in protein-protein interactions. *Bioinformatics* **23**, 1909-18 (2007).

121. Jones, S. & Thornton, J.M. Principles of protein-protein interactions. *Proc Natl Acad Sci U S A* **93**, 13-20 (1996).

122. Barlow, D.J. & Thornton, J.M. Helix geometry in proteins. *J Mol Biol* **201**, 601-19 (1988).

123. Guharoy, M. & Chakrabarti, P. Conservation and relative importance of residues across protein-protein interfaces. *Proc Natl Acad Sci U S A* **102**, 15447-52 (2005).

124. Henchey, L.K., Jochim, A.L. & Arora, P.S. Contemporary strategies for the stabilization of peptides in the alpha-helical conformation. *Curr Opin Chem Biol* **12**, 692-7 (2008).

125. Edwards, T.A. & Wilson, A.J. Helix-mediated protein--protein interactions as targets for intervention using foldamers. *Amino Acids* **41**, 743-54 (2011).

126. Tyndall, J.D., Nall, T. & Fairlie, D.P. Proteases universally recognize beta strands in their active sites. *Chem Rev* **105**, 973-99 (2005).

127. Garner, J. & Harding, M.M. Design and synthesis of alpha-helical peptides and mimetics. *Org Biomol Chem* **5**, 3577-85 (2007).

128. Goodman, C.M., Choi, S., Shandler, S. & DeGrado, W.F. Foldamers as versatile frameworks for the design and evolution of function. *Nat Chem Biol* **3**, 252-62 (2007).

129. Davis, J.M., Tsou, L.K. & Hamilton, A.D. Synthetic non-peptide mimetics of alpha-helices. *Chem Soc Rev* **36**, 326-34 (2007).

130. Taylor, J.W. The synthesis and study of side-chain lactam-bridged peptides. *Biopolymers* **66**, 49-75 (2002).

131. Brunel, F.M. & Dawson, P.E. Synthesis of constrained helical peptides by thioether ligation: application to analogs of gp41. *Chem Commun (Camb)*, 2552-4 (2005).

132. Kelso, M.J. et al. Alpha-turn mimetics: short peptide alpha-helices composed of cyclic metallopentapeptide modules. *J Am Chem Soc* **126**, 4828-42 (2004).

133. Cabezas, E. & Satterthwait, A. The Hydrogen Bond Mimic Approach: Solid-Phase Synthesis of a Peptide Stabilized as an alpha-Helix with a Hydrazone link. *J Am Chem Soc* **121**, 3862-3875 (1999).

134. Liu, J., Wang, D., Zheng, Q., Lu, M. & Arora, P.S. Atomic structure of a short alpha-helix stabilized by a main chain hydrogen-bond surrogate. *J Am Chem Soc* **130**, 4334-7 (2008).

135. Patgiri, A., Yadav, K.K., Arora, P.S. & Bar-Sagi, D. An orthosteric inhibitor of the Ras-Sos interaction. *Nat Chem Biol* **7**, 585-7 (2011).

136. Zhang, F., Sadovski, O., Xin, S.J. & Woolley, G.A. Stabilization of folded peptide and protein structures via distance matching with a long, rigid cross-linker. *J Am Chem Soc* **129**, 14154-5 (2007).

137. Fujimoto, K., Kajino, M. & Inouye, M. Development of a series of cross-linking agents that effectively stabilize alpha-helical structures in various short peptides. *Chemistry* **14**, 857-63 (2008).

138. Kawamoto, S.A. et al. Design of triazole-stapled BCL9 alpha-helical peptides to target the beta-catenin/B-cell CLL/lymphoma 9 (BCL9) protein-protein interaction. *J Med Chem* **55**, 1137-46 (2012).

139. Blackwell, H.E. et al. Ring-closing metathesis of olefinic peptides: design, synthesis, and structural characterization of macrocyclic helical peptides. *J Org Chem* **66**, 5291-302 (2001).

140. Schafmeister, C., Po, J. & Verdine, G.L. An All-Hydrocarbon Cross-Linking System for Enhancing the Helicity and Metabolic Stability of Peptides. *J Am Chem Soc* **122**, 5891-5892 (2000).

141. LaBelle, J.L. et al. A stapled BIM peptide overcomes apoptotic resistance in hematologic cancers. *J Clin Invest* **122**, 2018-31 (2012).

142. Stewart, M.L., Fire, E., Keating, A.E. & Walensky, L.D. The MCL-1 BH3 helix is an exclusive MCL-1 inhibitor and apoptosis sensitizer. *Nat Chem Biol* **6**, 595-601 (2010).

143. Bernal, F. et al. A stapled p53 helix overcomes HDMX-mediated suppression of p53. *Cancer Cell* **18**, 411-22 (2010).

144. Kutchukian, P.S., Yang, J.S., Verdine, G.L. & Shakhnovich, E.I. All-atom model for stabilization of alpha-helical structure in peptides by hydrocarbon staples. *J Am Chem Soc* **131**, 4622-7 (2009).

145. Bird, G.H. et al. Hydrocarbon double-stapling remedies the proteolytic instability of a lengthy peptide therapeutic. *Proc Natl Acad Sci U S A* **107**, 14093-8 (2010).

146. Wells, J.A. & McClendon, C.L. Reaching for high-hanging fruit in drug discovery at protein-protein interfaces. *Nature* **450**, 1001-9 (2007).

147. Weng, A.P. et al. Activating mutations of NOTCH1 in human T cell acute lymphoblastic leukemia. *Science* **306**, 269-71 (2004).

148. Nefedova, Y., Cheng, P., Alsina, M., Dalton, W.S. & Gabrilovich, D.I. Involvement of Notch-1 signaling in bone marrow stroma-mediated de novo drug resistance of myeloma and other malignant lymphoid cell lines. *Blood* **103**, 3503-10 (2004).

149. Nam, Y., Sliz, P., Song, L., Aster, J.C. & Blacklow, S.C. Structural basis for cooperativity in recruitment of MAML coactivators to Notch transcription complexes. *Cell* **124**, 973-83 (2006).

150. Weng, A.P. et al. Growth suppression of pre-T acute lymphoblastic leukemia cells by inhibition of notch signaling. *Mol Cell Biol* **23**, 655-64 (2003).

151. Moellering, R.E. et al. Direct inhibition of the NOTCH transcription factor complex. *Nature* **462**, 182-8 (2009).

152. Takada, K. et al. Targeted disruption of the BCL9/beta-catenin complex inhibits oncogenic Wnt signaling. *Sci Transl Med* **4**, 148ra117 (2012).

153. Zhang, H. et al. Antiviral activity of alpha-helical stapled peptides designed from the HIV-1 capsid dimerization domain. *Retrovirology* **8**, 28 (2011).

154. Zhang, H. et al. A cell-penetrating helical peptide as a potential HIV-1 inhibitor. *J Mol Biol* **378**, 565-80 (2008).

155. Braun, C.R. et al. Photoreactive stapled BH3 peptides to dissect the BCL-2 family interactome. *Chem Biol* **17**, 1325-33 (2010).

156. Carpenter, E.P., Beis, K., Cameron, A.D. & Iwata, S. Overcoming the challenges of membrane protein crystallography. *Curr Opin Struct Biol* **18**, 581-6 (2008).

157. Bill, R.M. et al. Overcoming barriers to membrane protein structure determination. *Nat Biotechnol* **29**, 335-40 (2011).

158. Bonvin, A.M., Boelens, R. & Kaptein, R. NMR analysis of protein interactions. *Curr Opin Chem Biol* **9**, 501-8 (2005).

159. Hu, Q. et al. The Orbitrap: a new mass spectrometer. *J Mass Spectrom* **40**, 430-43 (2005).

160. Anderson, G.W., Zimmerman, J.E. & Callahan, F.M. The Use of Esters of N-Hydroxysuccinimide in Peptide Synthesis. *J Am Chem Soc* **86**, 1839-1842 (1964).

161. Kim, Y. et al. Efficient site-specific labeling of proteins via cysteines. *Bioconjug Chem* **19**, 786-91 (2008).

162. Novak, P. & Kruppa, G.H. Intra-molecular cross-linking of acidic residues for protein structure studies. *Eur J Mass Spectrom (Chichester, Eng)* **14**, 355-65 (2008).

163. Deiters, A. et al. Adding amino acids with novel reactivity to the genetic code of Saccharomyces cerevisiae. *J Am Chem Soc* **125**, 11782-3 (2003).

164. Chin, J.W. et al. Addition of p-azido-L-phenylalanine to the genetic code of Escherichia coli. *J Am Chem Soc* **124**, 9026-7 (2002).

165. Wang, L., Zhang, Z., Brock, A. & Schultz, P.G. Addition of the keto functional group to the genetic code of Escherichia coli. *Proc Natl Acad Sci U S A* **100**, 56-61 (2003).

166. Wittelsberger, A., Mierke, D.F. & Rosenblatt, M. Mapping ligand-receptor interfaces: approaching the resolution limit of benzophenone-based photoaffinity scanning. *Chem Biol Drug Des* **71**, 380-3 (2008).

167. Sohn, C.H. et al. Designer reagents for mass spectrometry-based proteomics: clickable cross-linkers for elucidation of protein structures and interactions. *Anal Chem* **84**, 2662-9 (2012).

168. Back, J.W. et al. A new crosslinker for mass spectrometric analysis of the quaternary structure of protein complexes. *J Am Soc Mass Spectrom* **12**, 222-7 (2001).

Chapter 2

Production of Full-Length Monomeric BAK

Abstract

BCL-2 family members BAX and BAK execute apoptosis in response to stress stimuli by porating the mitochondrial outer membranes and releasing apoptogenic factors. Despite this central role as a critical control point of apoptosis, the biochemical mechanisms underlying BAX and especially BAK activation are poorly understood.

The longstanding inability to express full-length BAK as a recombinant protein has precluded a complete biochemical and structural dissection of its activation mechanism. Here, I report the successful production of monomeric, full-length BAK (FL-BAK) by increasing the solubility of its carboxy-terminal surface through point mutagenesis.

Introduction

BAK is a member of the BCL-2 protein family that regulates programmed cell death, or apoptosis. BAK resides as an inactive monomer in the outer membrane of the mitochondria, the energy-generating organelle of the cell, until stimulated by cellular stress to undergo conformational activation. The activated BAK protein self-associates to form pores in the mitochondrial outer membrane, allowing the release of critical signaling factors that drive the apoptotic process. Because BAK activation is one of the ultimate control points for apoptosis, the elusive mechanisms underlying BAK regulation and channel formation remain a research area of high priority in the cell death field. The longstanding inability to express full-length BAK as a recombinant protein has precluded a complete biochemical and structural dissection of its activation mechanism.

BAK shares functional homology with another BCL-2 family protein named BCL-2–associated X or BAX. Each protein contains an essential α-helical motif, termed BCL-2 homology domain 3 (BH3), which is required for oligomerization-based killing activity. Apoptosis is blocked when exposed BAK and BAX BH3 domains are sequestered in a groove on the surface of anti-apoptotic BCL-2 family proteins[1]. This mode of BAK and BAX suppression is so effective in preventing apoptosis that cancer cells are known to hijack and amplify this natural regulatory mechanism to enforce pathologic cell survival. Indeed, major efforts are underway to pharmacologically disrupt these inhibitory BAK and BAX interactions in order to reactivate the death pathway in human cancer. Although much is known about how BAK and BAX are blocked through this canonical "BH3-in-groove" interaction, the mechanisms that

activate BAK and BAX, and whether BAK and BAX are directly activated in the first place, have been the subject of much debate.

In recent years, tremendous progress has been made in deciphering thestructure, biochemical behavior, and activation patterns and mechanisms of pro-apoptotic BAX, owing in large part to the successful isolation of BAX in a pure monomeric form. Full-length recombinant BAX was successfully employed in NMR studies to solve its solution structure[2]. Much less is known about BAK, because as a membrane protein, it has been refractory to expression and purification in monomeric form[3]. To our knowledge, the successful production and purification of the full-length monomeric form of BAK has not been achieved.

Results

Production of C-terminally truncated BAK

Because BAK is a membrane protein, there are intrinsic difficulties associated with its production and purification, including toxicity for heterologous expression (*E.coli*), low expression levels, and aggregation upon purification[4]. A standard approach for purification of membrane proteins has been truncation of their membrane domains, especially if it is clearly identifiable and does not represent the bulk of the protein. In the case of BAK protein, its C-terminal helix, α9, is the hydrophobic helix that anchors it in the mitochondrial outer membrane[5]. I first eliminated this helix and expressed the truncated form as a GST-fusion, followed by affinity purification on GST beads, thrombin cleavage to remove the tag, and size exclusion chromatography (FPLC). The elution profile is shown on Figure 2.1, *A*. Gratifyingly, this approach allowed us to isolate large quantities of BAKΔC. Unfortunately, this protein was not functional as assessed by liposomal release assay, either alone or in combination with a BH3-only activator protein tBID, using BAKΔC concentrations of up to 5 μM (data not shown). Based on these data, I concluded that BAK's hydrophobic C-teminal helix is critical to its function. Thus, I set out to explore experimental approaches for producing full-length BAK.

Screening different conditions for full-length BAK production and purification

Having verified the importance of the full-length form of BAK for biochemical and functional analysis, we began screening different conditions for full-length BAK production. Several variable parameters were explored: expression vector/fusion tag; temperature; and bacterial expression strain, all with limited success.

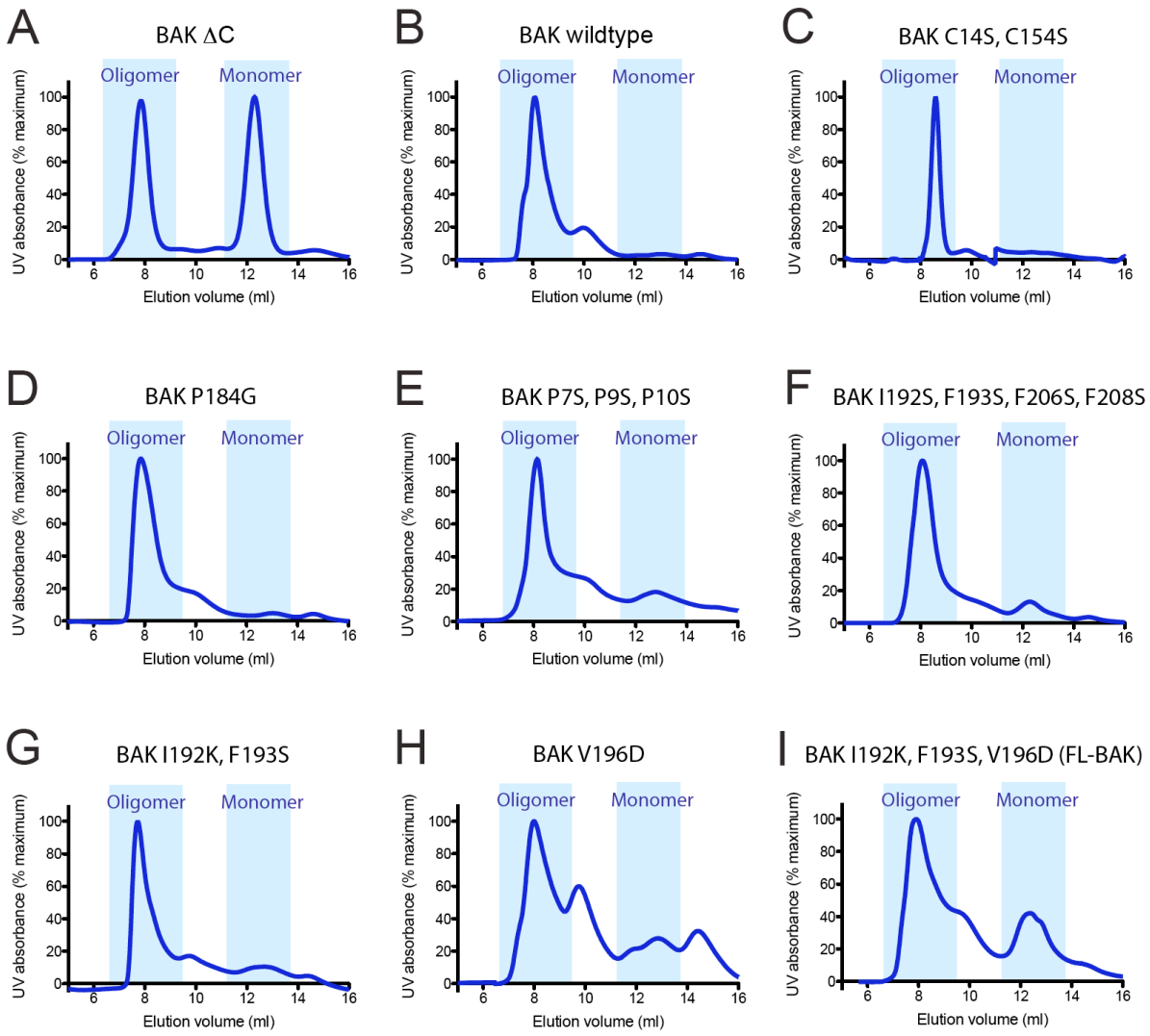

Figure 2.1. Expression and purification of select BAK mutant constructs. (*A*) Size exclusion chromatography (SEC) profile of BAKΔC demonstrates successful production of the BAKΔC monomer. (*B*) SEC profile of wild-type full-length BAK reflects the inability to isolate BAK monomer. (*C*) SEC elution profile of BAK C14S/C154S demonstrates that Cys to Ser substitutions did not remedy the inability to produce BAK monomer. (*D, E*) SEC elution profiles of proline-modified BAK proteins: BAK P184G (*D*) and BAK P7S/P9S/P10S (*E*). (*F-I*) SEC elution profiles of C-terminally modified BAK proteins: BAK I192S/F193S/F206S/F207S (*F*);

Figure 2.1 (Continued).

BAK I192K/I193S (*G*); BAK V196D (*H*); BAK I192K/F193S/V196D (*I*). Only triply mutant BAK I192K/F193S/V196D (hereafter referred to as FL-BAK) resulted in the successful isolation of a monomeric BAK species.

The summary of tested conditions is provided in Table 2.1. Based on our findings, we decided to focus our efforts on a chitin binding domain fusion tag-containing expression system, as it provided the most promising results for BAK; it is also known to be the system of choice for producing full-length BAX.

Point mutagenesis approach to the production of a full-length form of BAK

Introducing point mutations into the protein sequence can stabilize protein structure and promote the expression of a stable monomeric preparation[4,6]. One common strategy is to remove the cysteines from the protein sequence by substituting serines or other amino acids. Since cysteines promote disulfide bond formation, removing them can stabilize the protein by preventing its aggregation. Unfortunately, replacing cysteines with serines did not provide the desired effect for BAK (Figure 2.1, *B* and *C*), so we turned to alternative strategies.

Elimination of a proline residue at a kink between the C-terminal pocket and the α9 helix of BAX was previously shown to dramatically stabilize the monomeric form of BAX [7]. By analogy, we mutated the corresponding proline in full-length BAK (Figure 2.1, *D*) and several prolines at the N-terminal unstructured region of the BAK protein (Figure 2.1, *E*). However, none of these substitutions produced significant improvements in expression or purification.

A prominent distinction between BAX and BAK is their respective cytosolic vs. mitochondrial outer membrane localization, which at least in part, is driven by the disposition of the proteins' C-terminal α-helices. Whereas the BAX α9 helix is tightly bound to its canonical binding groove[8], the corresponding α-helix in BAK is constitutively released for mitochondrial outer membrane insertion. This structural and functional difference between the two α-helices is reflected by a comparatively more hydrophobic BAK than BAX α9. We reasoned that the

Table 2.1. Purification systems employed for production of full-length, monomeric BAK.

Vector/tag	▪ pTYB4 / Chitin binding domain (C-terminal)
	▪ pTYB11 / Chitin binding domain (N-terminal)
	▪ pGEX4B / GST tag
	▪ pGEV2 / GB1 tag
	▪ pET system / His-tag (C- or N-terminal)
Host strain	▪ BL21(DE3)
	▪ Arabinose-inducible cells
	▪ Rosetta
	▪ BL21 Origami
Temperature	▪ 37°C
	▪ 30°C
	▪ 22°C
	▪ 14°C
Purification	▪ From soluble fractions
	▪ Refolding from inclusion bodies

increased hydrophobicity of BAK's C-terminus may account for its membrane tropism and propensity to aggregate upon bacterial protein expression, precluding the isolation of full-length monomer. To surmount this challenge, I modified the surface of BAK α9 by introducing point mutations to better match the amphipathic character of BAX α9. Most of the substitutions did not yield the desired monomeric peak on the FPLC trace (Figure 2.1, *F-H*). However, one triple mutant construct produced the full-length monomeric BAK (Figure 2.1, *I*), and is described below.

Production of full-length, monomeric BAK

The successful production of full-length monomeric BAK resulted from converting the hydrophobic Phe193 residue of BAK into a hydrophilic Ser, and replacing the hydrophobic Ile192 and Val196 pair with charged residues Lys and Asp, respectively, yielding a surface salt bridge (Figure 2.2, *A*). I employed the pTYB4 vector to generate a chitin binding domain fusion protein of murine BAK I192K/F193S/V196D (hereafter referred to as full-length BAK [FL-BAK]). The fusion protein was expressed in *E. Coli* BL21 bacteria, isolated by chitin column chromatography, and subjected to dithiothreitol (DTT)-based intein tag removal, as reported[8,9]. The elution profiles of wild-type vs. triply mutagenized full-length BAK were compared by size exclusion chromatography (SEC). Whereas the wild-type construct yielded predominantly an oligomeric peak accompanied by a small dimeric peak, the α9-mutagenized construct additionally produced the desired monomeric peak (Figure 2.2, *B*). The monomeric fraction (11-12 mL elution volume) migrated as a 23 kD protein by SDS PAGE, and the identity of FL-BAK protein was confirmed by anti-BAK western blot analysis (Fig. 2.2, *B*) and MS/MS of the electrophoresed band (Fig. 2.2, *C*).

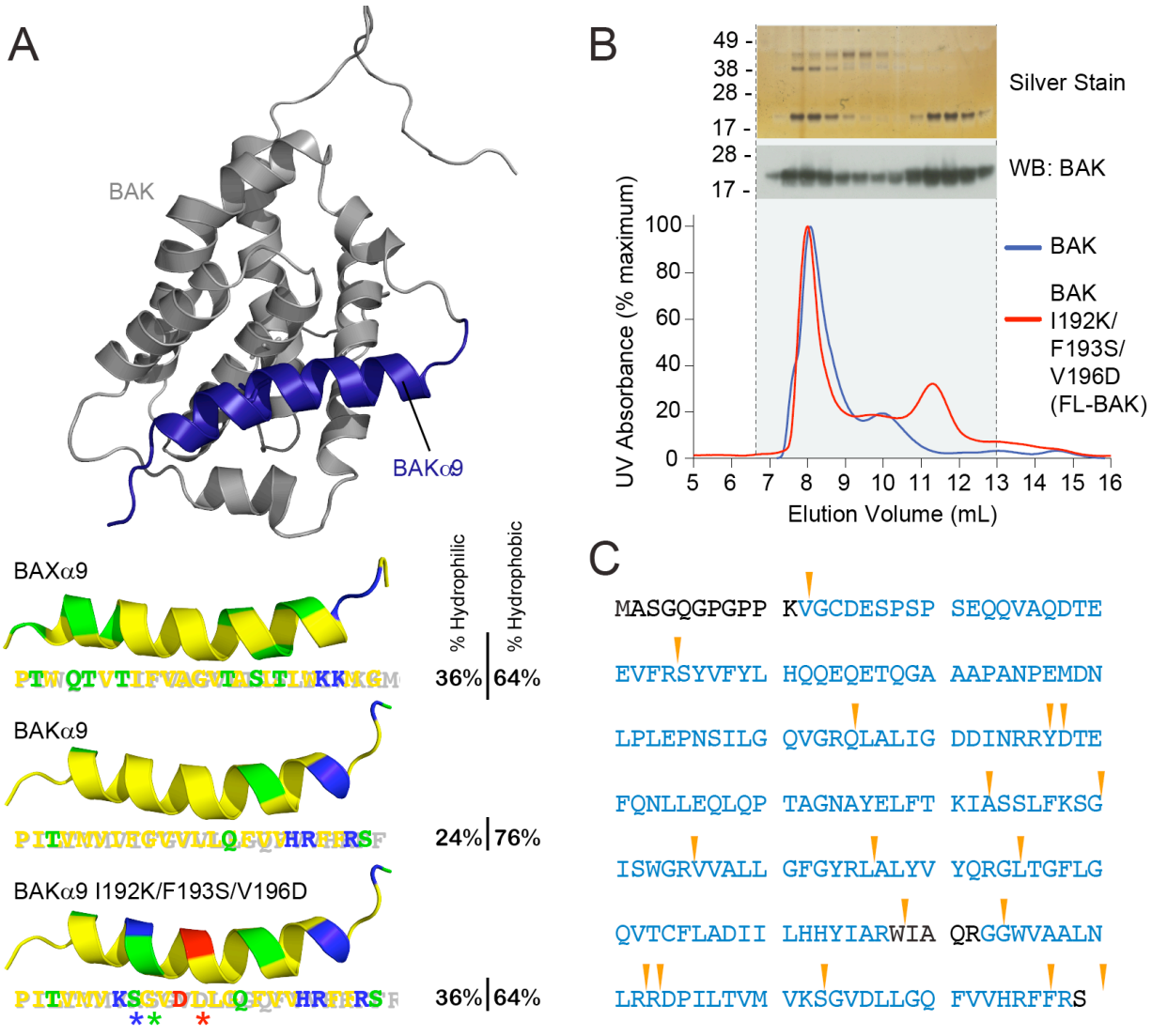

Figure 2.2. Expression and purification of recombinant, full-length, and monomeric BAK. (*A*) The α9 helix of BAK was subjected to triple mutagenesis (I192K/F193S/V196D) in order to increase its hydrophilicity and better match that of soluble, full-length BAX. The pictured model structure of BAK was calculated based on the solution structure of BAX using Modeller software[10], with BAK α9 colored blue. The hydrophobic, hydrophilic, positively charged, and negatively charged residues of the BAK and BAX α9 helices are colored yellow, green, blue, and red, respectively. (*B*) A comparison of the SEC elution profiles of BAK and BAK

Figure 2.2 (Continued).

I192K/F193S/V196D (FL-BAK) demonstrates that mutagenesis enabled the isolation of a monomeric species (11-12 mL fractions). Silver staining and anti-BAK western analysis of the electrophoresed FL-BAK fractions documented the isolation of monomeric BAK protein (~23 kDa). (*C*) The identity of the isolated, monomeric protein was confirmed to be FL-BAK by mass spectrometry analysis. Tryptic sites are highlighted by the arrowheads and the FL-BAK sequences identified by LC-MS/MS are colored blue.

FL-BAK induces apoptosis at a similar level as wild type BAK when transfected into cells

Importantly, I confirmed that this triple mutagenesis of BAK did not alter its functional activity, as evidenced by equivalently decreased viability of etoposide and staurosporine-treated *Bax*$^{-/-}$*Bak*$^{-/-}$ iBMK[11] cells upon expression of wild-type or the triply mutated full-length BAK (Fig. 2.3).

Summary

By employing structure-guided mutagenesis, I successfully generated, for the first time, pure, full-length, monomeric BAK by introducing the point mutations I192K/F193S/V196D. I confirmed the identity of the protein by mass spectrometry and western analysis, and documented its functionality in a cellular context by transiently expressing FL-BAK in *Bax*$^{-/-}$*Bak*$^{-/-}$ iBMK cells, which otherwisemanifest a severe deficiency in mitochondrial apoptosis. Upon transient expression and stimulation with cytotoxic drugs, triply mutant FL-BAK and wild-type BAK induced cell death at identical levels.

Methods

Expression and purification of full-length BAK

Production of monomeric, full-length BAK (FL-BAK) was achieved by introducing the point mutations I192K/F193S/V196D into the native mouse BAK sequence (Fig. 2.2, *A*; NCBI: NP_031549.2), which was subcloned into the pTYB4 vector (New England Biolabs) using NcoI and SmaI restriction sites. PCR-based site-directed mutagenesis was confirmed by DNA sequencing. The chitin binding domain fusion construct of FL-BAK was expressed in

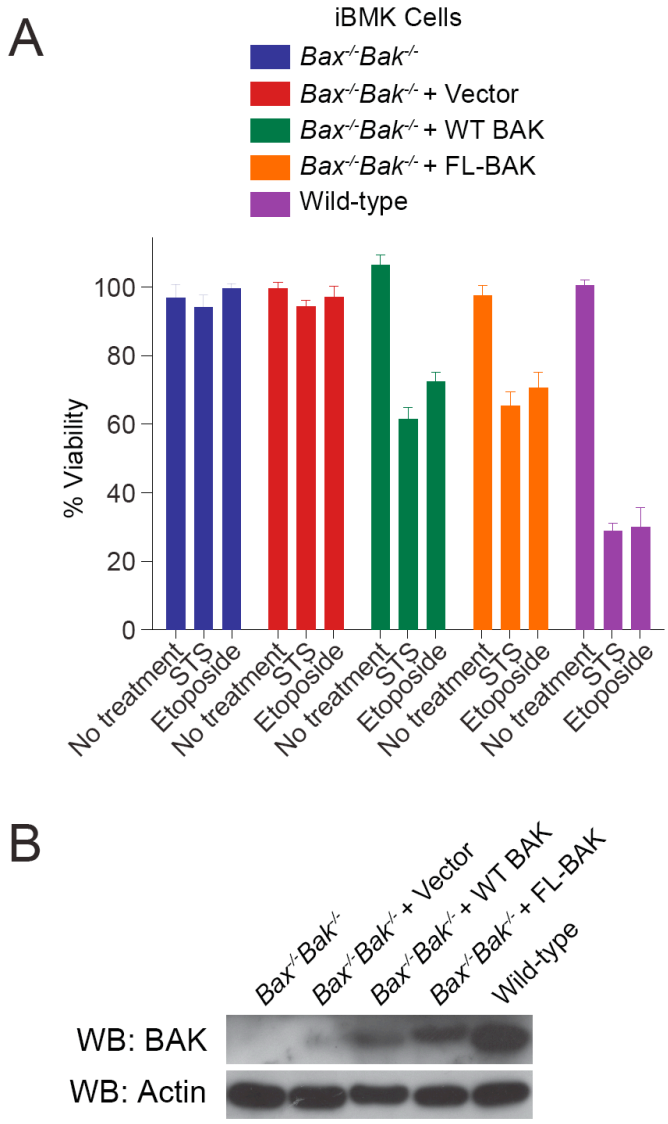

Figure 2.3. Equivalent pro-apoptotic activity of wild-type and FL-BAK.

(*A*) BAX/BAK-deficient immortalized baby mouse kidney epithelial (iBMK) cells reconstituted with wild-type BAK or FL-BAK were treated with etoposide (10 mM) or staurosporine (STS, 100 nM), and cell viability assessed by CellTiter-Glo at 24 hours. *Bax*$^{-/-}$*Bak*$^{-/-}$, *Bax*$^{-/-}$*Bak*$^{-/-}$ plus vector alone, and wild-type iBMK cells served as controls. Untreated controls were also included for all cell lines tested. Data are mean ± SEM for experiments performed in at least

Figure 2.3 (Continued).

triplicate. (*B*) BAK expression levels in the indicated cell lines were determined by anti-BAK western analysis. Whereas *Bax*$^{-/-}$*Bak*$^{-/-}$ and *Bax*$^{-/-}$*Bak*$^{-/-}$ plus vector iBMK cells showed no response to the etoposide or STS treatment, cells with introduced wild-type and triply mutant BAK (FL-BAK), which express at similar levels, exhibited equivalent impairment of viability in response to the pro-apoptotic stimuli. Of note, wild-type iBMK cells demonstrated the most robust response to etoposide and STS treatment, consistent with their expression of relatively higher levels of native BAK (in addition to the presence of native BAX).

BL21(DE3) *E. coli* and induced with 1 mM IPTG at 18°C overnight. Collected bacterial pellets were resuspended in lysis buffer (20 mM Tris, 250 mM NaCl, pH 7.6), lysed by microfluidization (Microfluidics M-110L), and centrifuged at 45,000 rpm for 1 h at 4°C (Beckman L-90K). The cleared cellular lysates were subjected to chitin affinity resin (New England Biolabs) chromatography followed by overnight on-bead intein-tag cleavage using 50 mM DTT. FL-BAK was eluted with lysis buffer, concentrated, and then subjected to size-exclusion chromatography (GE Life Sciences) at 4°C using 20 mM Hepes pH 7.8, 150 mM KCl buffer conditions. FL-BAK and its cysteine-mutant derivative were used immediately upon isolation, without further storage. FL-BAK C14S/A128C/C154S/L198C was maintained in the oxidized state by exposure to 2 mM glutathione disulfide (GSSG), whereas reduction of the disulfide tether was accomplished by 1 h incubation in 10 mM dithiothreitol (DTT). Recombinant full-length BAX and BCL-$X_L\Delta C$ were produced as described[8,9] and tBID was purchased from R&D Systems. Protein concentrations were determined by Bradford assay (Biorad).

iBMK transfection and cell viability assay.

Immortalized baby mouse kidney epithelial (iBMK) cells deficient in BAX and BAK[11] were transfected with the pORF mammalian expression vector alone or with the corresponding plasmid containing wild-type or FL-BAK using lipofectamine 2000 (Invitrogen), according to the manufacturer's protocol. The pORF plasmid containing wild-type murine BAK was purchased from Invivogen, and that containing FL-BAK was generated by PCR-based site-directed mutagenesis and confirmed by DNA sequencing. *bax*$^{-/-}$*bak*$^{-/-}$ iBMK cells were plated in 96-well plates ($4x10^4$ cells/well) in Dulbecco's Modified Eagle Media (DMEM) supplemented

with penicillin/streptomycin, glutamine, 2 mM dithiothreitol and 5% FBS. A mixture of plasmid DNA (0.2 μg) and 0.5 μl lipofectamine was added to each well, followed by 24 hour incubation. The transfected cells and control wild-type and *bax*$^{-/-}$*bak*$^{-/-}$ iBMK cells, were then treated with staurosporine (STS, 100 nM) or etoposide (10 μM), and cell viability was measured at 24 hours by CellTiter-Glo assay (Promega), according to the manufacturer's instructions.

Contributions

Elizaveta S. Leshchiner and Loren D. Walensky contributed to this portion of the work. E.S.L. and L.D.W. designed the experiments, E.S.L. screened and optimized protein production and purification conditions, isolated FL-BAK, and performed the biochemical and cell-based assays.

References

1. Sattler, M. et al. Structure of Bcl-xL-Bak Peptide Complex: Recognition Between Regulators of Apoptosis. *Science* **275**, 983-986 (1997).
2. Gavathiotis, E. et al. BAX activation is initiated at a novel interaction site. *Nature* **455**, 1076-81 (2008).
3. Willis, S.N. et al. Apoptosis initiated when BH3 ligands engage multiple Bcl-2 homologs, not Bax or Bak. *Science* **315**, 856-9 (2007).
4. Carpenter, E.P., Beis, K., Cameron, A.D. & Iwata, S. Overcoming the challenges of membrane protein crystallography. *Curr Opin Struct Biol* **18**, 581-6 (2008).
5. Willis, S.N. et al. Proapoptotic Bak is sequestered by Mcl-1 and Bcl-xL, but not Bcl-2, until displaced by BH3-only proteins. *Genes Dev* **19**, 1294-305 (2005).

6. Serrano-Vega, M.J., Magnani, F., Shibata, Y. & Tate, C.G. Conformational thermostabilization of the beta1-adrenergic receptor in a detergent-resistant form. *Proc Natl Acad Sci U S A* **105**, 877-82 (2008).

7. Schinzel, A. et al. Conformational control of Bax localization and apoptotic activity by Pro168. *J Cell Biol* **164**, 1021-32 (2004).

8. Suzuki, M., Youle, R.J. & Tjandra, N. Structure of Bax: Coregulation of Dimer Formation and Intracellular Localization. *Cell* **103**, 645-654 (2000).

9. Walensky, L.D. et al. A stapled BID BH3 helix directly binds and activates BAX. *Mol Cell* **24**, 199-210 (2006).

10. Fiser, A. & Sali, A. Modeller: generation and refinement of homology-based protein structure models. *Methods Enzymol* **374**, 461-91 (2003).

11. Mathew, R., Degenhardt, K., Haramaty, L., Karp, C.M. & White, E. Immortalized mouse epithelial cell models to study the role of apoptosis in cancer. *Methods Enzymol* **446**, 77-106 (2008).

Chapter 3

Biochemical Analysis of Full-Length Monomeric BAK

Abstract

The longstanding inability to express full-length BAK as a recombinant protein has precluded a complete biochemical and structural dissection of its activation mechanism. The 'indirect activation model' and 'direct activation model' were proposed to explain BAK and BAX membrane-permeabilization activity. The former postulates that BAX and BAK spontaneously oligomerize as soon as apoptotic inhibition is relieved, whereas the latter suggests that a direct triggering event, most likely by the BH3-only proteins, is necessary to initiate BAK and BAX activation.

I employed FL-BAK to address these unresolved questions. I find that soluble FL-BAK auto-translocates to isolated mitochondria, demonstrating a preference for the membrane environment that is consistent with the relative subcellular distributions of BAX and BAK *in vivo*. Translocation of FL-BAK does not permeabilize the mitochondria unless a BH3-only activator is also present, indicating that a definitive activation step is required either in the form of a direct trigger or inhibition of suppressive protein interactions. I found that the BH3-only protein tBID, or its essential BH3 helix in the form of a stapled BID BH3 peptide, activates and functionally oligomerizes FL-BAK in the absence of any other factors, definitively demonstrating a direct activation mechanism for full-length BAK. I used FL-BAK and a stapled BID BH3 peptide to measure the direct and sequence-dependent interaction between BAK and an activating BH3 helix.

Introduction

The primary function of pro-apoptotic BCL-2 family member proteins BAK and BAX is to execute mitochondrial apoptosis in response to stress stimuli[1-3]. In response to the apoptotic signal, activated BAX and BAK self-associate to form pores in the outer mitochondrial membrane [4,5], resulting in propagation and execution of the cell death cascade by releasing apoptogenic factors, such as cytochrome *c*, from mitochondria, thus triggering an irreversible capase-mediated cell death program.

BAK and BAX activation mechanisms have been the focus of much debate. Two models were proposed: "direct activation" and "indirect activation" [6,7]. The indirect activation model posits that BAK and BAX proteins exist in homeostatically primed forms and as soon as antiapoptotic inhibition is relieved, BAX and BAK proceed to form oligomers[8,9]. However, in the proposed indirect model, the stimulus responsible for the initial BAX and BAK priming is not explained, and only a small fraction of BAX and BAK is bound to antiapoptotic proteins in healthy, non-apoptotic cells[10]. The direct activation model suggests that in addition to preventing anti-apoptotic protein inhibition, a direct triggering interaction, most likely by the BH3-only proteins, is also necessary to activate BAK and BAX[11].

Several studies carefully examined BAX behavior and activation properties, confirming a critical role for direct triggering of BAX in initiating its apoptotic function[12,13]. However, little is known about the direct activation mechanism for BAK, an equally important mediator of cell death. Residing in the mitochondrial outer membrane environment[8], BAK may be one step closer to the activated state, as compared to BAX, which must first translocate from the cytosol to the mitochondrial membrane[14,15]. With FL-BAK in hand, I aimed to interrogate the BAK activation

mechanism and to clearly distinguish between direct and indirect BAK activation mechanisms in driving apoptosis.

Results

FL-BAK automatically translocates to mitochondrial membranes, but does not permeabilize them without an additional stimulus

With recombinant, monomeric FL-BAK in hand, I first sought to evaluate its biochemical behavior in aqueous solution containing isolated *Bak*$^{-/-}$ mouse liver mitochondria (MLM). Whereas recombinant, monomeric BAX requires ligand stimulation for mitochondrial translocation[16], I observed that FL-BAK auto-translocated to MLM in a dose-responsive fashion (Fig. 3.1, *A*). In contrast to ligand-stimulated BAX translocation[12], the auto-translocation of FL-BAK was not accompanied by cytochrome *c* release (Fig. 3.1, *B*). These data highlight the successful production of full-length monomeric BAK, which exhibits a natural preference for partitioning to mitochondria. Strikingly, this translocation is not accompanied by mitochondrial outer membrane permeabilization (MOMP), suggesting that a further activation step is required.

BH3-only activator tBID triggers BAK oligomerization and cytochrome c release from mouse liver mitochondria

I subjected the mixture of FL-BAK and *Bak*$^{-/-}$ MLM to the activator BH3-only protein tBID. I observed reciprocal dose-responsive activation of tBID-induced FL-BAK-mediated cytochrome *c* release, indicative of functionally intact BAK protein (Fig. 3.2, *A* and *B*). I monitored BAK oligomerization by using a chemical crosslinking approach. A small molecule

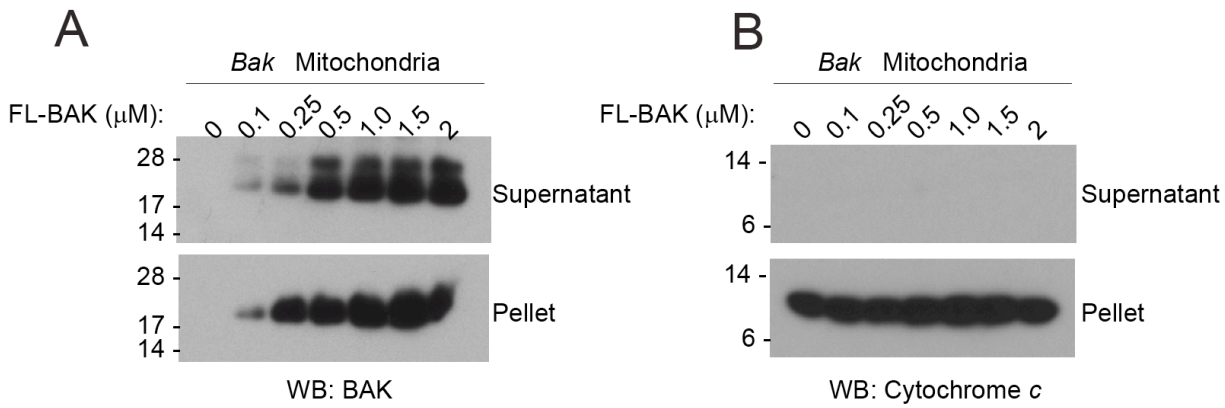

Figure 3.1. FL-BAK displays a natural tropism for the membrane environment.

(*A*) Upon exposure to isolated *Bak*$^{-/-}$ mouse liver mitochondria, FL-BAK dose-responsively translocated to the mitochondria-containing pellet fraction, as detected by anti-BAK western analysis. (*B*) Auto-translocation of FL-BAK to the mitochondrial fraction did not induce cytochrome *c* release from the pellet to the supernatant, as measured by anti-cytochrome *c* western analysis.

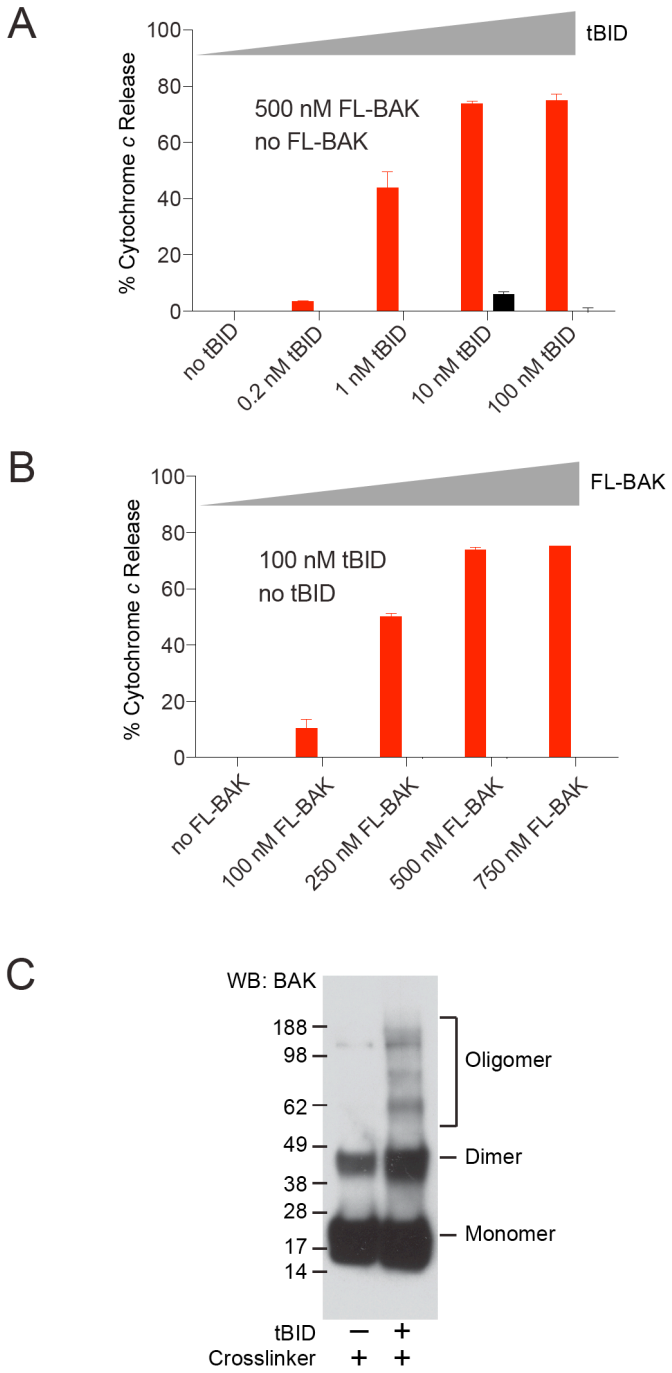

Figure 3.2. BH3-only protein tBID triggers FL-BAK-dependent mitochondrial release. (*A*, *B*) tBID dose-responsively triggered FL-BAK-mediated cytochrome *c* release from isolated *Bak*$^{-/-}$ mitochondria, as measured by cytochrome *c* ELISA. Likewise, FL-BAK dose-responsively induced cytochrome *c* release upon exposure to fixed dose tBID. No release was

Figure 3.2 (Continued).

observed upon exposure of the mitochondria to tBID or FL-BAK alone. Data are mean ± SD for experiments performed in duplicate and repeated at least three times using independent FL-BAK preparations with similar results. (*C*) tBID-induced and FL-BAK-mediated liposomal and mitochondrial release coincides with FL-BAK oligomerization. FL-BAK (500 nM) was incubated with *Bak*$^{-/-}$ mouse liver mitochondria in the presence or absence of tBID (100 nM), followed by a 15 minute incubation with bismaleimidohexane (BMH, 100 mM). After quenching with DTT, the reaction was subjected to SDS-PAGE and anti-BAK western analysis.

bifunctional cross-linker was applied to either a mixture of FL-BAK with tBID or FL-BAK alone in the presence of mitochondrial preparations, and the efficiency of oligomerization was assessed in each case by SDS-PAGE and western blotting. The observed FL-BAK oligomerization correlated with tBID-triggered and FL-BAK-mediated mitochondrial permeabilization (Fig. 3.2, *C*).

Direct activation of FL-BAK by tBID

Whereas the MLM experimental framework does not distinguish between tBID-induced direct activation of FL-BAK vs. derepression of FL-BAK as a result of anti-apoptotic inhibition by tBID, I further employed a reductionist liposomal system to evaluate FL-BAK release activity in the absence of other mitochondrial factors. Whereas incubating ANTS/DPX (fluorophore/quencher)-encapsulated liposomes with tBID or FL-BAK alone yielded little to no release of entrapped fluorophore, the combination of tBID and FL-BAK induced dose- and time-responsive liposomal release (Fig. 3.3, *A*). I confirmed by chemical crosslinking analysis that tBID-induced and FL-BAK-mediated liposomal release was accompanied by oligomerization of FL-BAK (Fig. 3.3, *B*). SEC analysis of the liposomal reaction mixtures further documented conversion of FL-BAK from a monomeric to an oligomeric form upon tBID exposure, with the majority of tBID remaining monomeric, consistent with the proposed "hit and run" mechanism for BH3-induced direct BAX/BAK activation[17] (Fig. 3.3, *C, D*).

The BID BH3 domain is responsible for direct BAK activation

To specifically link the FL-BAK-triggering activity of tBID to its BH3 domain, we generated stabilized alpha-helices of BCL-2 domains (SAHBs) modeled after the BID BH3

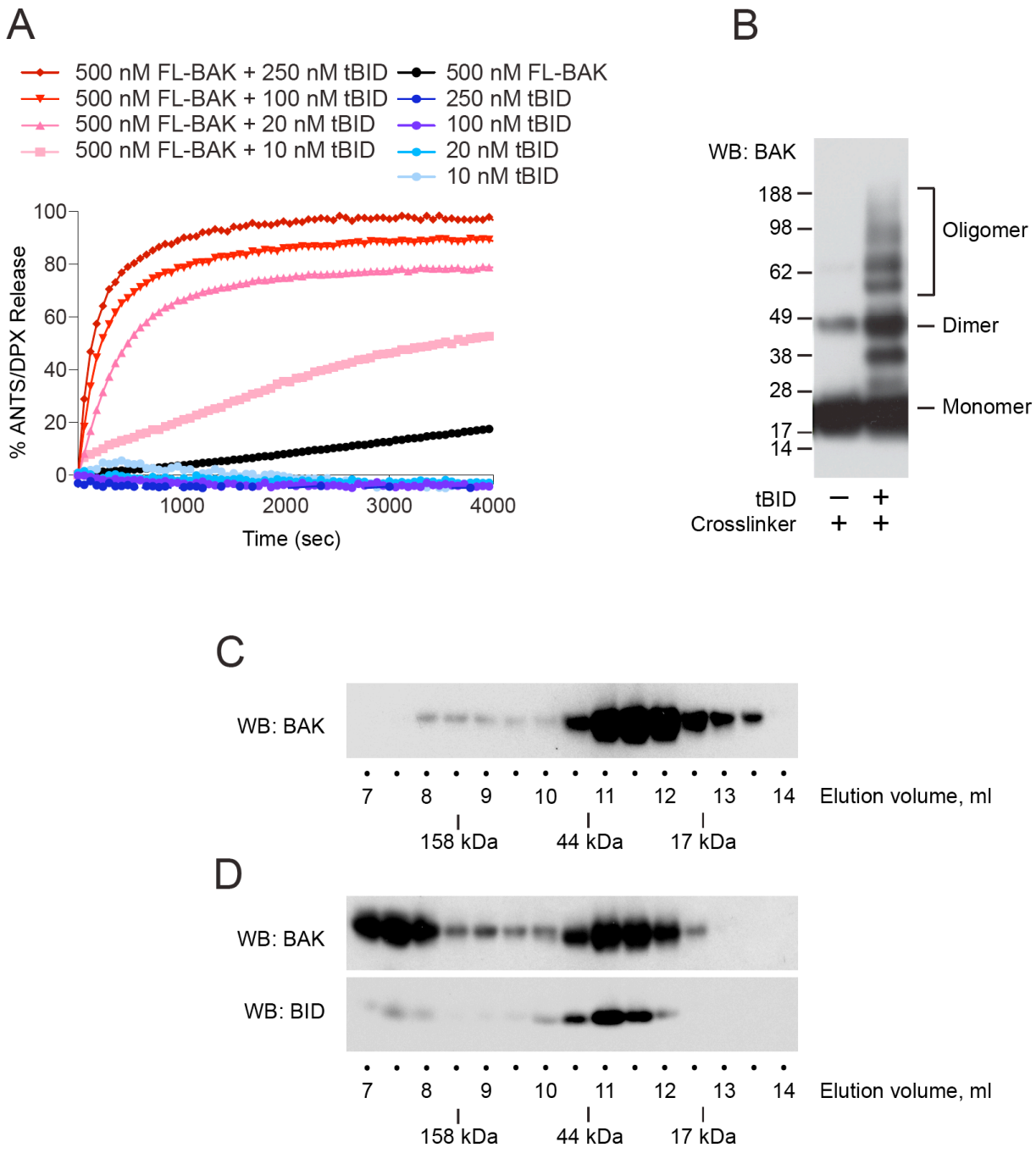

Figure 3.3. tBID triggers FL-BAK-dependent liposomal release. (*A*) tBID dose-responsively induced FL-BAK-mediated liposomal release of entrapped fluorophore, whereas tBID or FL-BAK alone had little to no effect. Data are representative of at least three independent experiments with similar results. (*B*) BAK-mediated liposomal release coincides with BAK

Figure 3.3 (Continued).

oligomerization. FL-BAK (500 nM) was incubated with liposomes in the presence or absence of tBID (100 nM) for 30 minutes, followed by a 15 minute incubation with disuccinimidyl suberate (DSS, 100 mM). After quenching with Tris base, the reaction mixture was subjected to SDS-PAGE and anti-BAK western analysis. (*C – D*) Size exclusion chromatography analysis of tBID-induced conversion of FL-BAK from monomer to oligomer. (*C*) FL-BAK (500 nM) was incubated with liposomes and analyzed by SEC after solubilization with CHAPS (0.5%). SEC fractions were collected, subjected to SDS-PAGE, and analyzed by anti-BAK western blotting. The elution fractions for molecular weight marker proteins (17, 44, and 158 kDa) are indicated. (*D*) The experiment was repeated with the inclusion of tBID (100 nM) and analyzed as above. In the presence of tBID (100 nm), FL-BAK (500 nM) is partially converted from monomer to oligomer after a 30 minute incubation. Of note, tBID predominantly remains in monomeric form, consistent with a "hit and run" mechanism for tBID-induced FL-BAK activation.

helix[12,18] for functional analysis (Fig. 3.4, *A*). We first performed fluorescence polarization (FP) binding analyses using FITC-BID SAHBs and FL-BAK, and, for the first time, detected and quantified the direct interaction between BID BH3 and full-length BAK. Whereas two differentially stapled BID SAHBs engaged FL-BAK with K_D values of 80-95 nM, single G94E point mutagenesis of the α-helical interface abrogated binding activity (Fig. 3.4, *B*). Correspondingly, BID SAHBs dose- and time-responsively activated FL-BAK-mediated liposomal release (Fig. 3.4, *C* and *D*), whereas little to no activity was observed for the point mutant SAHB (Fig. 3.4, *E*). Taken together, these data document that recombinant and monomeric FL-BAK is functionally active and can be induced to porate membranes as a result of direct and measurable interactions with BID BH3.

Summary

Having generated the full-length form of BAK for the first time, we show that it recapitulates BAK's native behavior. BAK translocated to mitochondria without a stimulus, and released cytochrome *c* upon tBID treatment. By employing a liposomal release assay we were able to distinguish between direct and indirect activation of BAK, and definitively conclude that in order to oligomerize and permeabilize lipidic membranes, BAK requires direct triggering, such as by BH3-only proteins.

Methods

SAHB synthesis and characterization

Peptide synthesis, hydrocarbon stapling by olefin metathesis, and derivatization with FITC and biotin were performed according to our established methods[19,20]. All peptides were

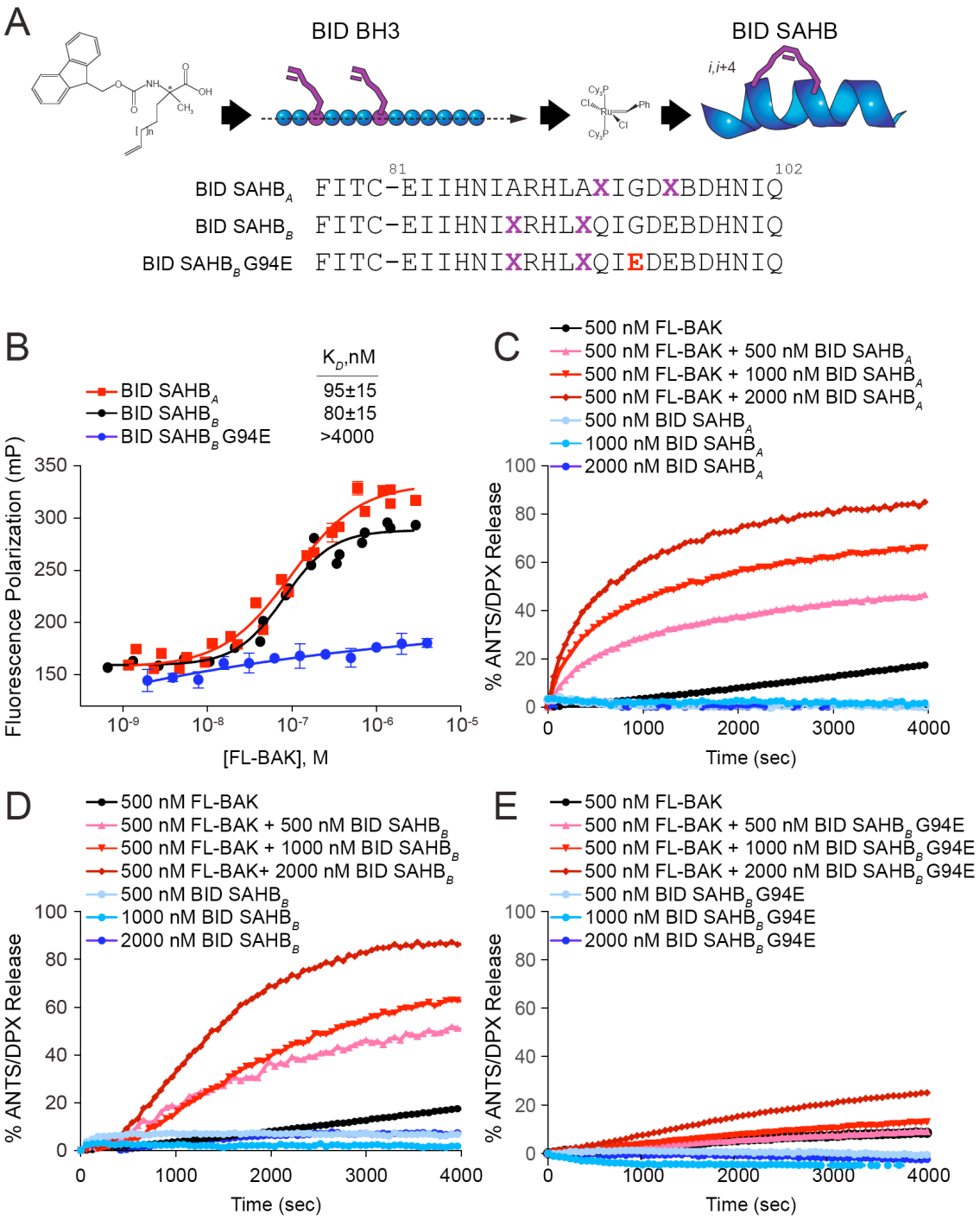

Figure 3.4. BID SAHBs bind to FL-BAK in a sequence-dependent manner and directly trigger FL-BAK activation. (*A*) Stabilized alpha-helix of BCL-2 domains (SAHBs) corresponding to the BH3 motif of BH3-only protein BID were generated by substituting non-

Figure 3.4 (Continued).

natural amino acids bearing olefin tethers at *i, i+4* positions followed by ruthenium-catalyzed olefin metathesis. G94E point mutagenesis of the hydrophobic binding interface yielded a negative control SAHB for biochemical studies. X, non-natural amino acid; B, norleucine (substituted for methionine to avoid thioether-based interference with ruthenium catalysis). (*B*) BID SAHBs A and B bound to FL-BAK with nanomolar affinity, whereas G94E point mutagenesis abrogated the interaction, as measured by fluorescence polarization assay. Data are mean ± SEM for experiments performed in at least duplicate and repeated three times with independent preparations of FL-BAK. (*C* - *E*) BID SAHBs A and B dose-responsively induced FL-BAK-mediated liposomal release of entrapped fluorophore, whereas BID $SAHB_B$ G94E, or BID SAHBs or FL-BAK alone, had little to no effect. Data are representative of at least three independent experiments with similar results.

purified by LC/MS to >95% purity and quantified by amino acid analysis. Photoreactive SAHBs (pSAHBs) were generated as described[21] by incorporating Fmoc-L-p-benzoyphenylalanine (EMD Biosciences) at the indicated locations in the peptide sequence.

Mitochondrial translocation assay

Bak$^{-/-}$ mitochondria were isolated from the livers of *Bak*$^{-/-}$ mice as previously reported[12], resuspended in experimental buffer (125 mM KCl, 10 mM Tris-MOPS [pH 7.4], 5 mM glutamate, 2.5 mM malate, 1 mM KPO4, 10 uM EGTA-Tris [pH 7.4]), and then treated with the indicated concentrations of freshly purified FL-BAK. After 90 min incubation at room temperature followed by tabletop centrifugation at 5500 x g, the supernatant and pellet fractions were separated and subjected to SDS-PAGE and immunoblotting using BAK NT (Millipore) and cytochrome *c* (BD Pharmingen) antibodies.

Mitochondrial cytochrome c release assay

Cytochrome *c* release assays were performed as previously reported[12]. Briefly, *bak*$^{-/-}$ mitochondria were incubated with the indicated concentrations of FL-BAK and tBID for 45 min at room temperature in experimental buffer (see above). The pellet and supernatant fractions were isolated by centrifugation at 3,200 rpm, and cytochrome *c* quantitated using a colorimetric ELISA assay (R&D Systems). Percent cytochrome *c* released into the supernatant (%cytoc_{sup}) from releasable mitochondrial pools was calculated according to the following equation: %cyto$c$=[(cytoc_{sup}-cytoc_{backgr})/(cytoc_{total}-cytoc_{backgr})]*100, where background release represents cytochrome *c* detected in the supernatant of vehicle-treated samples and total release represents cytochrome *c* measured in 1% Triton-X 100 treated samples.

Liposomal release assay

The liposomal release assay was adapted from a previously described method[22]. Large unilamellar vesicles (LUVs) were generated from a lipid mixture containing 48% phosphatidylcholine, 28% phosphatidylethanolamine, 10% phosphatidylinositol, 10% dioleoyl phosphatidylserine and 4% tetraoleoyl cardiolipin (Avanti Polar Lipids). The lipid mixture (1 mg aliquots) was prepared from chloroform stocks and dried as a thin film in glass test tubes under nitrogen gas and then under vacuum for 15 h. The fluorescent dye ANTS (6.3 mg) and the quencher DPX (19.1 mg) were added to 1 mg of dry lipid film, and the mixture resuspended in assay buffer (200 mM KCl, 1 mM $MgCl_2$, 10 mM HEPES, pH 7.0). After five freeze-thaw cycles (liquid nitrogen/water bath), the lipid mixtures were extruded through a 100 nm nucleopore membrane (Whatman) using an Avanti mini extruder, followed by gravity flow SEC using a crosslinked Sepharose CL-2B column (Sigma Aldrich). LUVs (10 ml) were treated with the indicated concentrations of FL-BAK, tBID, and BID SAHBs, singly and in combination, in 96-well format (Corning) in a total reaction volume of 100 ml. Fluorescence was measured from t =0 (F0) to t =2 h, and then Triton X-100 was added to a final concentration of 0.2% (v/v) followed by measurement of fluorescence for an additional 10 min to determine maximal release (F100). Percent ANTS/DPX release was calculated as $((F - F0)/(F100 - F0)) \times 100$.

Fluorescence polarization binding assay

FP assays were performed as previously described[23]. Briefly, FITC-BID SAHBs (15 nM) were incubated with the indicated serial dilution of FL-BAK protein in binding buffer (50 mM Tris, 100 mM NaCl, pH 8.0) until equilibrium was reached. FP was measured using a

SpectraMax M5 microplate reader (Molecular Devices). Dissociation constants (K_D) were calculated by nonlinear regression analysis of dose-response curves using Prism software (GraphPad).

Fractionation of FL-BAK to monitor its oligomerization

FL-BAK (500 nM) was incubated with liposomes in the presence or absence of tBID (100 nM) at room temperature for 30 minutes. Following solubilization by CHAPS (0.5%), the mixture was subjected to size exclusion chromatography (SEC) at 4°C in 20 mM Hepes pH 7.8, 150 mM KCl, 0.5% CHAPS. The fractions were collected, subjected to SDS-PAGE, and then analyzed by western blot using BAK (BAK NT, Millipore) and BID (FL-195, Santa Cruz) antibodies.

Chemical crosslinking analysis of FL-BAK upon tBID-induced liposomal and mitochondrial release

FL-BAK (500 nM) was incubated with liposomes or *Bak*$^{-/-}$ mouse liver mitochondria in the presence or absence of tBID (100 nM) at room temperature for 30 minutes. Disuccinimidyl suberate (DSS) and bismaleimidohexane (BMH) were added to the liposomal and mitochondrial mixtures, respectively, at a final concentration of 100 mM, and incubated for 15 minutes. After quenching the liposomal and mitochondrial crosslinking reactions with 1M Tris base and 50 mM dithiothreitol (DTT), respectively, the mixtures were subjected to SDS-PAGE and anti-BAK western analysis.

Contributions

Elizaveta S. Leshchiner, Gregory H. Bird and Loren D. Walensky contributed to this section of the work. E.S.L. and L.D.W. designed experiments and conducted data analysis. E.S.L. and G.H.B. synthesized and purified staples peptides (SAHBs). E.S.L. performed protein purification, translocation experiments, cytochrome *c* release and liposomal release assays, fluorescence polarization experiments, fractionation, and cross-linking experiments.

References

1. Annis, M.G. et al. Bax forms multispanning monomers that oligomerize to permeabilize membranes during apoptosis. *EMBO J* **24**, 2096-103 (2005).

2. Kiefer, M.C. et al. Modulation of apoptosis by the widely distributed Bcl-2 homologue Bak. *Nature* **374**, 736-9 (1995).

3. Chittenden, T. et al. Induction of apoptosis by the Bcl-2 homologue Bak. *Nature* **374**, 733-6 (1995).

4. Wei, M.C. et al. tBID, a membrane-targeted death ligand, oligomerizes BAK to release cytochrome c. *Genes & Development* **14**, 2060-2071 (2000).

5. Wei, M.C. et al. Proapoptotic BAX and BAK: A Requisite Gateway to Mitochondrial Dysfunction and Death. *Science* **292**, 727-730 (2001).

6. Chipuk, J.E. & Green, D.R. How do BCL-2 proteins induce mitochondrial outer membrane permeabilization? *Trends Cell Biol* **18**, 157-64 (2008).

7. Dewson, G. & Kluck, R.M. Mechanisms by which Bak and Bax permeabilise mitochondria during apoptosis. *J Cell Sci* **122**, 2801-8 (2009).

8. Willis, S.N. et al. Proapoptotic Bak is sequestered by Mcl-1 and Bcl-xL, but not Bcl-2, until displaced by BH3-only proteins. *Genes Dev* **19**, 1294-305 (2005).

9. Willis, S.N. et al. Apoptosis initiated when BH3 ligands engage multiple Bcl-2 homologs, not Bax or Bak. *Science* **315**, 856-9 (2007).

10. Leber, B., Lin, J. & Andrews, D.W. Embedded together: the life and death consequences of interaction of the Bcl-2 family with membranes. *Apoptosis* **12**, 897-911 (2007).

11. Letai, A. et al. Distinct BH3 domains either sensitize or activate mitochondrial apoptosis, serving as prototype cancer therapeutics. *Cancer Cell* **2**, 183-192 (2002).

12. Walensky, L.D. et al. A stapled BID BH3 helix directly binds and activates BAX. *Mol Cell* **24**, 199-210 (2006).

13. Lovell, J.F. et al. Membrane Binding by tBid Initiates an Ordered Series of Events Culminating in Membrane Permeabilization by Bax. *Cell* **135**, 1074-1084 (2008).

14. Hsu, Y.T., Wolter, K.G. & Youle, R.J. Cytosol-to-membrane redistribution of Bax and Bcl-X(L) during apoptosis. *Proc Natl Acad Sci U S A* **94**, 3668-72 (1997).

15. Hsu, Y.T. & Youle, R.J. Bax in murine thymus is a soluble monomeric protein that displays differential detergent-induced conformations. *J Biol Chem* **273**, 10777-83 (1998).

16. Gavathiotis, E., Reyna, D.E., Davis, M.L., Bird, G.H. & Walensky, L.D. BH3-triggered structural reorganization drives the activation of proapoptotic BAX. *Mol Cell* **40**, 481-92 (2010).

17. Wei, M.C. et al. tBID, a membrane-targeted death ligand, oligomerizes BAK to release cytochrome c. *Genes Dev* **14**, 2060-71 (2000).

18. Walensky, L.D. et al. Activation of apoptosis in vivo by a hydrocarbon-stapled BH3 helix. *Science* **305**, 1466-70 (2004).

19. Bird, G.H., Crannell, C.W. & Walensky, L.D. Chemical Synthesis of Hydrocarbon-Stapled Peptides for Protein Interaction Research and Therapeutic Targeting. *Curr Protoc Chem Biol* **3**, 99-117 (2011).

20. Bird, G.H., Bernal, F., Pitter, K. & Walensky, L.D. Synthesis and biophysical characterization of stabilized alpha-helices of BCL-2 domains. *Methods Enzymol* **446**, 369-86 (2008).

21. Braun, C.R. et al. Photoreactive stapled BH3 peptides to dissect the BCL-2 family interactome. *Chem Biol* **17**, 1325-33 (2010).

22. Lovell, J.F. et al. Membrane binding by tBid initiates an ordered series of events culminating in membrane permeabilization by Bax. *Cell* **135**, 1074-84 (2008).

23. Pitter, K., Bernal, F., Labelle, J. & Walensky, L.D. Dissection of the BCL-2 family signaling network with stabilized alpha-helices of BCL-2 domains. *Methods Enzymol* **446**, 387-408 (2008).

Chapter 4

Comparative Structural Analysis of the Activation of Full-Length Proapoptotic BAK and BAX

Abstract

It has been recently shown that BAX is directly activated by BIM BH3 and the binding site was located by NMR spectroscopy[1]. Surprisingly, the triggering BH3-binding site on BAX is found at the opposite side of the protein from the canonical binding pocket of anti-apoptotic proteins. The nature of the binding interaction also differs from that of BH3 engagement of anti-apoptotic proteins, in that the BAX interaction is a transient, hit-and-run phenomenon.

Much less is known about BAK, in part due to the inability to obtain full-length protein for biochemical and structural studies. Not only was a site for BH3 interaction with BAK unknown, but whether BH3-only proteins directly engage BAK to begin with was unknown. With full-length BAK in hand, we were in a position to determine if direct BH3 interactions occur, and if so, where the site of interaction is located. By applying photoreactive BH3 helices and mass spectrometry analysis, we mapped the trigger site for direct BAK activation to its canonical BH3-binding pocket located at the C-terminal face of the protein, whereas the same ligands crosslinked to the N-terminal BH3 trigger site of BAX. Thus, BAK and BAX activation are initiated by direct BH3 interaction, but at distinct trigger sites.

Introduction

The structural conformations of BCL-2 family of proteins have been an intensive focus of cell death research. The interactions between BCL-2 family proteins are mediated by the binding of the BH3 domains of proapoptotic BAK, BAX, and BH3-only proteins to the hydrophobic C-terminal canonical binding pocket, or groove, on antiapoptotic proteins such as MCL-1, BCL-2, BCL-X_L. Structures of antipoptotic proteins complexed with peptides corresponding to BH3 domains of other BCL-2 family members all follow described consistent structural pattern[2-5]. The paradigm for antiapoptotic sequestering of the BH3 helices of activated BAK and BAX has translated into pharmacological disruption of this interaction to reactivate apoptosis in human cancer[6-8].

The interactions of the same BH3-only proteins with BAK and BAX were much more elusive, especially in deciphering between the 'direct' vs. 'indirect' activation models: the indirect activation model implied that BH3-only interactions with BAX and BAK may not occur in the first place.

Structural and biochemical analyses of the interactions between full-length recombinant BAX and a stapled BIM BH3 helix revealed a novel, non-canonical BH3 interaction site at the confluence of BAX α-helices 1 and 6, which has been termed a trigger site for BH3-mediated direct BAX activation[1]. Upon interaction with a triggering BH3 ligand, BAX undergoes a major conformational change that includes allosteric release of its C-terminal helix for mitochondrial translocation and exposure of its BH3 domain, which both propagates BAX activation and results in functional oligomerization within the mitochondrial outer membrane[9].

In contrast to BAX, full-length BAK has been refractory to protein expression and purification[10], precluding the corresponding structural and biochemical studies using fully intact

recombinant protein. Instead, truncated forms of BAK have been used[11-14], documenting BAKΔC dimeric structures with severely occluded canonical pocket[11,12] and the interactions of select BH3 peptides to the canonical pocket region of BAKΔC[13,14].

By employing FL-BAK, we aimed to interrogate its BH3 binding capability and site of activation, and determine whether the N-terminal trigger site found in BAX also exists on BAK, and/or whether the C-terminal canonical pocket plays a role in direct BAK activation.

Results

Photoreactive BID SAHBs localize the canonical BH3 binding pocket of BCL-X_L

We previously developed photoreactive SAHBs (pSAHBs), containing differentially localized benzophenone moieties, as novel tool reagents for covalently trapping protein interactors and explicitly localizing the sites of intercalation by mass spectrometry[15]. pSAHBs are ideally suited for rapid binding site identification in the absence of protein solution or crystal structures. Here, we synthesized and deployed a panel of BID pSAHBs (Fig. 4.1, *A*) to locate the BH3 interaction site on FL-BAK. To validate the binding specificity and utility of BID pSAHBs 1-3, we first conducted crosslinking analysis with anti-apoptotic BCL-X_LΔC, for which definitive structures are known. We found that the differentially-placed benzophenone moieties in each BID pSAHB crosslinked to discrete subregions of the canonical BH3 binding pocket, precisely corresponding to the established structures of BH3 helix/BCL-XLΔC complexes (e.g. PDB ID# 2YJ1, 3FDL, 1BXL, 3PL7) (Fig. 4.1, *B-E*).

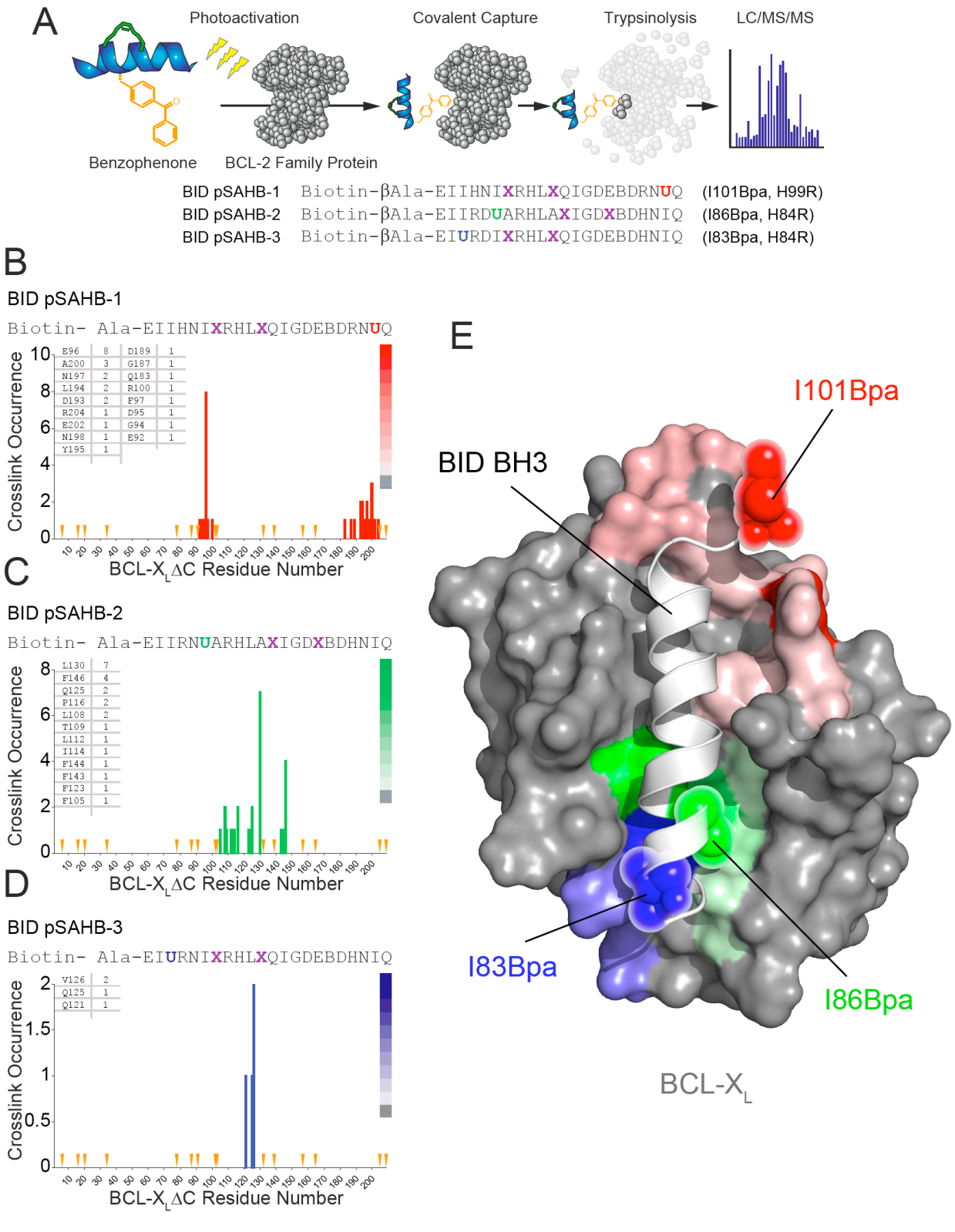

Figure 4.1. Photoreactive BID SAHBs localize BH3 interaction sites with high fidelity.

Figure 4.1. (Continued).

(*A*) Photoreactive stabilized alpha-helix of BCL-2 domains (pSAHBs) modeled after the BH3 domain of BID were generated for protein capture and binding site identification by replacing select native residues with 4-benzoyl-phenylalanine (Bpa), followed by ring closing metathesis of olefinic non-natural amino acids installed at *i, i+4* positions. To facilitate tryptic digestion of pSAHBs into shorter and more identifiable fragments by MS, single arginine substitutions were made as indicated, taking advantage of natural sites of homology between the human and mouse BID BH3 domains (i.e. H84R, H99R).

(*B – D*) BID pSAHBs 1-3 were incubated individually with antiapoptotic BCL-$X_L\Delta C$ and the mixtures subjected to UV irradiation, electrophoresis, excision of the crosslinked protein, trypsin proteolysis, and LC-MS/MS analysis. The plots depict the frequency of crosslinked sites identified across the BCL-$X_L\Delta C$ polypeptide sequence. Orange arrowheads indicate trypsin digestion sites. (*E*) Mapping of BID pSAHB-crosslinked amino acids onto the BCL-$X_L\Delta C$ structure (PDB ID 2BZW) highlighted the capacity of individual pSAHBs to explicitly localize sites of interaction to circumscribed regions along the canonical BH3-binding pocket corresponding to the relative N- to C-terminal disposition of benzophenone residues within the pSAHB sequence. Docking was performed using crystallography and NMR system solve (CNS) within HADDOCK 2.0 [16] and results displayed by PYMOL [17]. The frequency of crosslinking occurrence is reflected on the BCL-$X_L\Delta C$ structure by the color scale for each BID pSAHB (1, red; 2, green; 3, blue).

Photoreactive BID SAHBs localize the BH3 trigger site on BAK

Having validated the fidelity of BID pSAHBs 1-3, we next subjected FL-BAK to the crosslinking analysis. Walking the benzophenone moiety from the C- to N-terminus of BID pSAHB led to sequential crosslinking of discrete residue clusters along the canonical BH3 binding pocket of FL-BAK (Fig. 4.2, *A*-*C*). Interestingly, BID pSAHB-3, which contained the most N-terminal benzophenone substitution also crosslinked to select internal face residues of BAK α9, suggesting that the BID BH3 helix directly displaces the C-terminal helix, whose hydrophobic face becomes exposed for interaction (Fig. 4.2, *C*).

Occlusion of the C-terminal BH3 trigger site by disulfide tethering leads to disruption of BID BH3 binding to BAK

We mutated Leu198 of α9 and Ala128 of α5 to cysteine residues, and converted native cysteines C14 and C154 to serines, in order to generate a FL-BAK construct in which α9 can be reversibly locked into its canonical binding pocket based on redox conditions (Fig. 4.3, *A*). Whereas FITC-BID SAHB$_B$ bound to FL-BAK C14S/A128C/C154S/L198C under reducing conditions (10 mM DTT), no interaction was observed under oxidizing conditions (2 mM GSSG) (Fig. 4.3, *B*). Of note, the reducing and oxidizing conditions had no effect on the interaction between FITC-BID SAHB$_B$ and the parental FL-BAK construct (Fig. 4.3, *C*). Thus, the data suggest that when the canonical BH3-binding pocket is blocked by locking the C-terminus in place, no further binding can occur between BID SAHB and FL-BAK. This result stands in striking contrast to the biochemical- and NMR-based analyses of the interaction between BIM SAHB and BAX, whereby covalent tethering of the BAX C-terminus to its canonical pocket had no disruptive effect on BIM SAHB binding, which was maintained at the α1/α6 trigger site[9].

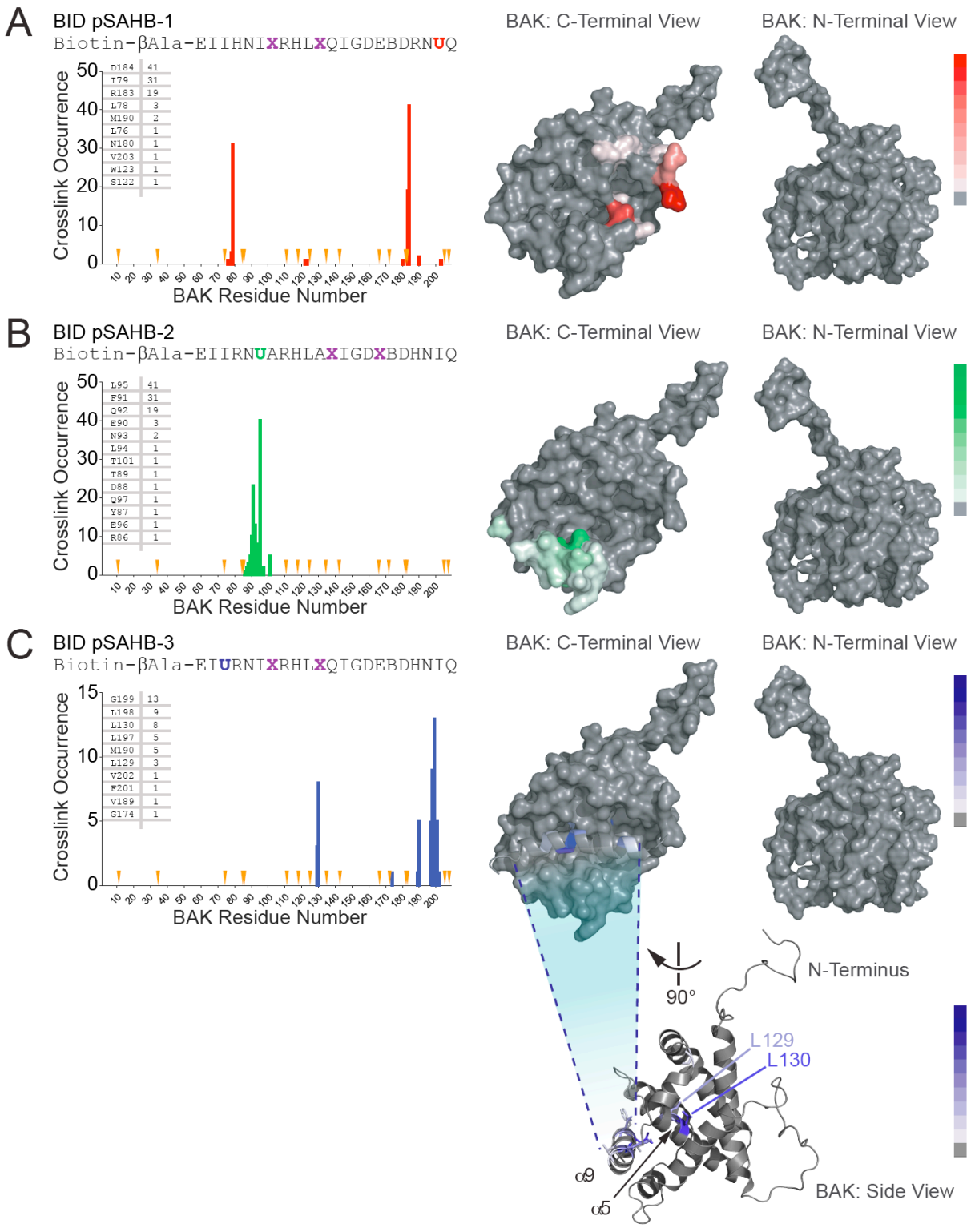

Figure 4.2. Photoreactive BID pSAHBs localize the BH3 trigger site on BAK to its canonical BH3-binding pocket. (*A-C*) BID pSAHBs 1-3 were incubated individually with

Figure 4.2 (Continued).

FL-BAK and the mixtures subjected to UV irradiation, electrophoresis, excision of the crosslinked protein, trypsin proteolysis, and LC-MS/MS analysis. The plots depict the frequency of crosslinked sites identified across the FL-BAK polypeptide sequence, with crosslinked residues mapped onto a calculated model structure of FL-BAK (based on sequence homology to BAX) and colored according to the frequency of occurrence for each pSAHB (1, red; 2, green; 3, blue). For BID pSAHBs 1 and 2, which do not crosslink to residues of the C-terminal helix of FL-BAK, α9 has been removed from the structure to better visualize the crosslinked residues at the surface of the canonical BH3-binding pocket. For BID pSAHB-3, a side view of FL-BAK is also shown in order to demonstrate the localization of crosslinked residues at both the surface of the canonical BH3-binding pocket and the inner surface of α9. The latter dataset highlights that, after α9 displacement, previously unexposed and inward-facing α9 residues become available for interaction with BID pSAHB-3.

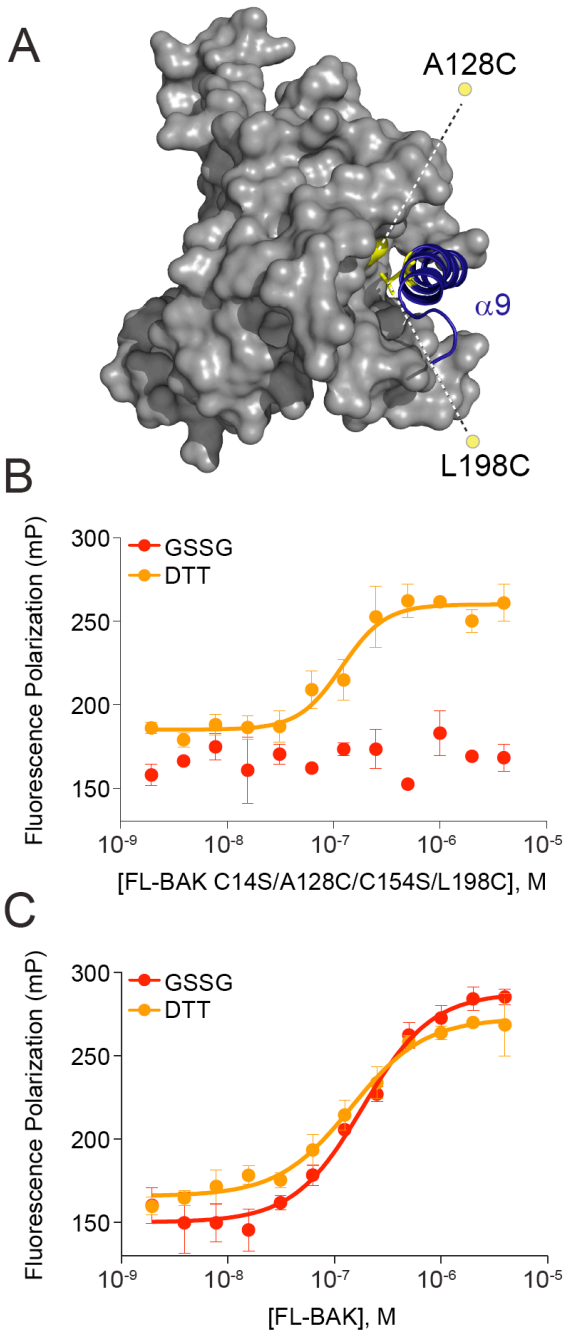

Figure 4.3. The binding interaction between BID SAHB and FL-BAK requires access to the canonical BH3-binding pocket. (*A*) To determine if the BID SAHB/FL-BAK interaction is explicitly dependent on displacement of α9 (blue) and exposure of the canonical pocket, FL-BAK residues A128 of α5 and L198 of α9 were mutated to cysteines (yellow) and native cysteines C14 and C154 were mutated to serines, yielding an α9-tethered FL-BAK construct in

Figure 4.3 (Continued)

which the C-terminal helix is reversibly locked into its binding pocket by redox conditions. (*B*) Oxidized FL-BAK (C14S/A128C/C154S/L198C) (2 mM GSSG) showed no interaction with FITC-BID $SAHB_B$, whereas binding activity was completely restored upon addition of reducing agent (10 mM DTT), as assessed by fluorescence polarization assay. Data are mean ± SEM for experiments performed in at least duplicate and repeated at least two times with independent preparations of FL-BAK (C14S/A128C/C154S/L198C). (*C*) In contrast, redox conditions have no effect on the binding interaction between FITC-BID $SAHB_B$ and FL-BAK. Data are mean ± SEM for experiments performed in at least duplicate and repeated at least two times with independent preparations of FL-BAK.

The BH3 trigger site is identical in soluble and membrane-bound BAK

Importantly, we confirmed that BID pSAHB engagement of the canonical BH3-interaction site likewise occurred in the membrane context. We generated and purified FL-BAK-embedded and ANTS/DPX-loaded liposomes, confirming by proteinase K digestion and anti-BAK western blot that FL-BAK was susceptible to proteolysis and thus surface exposed (Fig. 4.4, *A*). The FL-BAK-containing liposomes preserved membrane integrity, as reflected by release of fluorophore upon Triton X-100 lysis (Fig. 4.4, *B*), and underwent dose-responsive, ligand-triggered release upon exposure to tBID (Fig. 4.4, *C*). Having validated the functional reconstitution of FL-BAK into liposomes, we then incubated the liposomes with BID pSAHB-1 in the presence of UV light and subjected the mixture to our MS-based crosslinking analysis. Although the crosslinking and site-identification method was less efficient in the liposomal context, discrete residues of the FL-BAK canonical pocket were again detected by BID pSAHB-1 photoaffinity labeling (Fig. 4.4, *D*). Thus, we find that whether performed in solution or in the membrane environment, BID SAHB directly engages residues of the canonical BH3-binding groove of FL-BAK.

Activator BID pSAHBs detect distinct trigger sites for BAK and BAX

Because photoactivated benzophenone crosslinking may favor stable over transient BH3 interactions, we sought to further interrogate the BID pSAHB crosslinking results to rule out the possibility of an alternative BH3 interaction site on BAK, as discovered for BAX by NMR analysis[1].

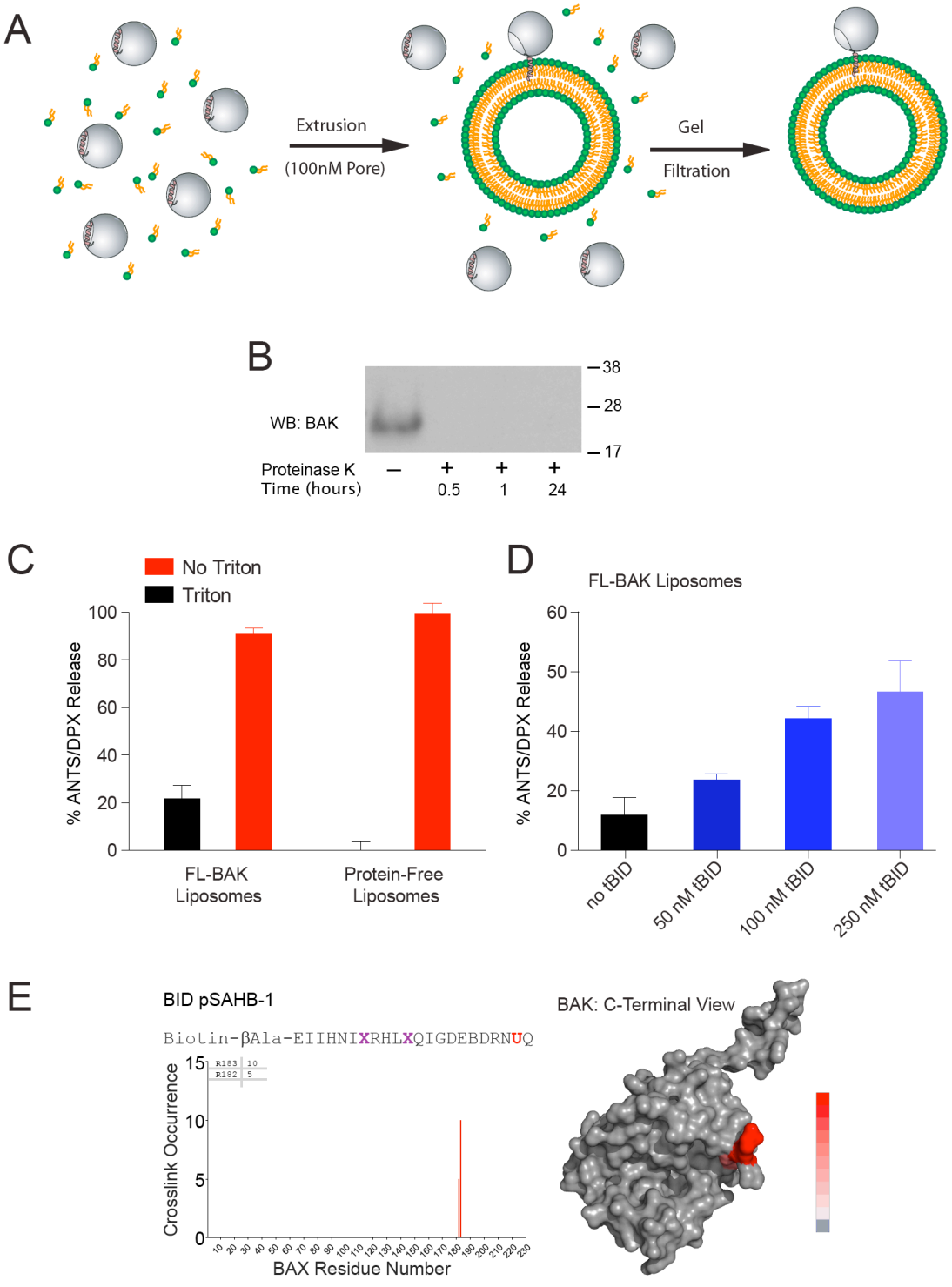

Figure 4.4. BID pSAHB-1 crosslinks to discrete residues of the BH3-binding pocket of membrane-embedded FL-BAK. (*A*) Liposomes generated in the presence of FL-BAK and ANTS/DPX were purified by SEC. (*B*) Incorporation of FL-BAK was documented by anti-BAK

Figure 4.4 (Continued).

western analysis. Upon treatment with proteinase K, FL-BAK was efficiently proteolyzed, consistent with protein exposure at the liposomal surface. (*C*) Protein-free and FL-BAK-embedded liposomes manifested a similar degree of ANTS/DPX release upon lysis with Triton X-100, confirming that FL-BAK liposomes maintain membrane integrity and stably encapsulate ANTS/DPX. Data are mean ± SEM for experiments performed in at least duplicate and are representative of two independent experiments. (*D*) FL-BAK liposomes likewise maintained signaling functionality, as demonstrated by dose-responsive release of ANTS/DPX upon exposure to tBID. Data are mean ± SEM for experiments performed in at least duplicate and are representative of two independent experiments. (*E*) BID pSAHB-1 was incubated with FL-BAK liposomes and the mixture subjected to UV irradiation, solubilization, electrophoresis, excision of the crosslinked protein, trypsin proteolysis, and LC-MS/MS analysis. The plots depict the frequency of crosslinked sites identified across the FL-BAK polypeptide sequence (left), with crosslinked residues mapped onto a calculated model structure of FL-BAK (based on sequence homology to BAX) and colored according to the frequency of occurrence (right). As no crosslinks to residues of the C-terminal helix of FL-BAK were observed, α9 was removed from the structure to better visualize the crosslinked residues at the surface of the canonical BH3-binding pocket. Of note, residues of this same region were crosslinked by BID pSAHB-1 upon incubation with FL-BAK in solution (Fig. 4.2, *A*).

Next, we subjected recombinant full-length BAX to BID pSAHB crosslinking analysis to determine if pSAHBs were capable of detecting the α1/α6 trigger site. Indeed, we find that BID pSAHBs crosslinked to a series of residues located within the previously defined BH3 trigger site at the N-terminal face of BAX (Fig. 4.5, *A* and *B*). Interestingly, BID pSAHB-2 also crosslinked to discrete residues within the canonical BH3 binding pocket of BAX (Fig. 4.5, *B*), suggesting that once triggered at the α1/α6 site, which was previously defined by biochemical and NMR studies as the initiating interaction for BAX activation[9], compatible BH3 binding at the canonical groove upon allosteric release of BAX α9 can also occur.

Another BH3-only activator helix, BIM pSAHB, detects differential binding and trigger sites for BAK and BAX

To document that this paradigm holds for another activator BH3 helix, we generated and applied a BIM pSAHB in crosslinking analyses of both full-length BAK and BAX. Again, we found that BIM pSAHB crosslinked exclusively to residues of the canonical BH3-binding pocket on BAK (Fig. 4.5, *C*), whereas a series of α1, α1-α2 loop, and α6 residues are also crosslinked only in BAX (Fig. 4.5, *D*).

Self-propagating interactions of BAK/BAX BH3 SAHBs are analogous to those of BID and BIM and localize to differential binding pockets on BAK and BAX proteins

Finally, to explore whether the distinct trigger sites for initiating direct activation of BAK/BAX by BID/BIM BH3 helices are also invoked during the self-propagation and/or oligomeric self-association steps of BAK/BAX activation[9,18,19], we generated BAK and BAX

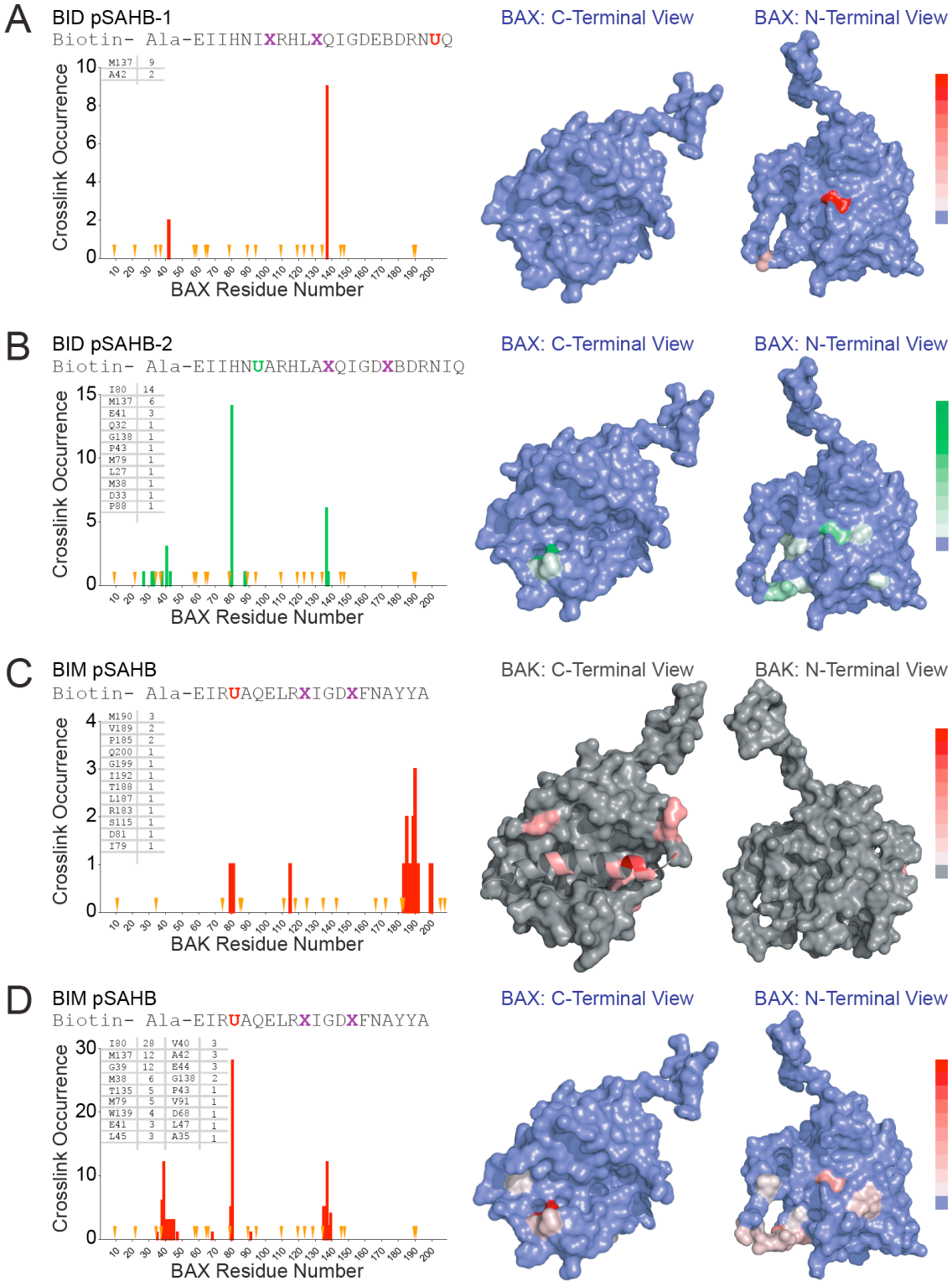

Figure 4.5. BID and BIM pSAHBs crosslink to the α1/α6 trigger site on BAX but not FL-BAK. (*A, B*) In contrast to the results obtained with FL-BAK (Fig. 4.2), BID pSAHBs

Figure 4.5 (Contunued).

crosslinked to a series of BAX surface residues located within the previously defined BH3 trigger site formed by the confluence of α-helices 1 and 6 at the N-terminal face of BAX. BID pSAHB-2 crosslinked to two additional amino acids of the canonical BH3-binding pocket of BAX. The plots depict the frequency of crosslinked sites identified across the BAX polypeptide sequence, with crosslinked residues mapped onto the solution structure of BAX and colored according to the frequency of occurrence for each pSAHB (1, red; 2, green). As BID pSAHB-crosslinks to BAX α9 were not evident, the C-terminal helix was removed from the BAX structure to better visualize the crosslinked residues at the surface of the canonical BH3-binding pocket. (*C, D*) To compare sites of interaction for another direct activator BH3 helix with distinct sequence composition from BID BH3, a BIM pSAHB was employed in crosslinking analysis with FL-BAK and BAX. BIM pSAHB exclusively crosslinked to residues at the C-terminal face of FL-BAK, including amino acids of the canonical BH3-binding pocket and α9 helix, as observed for the corresponding BID pSAHB with an N-terminally located benzophenone moiety (Fig. 4.2, *C*). In contrast, the identical BIM pSAHB construct engaged a host of BAX surface residues at the α1/α6 trigger site on BAX in addition to select residues of the canonical groove. The plots depict the frequency of crosslinked sites identified across the FL-BAK and BAX polypeptide sequences, with crosslinked residues mapped onto the FL-BAK (grey) and BAX (blue) structures and colored according to the frequency of occurrence. As BIM pSAHB-crosslinks to BAX α9 were not evident, the C-terminal helix was removed from the BAX structure to better visualize the crosslinked residues at the surface of the canonical BH3-binding pocket.

pSAHBs for crosslinking analyses. Consistent with the results observed for BID and BIM pSAHBs, BAK and BAX pSAHBs exclusively crosslinked to residues of the canonical BH3-binding pocket of FL-BAK (Fig. 4.6, *A* and *B*), whereas the same pSAHBs either additionally or exclusively crosslinked to residues of the α1/α6 trigger site on BAX (Fig. 4.6, *C* and *D*). Whether or not the identified BAK BH3 in groove interaction reflects a propagation mechanism defined by nucleation of dimers that then oligomerize through a second stable binding interface as previously proposed[20,21], or a linear auto-activation mechanism that ultimately produces a membrane-embedded oligomer of conformationally-altered monomers, remains to be structurally determined. If the former case, the identified crosslinks between BAK SAHB and the canonical pocket of FL-BAK could likewise reflect a stable component of the homo-dimer or homo-oligomer of BAK. Taken together, these data suggest that the initiating step for direct BAK and BAX activation, whether triggered by activator BH3-only domains or propelled by BAK/BAX BH3 domains, employs distinct BH3-binding interfaces on the two pro-apoptotic multidomain proteins – the canonical groove for full-length BAK and the non-canonical α1/α6 site for full-length BAX.

Summary

To define the mechanism of direct BAK activation and the binding modes of activating BH3 domains, we employed a affinity labeling and mass spectrometry approach. We synthesized photoreactive SAHBs (pSAHBs) corresponding to the BH3 domains of BH3-only proteins BID and BIM, and to the BH3 domains of BAK and BAX, which have been hypothesized to participate in BAK and BAX auto-propagation. Using our novel pSAHBs and full-length BAK and BAX constructs, we defined the differential BH3 binding modes of BAK and BAX proteins.

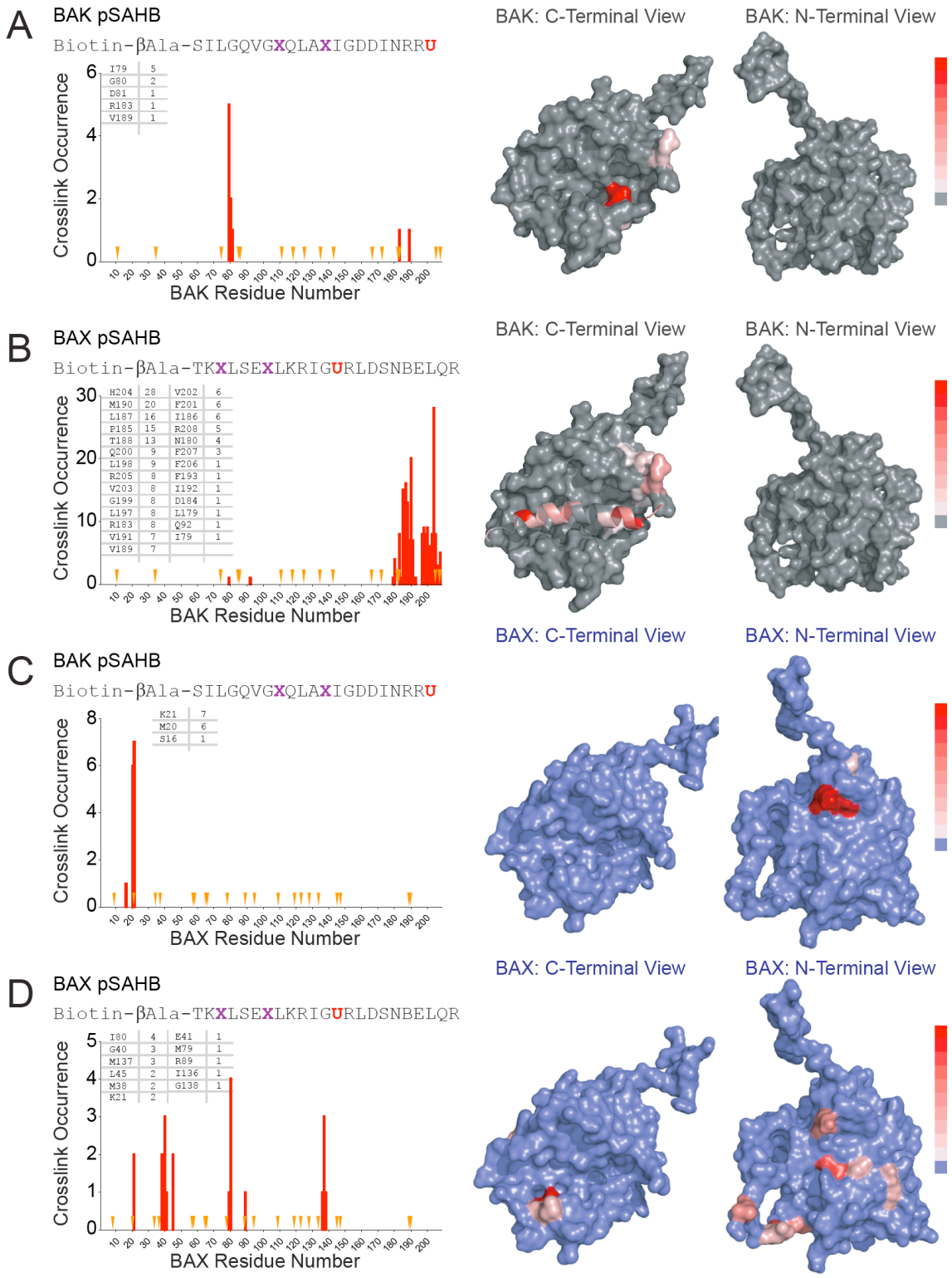

Figure 4.6. The BAK/BAX BH3 helices likewise engage distinct trigger surfaces on FL-BAK and BAX. (*A*, *B*) BAK and BAX pSAHBs were incubated individually with FL-BAK and

Figure 4.6 (Continued).

the mixtures subjected to UV irradiation, electrophoresis, excision of the crosslinked protein, trypsin proteolysis, and LC-MS/MS analysis. The plots depict the frequency of crosslinked sites identified across the FL-BAK polypeptide sequence, with crosslinked residues mapped onto the calculated model structure of FL-BAK structure (grey) and colored according to the frequency of occurrence. As BAK pSAHB-crosslinks to FL-BAK α9 were not identified, the C-terminal helix was removed from the calculated FL-BAK structure to better visualize the crosslinked residues at the surface of the canonical BH3-binding pocket. (*C*, *D*) When exposed to full-length BAX, the identical BAK and BAX pSAHBs crosslinked to a series of residues at the α1/α6 trigger site, with no canonical site crosslinks observed for BAK pSAHB and a select few identified for BAX pSAHB. The plots depict the frequency of crosslinked sites identified across the BAX polypeptide sequence, with crosslinked residues mapped onto the structure of BAX (blue) and colored according to the frequency of occurrence. As pSAHB crosslinks to BAX α9 were not evident, the C-terminal helix was removed from the BAX structure to better visualize the BAX pSAHB-crosslinked residues at the surface of the canonical BH3-binding pocket.

All of the above SAHBs bind BAK exclusively at the C-terminal canonical pocket (also found in antiapoptotic proteins), whereas the initial activation step of BAX is mediated by BH3 engagement of an N-terminal trigger site.

Methods

Photoreactive SAHB Synthesis and Characterization

Photoreactive SAHBs (pSAHBs) were generated as described[15] by incorporating Fmoc-L-p-benzoyphenylalanine (EMD Biosciences) at the indicated locations in the peptide sequence.

Photoaffinity labeling

pSAHBs were mixed with FL-BAK or BAX at a 1:1 ratio (10 mM) in Buffer A (20 mM Tris, 250 mM NaCl, pH 7.6), incubated for 10 min, and then irradiated at 365 nm for 2 hr on ice, in accordance with our previously reported method[15]. Unreacted pSAHBs were removed by dialyzing overnight at 4°C in Buffer B (200 mM NaCl, 50 mM Tris, pH 7.4) using 6-8 MWCO D-tube dialyzers (EMD Biosciences). Biotin capture was accomplished by incubating the reaction mixture with high-capacity streptavidin agarose (Thermo) in Buffer B. Streptavidin beads were washed with 1% SDS in PBS (3x), 1 M NaCl in PBS (3x), and then 10% ethanol in PBS (3x). Biotinylated proteins were eluted by boiling in 10% SDS solution (Promega) containing 10 mg/ml D-biotin, subjected to SDS-PAGE, and then visualized by Coomassie staining (Simply Blue Safestain, Invitrogen). Bands corresponding to crosslinked species were excised, subjected to in-gel digestion with trypsin, and then analyzed by LC-MS/MS (see below).

Mass spectrometry analysis

Mass spectrometry analysis of covalent pSAHB interaction sites was performed as previously described[15]. Excised gel bands were destained, washed by dehydration, reduced with 20 mM DTT in 100 mM ammonium bicarbonate, washed again, and then alkylated by incubation with 10 mM iodoacetamide in the dark. After washing and dehydration with acetonitrile, gel slices were rehydrated overnight in trypsin digestion buffer (12.5 ng/ml sequencing grade modified trypsin [Promega] in 50 mM ammonium bicarbonate). Following digestion, samples were extracted from the gel with 50% acetonitrile/5% formic acid in water, the solvent evaporated by speedvac, and the samples resuspended in 0.5% trifluoroacetic acid in 1M urea followed by desalting using C18 STAGE tips[22]. Samples were then subjected to nano LC-MS/MS using a 20 cm column composed of a 100 mm i.d. fused silica capillary that was flame pulled in-house to produce an approximately 5 mm tip, and packed with Maccel C18 Resin (3m, 200Å, The Nest Group, Inc.). Data was collected on an LTQ Orbitrap Discovery hybrid mass spectrometer (ThermoFisher) operated in data-dependent mode[15]. The MS/MS spectra were assigned by searching with the SEQUEST algorithm[23] against a sequence-reversed database containing BAK, the corresponding mutated BAK sequences, BAX, $BCLX_L\Delta C$, trypsin, and common keratin contaminants. Peptide false detection rates (FDR) were limited to <5% by filtering peptide spectral matches according to their XCorr, mass accuracy, tryptic state, charge state, and peptide length. When filtering for crosslinked species, spectral matches corresponding to multiply crosslinked peptides or crosslinked keratins were considered contaminants and included in the FDR 5% limit. The resultant list of high confidence sites of covalent modification were plotted by frequency of occurrence across the polypeptide sequence.

Generation and characterization of FL-BAK liposomes

ANTS/DPX-loaded liposomes were generated as described in the liposomal assay method, except that FL-BAK (20 μM) was also added to the lipid film (1 mg) mixture in 200 mM KCl, 1 mM $MgCl_2$, 10 mM HEPES, pH 7.0. After extrusion (Avanti extruder) through a 100 nm nucleopore membrane, FL-BAK-containing liposomes were purified by gravity-flow SEC, removing any non-incorporated FL-BAK from the preparation. Proteinase K digestion was performed at room temperature for the indicated durations. tBID treatment and Triton X-100 lysis were performed as described in the liposomal assay method.

Photoaffinity labeling and mass spectrometry analysis of membrane-embedded FL-BAK

Site identification analysis using BID pSAHB-1 was performed as described for FL-BAK in solution except that (1) FL-BAK liposomes were used instead and (2) after UV irradiation, the mixture was incubated with 1% CHAPS to solubilize the FL-BAK liposomes prior to the overnight dialysis step that removes unreacted pSAHB.

Contributions

Elizaveta S. Leshchiner, Craig R. Braun, Gregory H. Bird and Loren D. Walensky contributed to this part of the work. E.S.L. expressed and purified recombinant proteins, conducted crosslinking experiments and analyzed data. C.R.B. conducted mass spectrometry experiments, analyzed data, and performed *in silico* docking. E.S.L., C.R.B. and G.H.B. designed, synthesized, and purified photoreactive SAHBs.

References

1. Gavathiotis, E. et al. BAX activation is initiated at a novel interaction site. *Nature* **455**, 1076-81 (2008).

2. Day, C.L. et al. Solution structure of prosurvival Mcl-1 and characterization of its binding by proapoptotic BH3-only ligands. *J Biol Chem* **280**, 4738-44 (2005).

3. Sattler, M. et al. Structure of Bcl-xL-Bak Peptide Complex: Recognition Between Regulators of Apoptosis. *Science* **275**, 983-986 (1997).

4. Petros, A.M. et al. Rationale for Bcl-xL/Bad peptide complex formation from structure, mutagenesis, and biophysical studies. *Protein Sci* **9**, 2528-34 (2000).

5. Liu, X., Dai, S., Zhu, Y., Marrack, P. & Kappler, J.W. The structure of a Bcl-xL/Bim fragment complex: implications for Bim function. *Immunity* **19**, 341-52 (2003).

6. Walensky, L.D. et al. Activation of apoptosis in vivo by a hydrocarbon-stapled BH3 helix. *Science* **305**, 1466-70 (2004).

7. Oltersdorf, T. et al. An inhibitor of Bcl-2 family proteins induces regression of solid tumours. *Nature* **435**, 677-81 (2005).

8. Nguyen, M. et al. Small molecule obatoclax (GX15-070) antagonizes MCL-1 and overcomes MCL-1-mediated resistance to apoptosis. *Proc Natl Acad Sci U S A* **104**, 19512-7 (2007).

9. Gavathiotis, E., Reyna, D.E., Davis, M.L., Bird, G.H. & Walensky, L.D. BH3-triggered structural reorganization drives the activation of proapoptotic BAX. *Mol Cell* **40**, 481-92 (2010).

10. Willis, S.N. et al. Apoptosis initiated when BH3 ligands engage multiple Bcl-2 homologs, not Bax or Bak. *Science* **315**, 856-9 (2007).

11. Wang, H. et al. Novel dimerization mode of the human Bcl-2 family protein Bak, a mitochondrial apoptosis regulator. *J Struct Biol* **166**, 32-7 (2009).

12. Moldoveanu, T. et al. The X-ray structure of a BAK homodimer reveals an inhibitory zinc binding site. *Mol Cell* **24**, 677-88 (2006).

13. Dai, H. et al. Transient binding of an activator BH3 domain to the Bak BH3-binding groove initiates Bak oligomerization. *J Cell Biol* **194**, 39-48 (2011).

14. Du, H. et al. BH3 domains other than Bim and Bid can directly activate Bax/Bak. *J Biol Chem* **286**, 491-501 (2011).

15. Braun, C.R. et al. Photoreactive stapled BH3 peptides to dissect the BCL-2 family interactome. *Chem Biol* **17**, 1325-33 (2010).

16. de Vries, S.J., van Dijk, M. & Bonvin, A.M. The HADDOCK web server for data-driven biomolecular docking. *Nat Protoc* **5**, 883-97 (2010).

17. DeLano, W.L. *The PyMOL Molecular Graphics System*, (DeLano Scientific, San Carlos, 2002).

18. Llambi, F. et al. A unified model of mammalian BCL-2 protein family interactions at the mitochondria. *Mol Cell* **44**, 517-31 (2011).

19. Tan, C. et al. Auto-activation of the apoptosis protein Bax increases mitochondrial membrane permeability and is inhibited by Bcl-2. *J Biol Chem* **281**, 14764-75 (2006).

20. Dewson, G. et al. Bak activation for apoptosis involves oligomerization of dimers via their alpha6 helices. *Mol Cell* **36**, 696-703 (2009).

21. Dewson, G. et al. To trigger apoptosis, Bak exposes its BH3 domain and homodimerizes via BH3:groove interactions. *Mol Cell* **30**, 369-80 (2008).

22. Rappsilber, J., Mann, M. & Ishihama, Y. Protocol for micro-purification, enrichment, pre-fractionation and storage of peptides for proteomics using StageTips. *Nat Protoc* **2**, 1896-906 (2007).

23. Eng, J.K., McCormack, A.L. & Yates, J.R. An approach to correlate tandem mass spectral data of peptides with amino acid sequences in a protein database *J Am Soc Mass Spectrom* **5**, 976-989 (1994).

Chapter 5

Discussion and Future Directions

Discussion

The oligomerization of BAK and BAX in the mitochondrial outer membrane is one of the ultimate control points for mitochondrial apoptosis[1]. As such, the mechanisms that underlie BAK/BAX regulation and channel formation remain a high-priority research focus of the cell death field. The production of recombinant BCL-2 family proteins has been an essential step for both dissection of their biochemical functions and for translation of these insights into potential therapies to modulate cell death in human disease. For example, bacterial expression and purification of anti-apoptotic BCL-X_L, with the C-terminus removed and an unstructured loop trimmed, led to a fundamental understanding of how BCL-2 survival proteins trap the BH3 helices of pro-apoptotic proteins to block cell death[2,3] and provided a blueprint for the development of ABT-263, the first selective BCL-2/BCL-X_L inhibitor to advance to clinical testing in cancer[4-6]. Owing to the membrane-based activity of many BCL-2 family members, which is facilitated by a hydrophobic infrastructure including a C-terminal membrane insertion helix, the production of sufficient soluble, full-length, and monomeric recombinant protein for biochemical and structural analyses has been a longstanding challenge. Given the importance of the C-termini of BCL-2 family proteins in protein structural integrity, membrane trafficking, and functional insertion into a membrane[7-10], analysis of full-length constructs is highly preferred. For example, our understanding of the functional dynamics of BCL-w and BAX has been greatly advanced by the structural and biochemical analysis of the corresponding full-length proteins[8,10-13]. Whereas the cytosolic disposition of select multidomain BCL-2 family proteins has favored bacterial expression and purification of full-length monomeric protein, expression of membrane-localized members have been especially refractory.

To overcome the longstanding challenge of producing full-length, monomeric BAK, we undertook a surface mutagenesis approach to minimally hydrophilize its hydrophobic C-terminus. In doing so, we developed the first full-length BAK construct amenable to bacterial expression, affinity chromatography, and FPLC-based purification in monomeric form[14]. Interrogation of this recombinant FL-BAK has led to a number of novel insights. First, in contrast to full-length recombinant BAX, soluble FL-BAK auto-translocates to isolated mitochondria, demonstrating a differential membrane tropism that is consistent with the relative subcellular distributions of BAX and BAK *in vivo*. Potential differences in affinity of the BAX and BAK C-terminal α9 helices for their respective binding pockets, leading to distinct propensities to release α9 for membrane insertion, could account for this phenomenon. Second, translocation of FL-BAK, in and of itself, does not permeabilize the mitochondria, indicating that a definitive activation step is required either in the form of a direct trigger or inhibition of suppressive heterotypic protein interactions. Third, the combined use of FL-BAK and BID SAHB enabled the quantitation of a direct and sequence-dependent interaction between BAK and an activator BH3 helix. The BH3-only protein tBID or its essential BH3 helix in the form of BID SAHB, activates and functionally oligomerizes FL-BAK in the absence of any other factors, definitively validating a direct activation mechanism for BAK. Fourth, biochemical occlusion of the canonical BH3-binding pocket by disulfide tethering of the BAK C-terminal helix, abrogates the binding interaction between BID SAHB and FL-BAK, suggesting that, in contrast to BAX, the primary site for initiating direct BAK activation lies at the C-terminal face of the protein. Finally, with full-length BAK and BAX in hand, combined with the application of photoreactive SAHBs, we were able to perform the first comparative structural mapping of BH3 binding sites

on these essential executioner proteins, revealing distinct trigger sites for initiating and propelling their activation.

Installation of photoreactive benzophenone moieties along the sequence of BH3 peptide helices enables an unbiased analysis of covalent intercalation sites on a target protein using proteomic methods[15]. The capacity to rapidly and accurately map binding interfaces with this combined chemical biology and MS/MS strategy provides an alternative and complementary approach to bridging the often multi-year gap until such interfaces are characterized by definitive structural methods such as NMR or X-ray crystallography. In this case, the application of BH3-only direct activator helices[8,16-18] (BID, BIM, BAK and BAX pSAHBs) all pointed to an exclusive site of direct FL-BAK interaction at its canonical binding groove. In striking contrast, the same pSAHBs consistently crosslinked to a distinct BH3-binding site localized to the opposite side of the full-length BAX protein, previously characterized by a battery of NMR and biochemical analyses as the trigger site for direct BAX activation[16]. Thus, to initiate BAK and BAX activation, membrane-localized BAK and cytosolic BAX employ distinct triggering surfaces. Interestingly, a subset of activator pSAHBs showed dual crosslinking to both the N-terminal trigger ($\alpha1/\alpha6$) and C-terminal canonical BH3-binding sites on BAX, suggesting that once triggered at the N-terminus, release of the BAX C-terminus exposes a second BH3-compatible binding interface at the canonical groove. Indeed, this concept of sequential BH3-only binding interactions to drive BAX activation is supported by a prior stepwise analysis of tBID-induced BAX oligomerization[19]. Taken together, our data suggest that activator BH3-engagement at the canonical pocket in the context of the mitochondrial outer membrane may represent a common mechanism for maintaining BAK and BAX in an activation-competent

state, with the α1/α6 triggering mechanism of BAX representing a unique afferent step required to regulate the activation and mitochondrial translocation of cytosolic BAX (Figure 5.1).

Future directions

BAX/BAK oligomeric pore structure

The functional endpoint of BAK and BAX activation is membrane integration in the form of oligomeric pores, critical structures that remain to be defined. Indeed, the development of full-length forms of BCL-2 family members, such as BAK, is an essential step to advancing our structural and biochemical understanding of the protein interaction dynamics that dictate their pro-apoptotic function in the membrane environment.

The final structure of the apoptotic pore in the outer mitochondrial membrane has been elusive due to notorious difficulties associated with production, purification and structural characterization of BCL-2 family proteins. Intrinsic properties allow these proteins to (1) either exist in the membrane environment (BAK) or shuttle between cytoplasm and the mitochondrial membrane (BAX), perhaps reversibly[20]; (2) undergo dramatic conformational changes that involve the exposure of the protein hydrophobic core ; and (3) self-propagate and oligomerize. Importantly, the oligomeric pore of BAX/BAK has been reported to continuously propagate in size, resembling a chain reaction with more and more molecules of BAX recruited to the pore, making it challenging to isolate a single species of BAX/BAK oligomer[21]. Lipids are also an important part of the pore; proteinaceous, toroidal lipidic pores have been attributed to BAX/BAK oligomers, as opposed to clearly defined protein channels[22]. All of these technical challenges have prevented definitive structural determination of the BAX/BAK pore, which remains a high priority goal for the field.

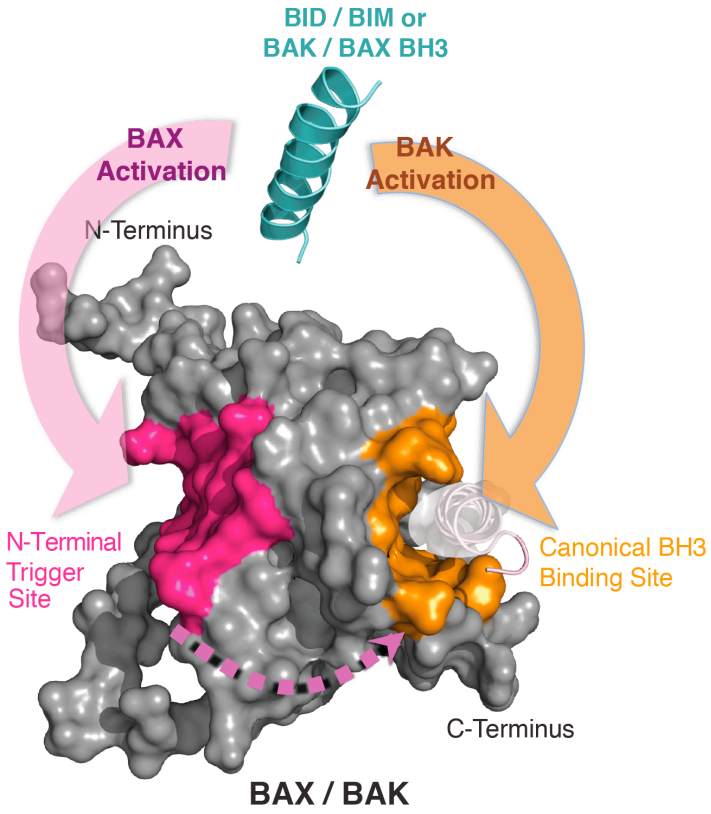

Figure 5.1. Differential BH3 binding modes initiate the direct activation of full-length BAK and BAX. We interrogated the initiation site for BH3-mediated direct activation of BAK and BAX by employing a series of photoreactive activator BH3 helices. The BID, BIM, BAK and BAX BH3 helices engaged the α1/α6 trigger site on BAX but only the canonical BH3-binding pocket on BAK. Thus, activation of the full-length forms of both BAK and BAX are initiated by direct BH3 interaction, but at distinct trigger sites.

Dewson et al. undertook an extensive mutagenesis approach to study BAK oligomerization in cells[23]. Their study revealed that, during apoptosis, BH3 domains of BAK become temporarily exposed and then reburied in dimers or oligomers, which was detected by a conformation-specific anti-BH3 antibody. Chemical crosslinking by small molecule agents that oxidize cysteines to disulfides (e.g. CuPhe) were most efficient when cysteines were installed in the BH3 domain and hydrophobic pocket of BAK, suggesting a direct interface of interaction at some stage of BAK oligomerization. Additionally, a designed BH3 mutation in BAK BH3 rescued, albeit partially, a loss-of-function hydrophobic groove mutant of BAK.

Analogous studies on the opposite side of BAK, close to its N-terminus, revealed that BH3:groove dimers can oligomerize by forming a second interface at the α6 surface of neighboring BAK molecules[24]. Cysteine residues introduced in α6 could be crosslinked upon apoptotic stimulation once the BH3:groove dimer was formed, leading to the conclusion that BAK oligomers are composed of symmetrical BAK dimers, as schematically depicted in Figure 5.2, *A*. Furthermore, at least 18 BAK molecules are required to compose an oligomeric pore, althoughthe definitive size of the physiologic BAK oligomeric pore has not been defined. This induced cysteine crosslinking approach provided an explaination for how N-terminal α1/α6 exposure of BAK during apoptosis could contribute to BAK oligomerization. However, how the pore lumen is formed was not resolved. If the toroidal pore model is correct, then at least some parts of the BAK protein must be submerged in the lipidic bilayer, completely distorting the inactive BAK structure. Thus, the oligomer of dimers model may be a transient state during BAK oligomerization. Analogously, BAX was proposed to form a similar dimeric structure upon activation. Two BAX molecules inserting their BH3 domain into each other's canonical binding

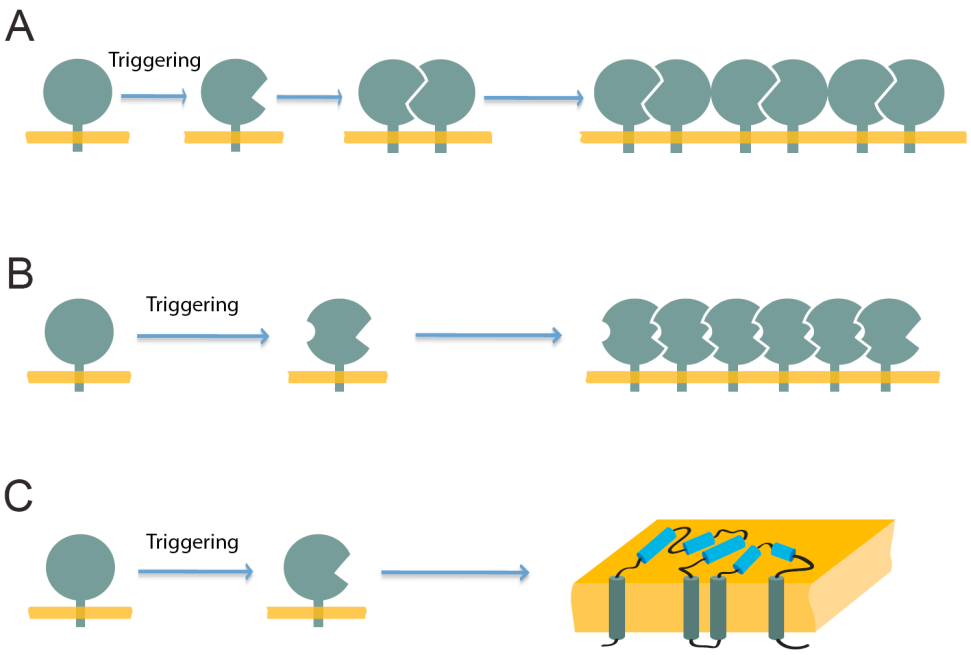

Figure 5.2. Alternative models for proapoptotic BAK and BAX oligomeric structures. (*A*) The "oligomer of dimers" model postulates that BH3:groove dimers are the fundamental unit of oligomeric pore formation. (*B*) Oligomeric chains of single conformers may alternatively comprise the pore structure of BAK and BAX. (*C*) Dramatic conformational changes accompany BAK and BAX oligomerization, including exposure of the BAK and BAX hydrophobic core and permeabilization of the lipidic bilayer.

groove form a symmetric dimer, which was proposed to also nucleate formation of the oligomeric pore[25,26].

An alternative view for BAK oligomerization was proposed by Pang et al[27]. By using molecular dynamics simulations, BAK was proposed to form asymmetric single-conformer oligomeric chains (Figure 5.2, *B*), as opposed to the "oligomer of dimers" model. Other observations may suggest yet another mechanism. All of the above models assume that the structure of BAX/BAK molecules in the final oligomeric pores is similar to the initial monomeric structures. However, these proteins possess a highly hydrophobic core, which may become exposed to the membrane environment during BAX/BAK conformational changes. This would promote a very dramatic conformational change in the monomeric unit structure in the pore as compared to the initial structure of BAK/BAX, consistent with protein unfolding in the membrane environment (Figure 5.2, *C*)[28].

New insights continue to emerge from strutcural analyses of BAX and BAK. In 2013, the first crystal structure representing a dimeric form of BAX was reported[26]. Even though severely truncated (only helices α2-α5 were included, which represents less than half of the protein sequence), the structural data suggestthat the canonical pocket interaction may be important in BAX dimerization and potentially oligomerization.

With full-length BAX and now BAK in hand, we are poised to generate more definitive structural data on BAK and BAX, and how they self-associate to form pores.

Development of new pharmacologic agents targeting pro-apoptotic BCL-2 family members

Cancer cells often hijack the apoptosis pathway mediated by the BCL-2 family of proteins by pathologically overexpressing antiapoptotic proteins. The structures of antiapoptotic BCL-2 family proteins and their complexes with BH3 peptides stimulated major efforts to develop inhibitors of antiapoptotic proteins capable of restoring cell sensitivity to apoptotic stimuli. Several small molecules[4-6] and stapled peptides[29,30] have since been developed that indirectly activate the mitochondrial apoptosis by binding to and inhibiting the hydrophobic binding groove of antiapoptotic proteins, reducing the antiapoptotic blockade. Some of these compounds are already being tested in clinical trials as promising next-generation cancer therapeutics[6].

Recently, a novel approach was undertaken to develop small molecule BAX activators. These novel pharmacologic agents employ a different strategy: instead of stimulating apoptosis indirectly via inhibition of antiapoptotic proteins, BAX activators directly bind to and activate BAX[31]. Our characterization of the differential trigger sites for BAK and BAX[14] allows for extension of the development of selective pharmacologic agents for BAK activation.

Whereas BAX/BAK activation promotes apoptosis, inhibition of BAX/BAK oligomerization and mitochondrial poration would potentially lead to inhibition of apoptosis and could hypothetically be used in diseases of acute cell death. Importantly, several findings have provided evidence that other forms of cell death, including necrosis, are also dependent on BAK and BAX[32,33]. This suggests that acute inhibition of BAX/BAK may be beneficial as a therapeutic strategy to prevent tissue loss at the earliest stages of myocardial infarction or stroke. Several BAX channel inhibitors have also been described[34]. The therapeutic potential of this entirely new class of agents, directed at activating or inhibiting BAX/BAK, represents an exciting drug development frontier.

Dissecting the BCL-2 family interactome

In addition to the essential roles of BCL-2 family proteins in regulating apoptosis, non-canonical functions have also been described. For example, unanticipated roles for BCL-2 family members (and BH3-only proteins in particular) in autophagy[35], the DNA damage response[36,37], glucose homeostasis[38,39], cell cycle progression[40] and calcium signaling have been reported[41,42].

With new chemical biology and proteomic tools in hand, we aim to advance a systematic study of the BCL-2 family interactome. Proteomic approaches such as immunoprecipitation of a tagged protein bait followed by mass spectrometry-based identification of bound targets has been widely used to search for novel protein interactions, and could be applied to BCL-2 family proteins. However, a major impediment to performing such screens in high-throughput fashion is the necessity to validate large sets of hits individually. Correct mass spectrometry identification of the protein target, confirmation of direct binding, and uncovering the functional consequences of interaction, represent a complex and time-consuming workflow. We propose to use stabilized peptides (SAHBs) corresponding to the BH3 domains of the BCL-2 family proteins as the first-pass validation screen, after an initial set of binding partners has been identified by direct protein immunoprecipitation. The benefits of using stapled peptides are four-fold. First, the native shape of the BH3 domain is preserved, maintaining a physiologically relevant bait. Second, SAHBs can be modified to include a biotin tag (for straptavidin pull-down), which provides an orthogonal means of identifying high-confidence targets, as non-specific binding to antibody-containing beads and streptavidin beads should not fully overlap. By filtering against non-specific binders under harsh conditions in both experimental setups, confident in the derived hits would be

increased. Third, use of photoreactive SAHBs, or pSAHBs, allows for covalent capture of the binding partners from cellular lysates upon UV irradiation, enabling detection of direct interaction partners in a high-throughput manner. Finally, an additional benefit of using pSAHBs is the structural determination of the binding site that can follow immediately after binding partner identification, provided that at least some structural information is available on theidentified 'hit' protein. The ability to quickly determine any structural information for the newly proposed interaction is crucial to validating the binding mechanism, designing expeirments to probe the functional consequences, and advancing pharmacologic approaches for targeting the protein interaction for potential therapeutic benefit. Piloting the approach BAK protein and BAK BH3 SAHBs, I can accurately detect known BAK interactors. For example, BCL-2 family interactors such as MCL-1 were detected in BAK SAHB immunoprecipitations but not in vehicle controls. These data highlight the promise of the proposed multi-step approach, with sequential verification of the obtained hits under stringent conditions.

By extensively studying tBID-mediated BAK and BAX activation in the course of this thesis work, I became increasingly interested in some of the unique properties of the BID protein. Structurally, BID more closely resembles the structure of multidomain than BH3-only proapoptotic proteins. In particular, BID contains the classical fold of multidomain BCL-2 family members: two hydrophobic helices at the core (α5 and α6) surrounded by several amphipathic helices[43]. In contrast, the majority of BH3-only proteins are unstructured, with the exception of their BH3 domain α-helices, some of which take shape only when bound to their protein targets. Interestingly, BID has been implicated in cellular processes other than apoptosis. For example, BID is believed to participate in the DNA damage response[36,37] (although

conflicting reports exist[44]) and also serves as a component of the inflammasome complex[45], potentiating innate immune signaling.

I observed that *Bid*$^{-/-}$ mouse embryonic fibrosblasts (MEFs) grow significantly more slowly when compared to wild-type MEFs (data not shown), suggesting a potential role for BID in cellular processes other than apoptosis. I set out to perform proteomics-based identification of BID binding targets using the methodology described above. Because overexpressing BID is cytotoxic, we instead conjugated recombinant BID protein to biotin. By measuring optical absorbance spectra, I quantified the number of biotin molecules attached to each BID protein molecule, and the yield was approximately 2 biotin moieties per molecule of BID protein. I incubated the biotinylated BID protein with streptavidin beads to generate BID-coated beads, which were then used to perform affinity capture from cellular lysates. After mass spectrometry-based identification of protein targets, a similar procedure was performed for BID SAHB, and the lists of hits were compared.

Importantly, I detected BID protein and BID SAHB interactions with select BCL-2 family proteins (e.g., BAX, BAK, MCL-1), as well as non-canonical interaction partners that have been described previously (e.g., ATM, ATR). Additionally, I detected several novel, unexpected targets, which I am currently validating experimentally. BID could potentially regulate or be regulated by[46] some of the identified protein targets. We further plan to extend the studies of BAK and BID interaction partners to include photoreactive crosslinker (pSAHBs) analyses. In a sequential validation step, I will perform reverse immunoprecipitations to validate the presence and abundance of the candidate protein interaction. I will create a cumulative confidence score based on the number of peptides detected in the mass spectrometry experiments, normalized to the molecular mass of the corresponding protein hit and to its

abundance in the cellular proteome (e.g. http://pax-db.org/#!home). Biological validation of novel protein interactions remains a critical step of this type of BCL-2 family interactome analysis.

Non-canonical pathways for direct BAX/BAK activation

Several studies have suggested the involvement of non-canonical regulation of mitochondrial apoptosis. One striking example involves the p53 protein, which inducescell cycle arrest and transcriptional upregulation of key apoptotic genes in response to discrete stimuli, such as DNA damage. A direct role for p53 in outer mitochondrial membrane permeabilization has also been described, involving BAX- [47] and BAK-dependent[48] mechanisms[49]. Thus, tumor suppressor pathways may engage the BAX/BAK machinery directly.

Studies undertaken by Keren Hilgendorf and Jacqueline Lees at MIT investigated a role for the retinoblastoma protein (pRB) in activating mitochondrial apoptosis. pRB has previously been detected outside of the nucleus, in both the cytoplasm[50,51] and mitochondria[52], although the function of pRB at these sites is unknown. Lees and colleagues observed that inducible expression of pRB in MEFs significantly increased TNF-α-induced apoptosis (personal communication). This apoptosis enhancement was only observed in wild-type and $Bak^{-/-}$ pRB-expressing MEFs, but not in $Bax^{-/-}$ or $Bak^{-/-}Bax^{-/-}$ (DKO) MEFs, suggesting a role for BAX in this process.

To explore a functional connection between BAX and pRB, we isolated liver mitochondria from $Alb\text{-}cre^{pos}Bax^{f/-}Bak^{-/-}$ mice. When incubated with recombinant BAX protein, pRB induced cytochrome *c* release, as documented by western blotting for cytochrome *c* in the supernatant and pellet (mitochondrial) fractions (Figure 5.3, *A*). This mitochondrial permeabilization was both dose-dependent and BAX-dependent.

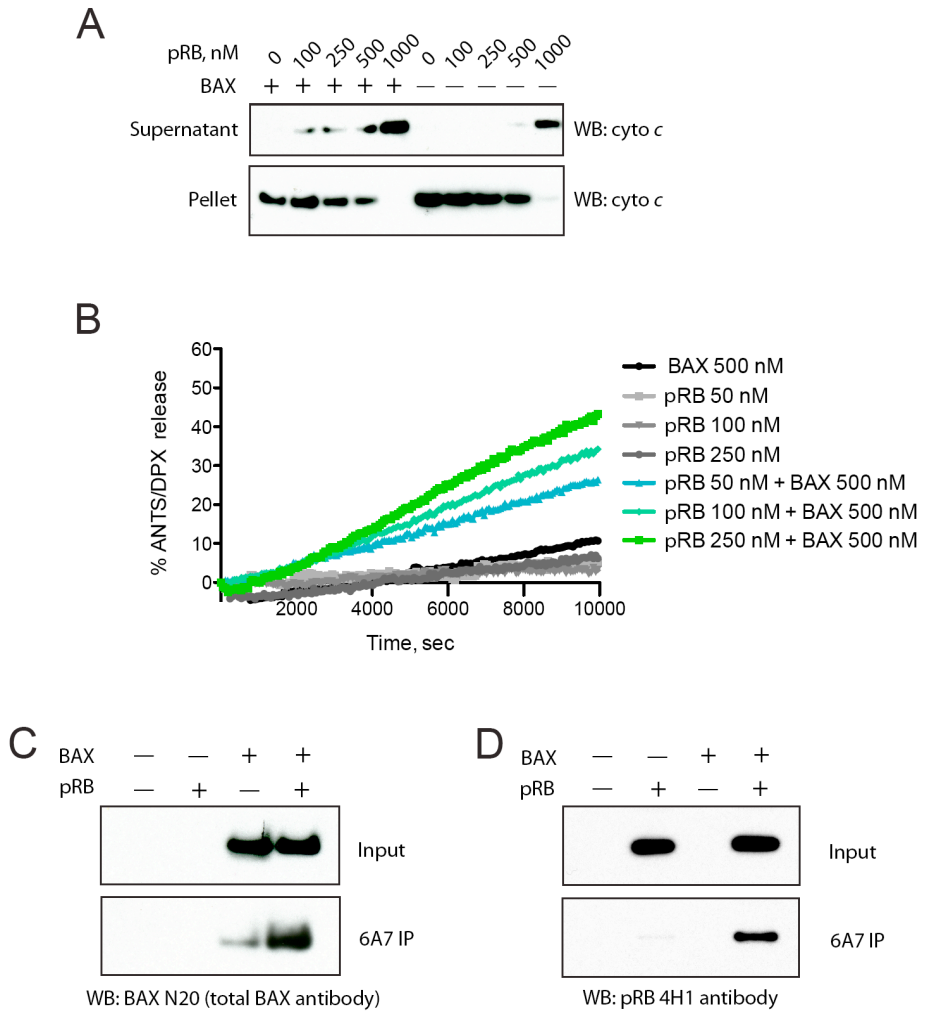

Figure 5.3. pRB induces mitochondrial and liposomal permeabilization by directly activating BAX.

(*A*) *Bax*$^{-/-}$*Bak*$^{-/-}$ mouse liver mitochondria were isolated, and supplemented with the indicated amounts of recombinant BAX and recombinant human pRB. Cytochrome *c* release was assessed after incubation and centrifugation by western blotting of the pellet and supernatant fractions. pRB dose-dependently promoted BAX-mediated cytochrome *c* release from mitochondria (*B*) ANTS/DPX-loaded liposomes were incubated with the indicated concentrations of recombinant pRB in the presence or absence of recombinant BAX. pRB yielded dose-dependent BAX-mediated liposomal permeabilization. (*C*) *In vitro* BAX activation as monitored by 6A7 epitope

Figure 5.3 (Continued).

exposure of activated BAX. Immunoprecipitations were performed by using the 6A7 conformation-specific BAX antibody. (*D*) pRB was co-precipitated with activated BAX as assessed by the 6A7 immunoprecipitation assay. (*A-D*) Data are representative of at least three independent experiments.

I then tested pRB-induced BAX activation in a liposomal context that lacks potentially confounding mitochondrial factors. I generated ANTS (fluorescent dye)/DPX (quencher)-loaded liposomes and monitored their permeabilization fluorometrically. Consistent with the cytochrome *c* release experiments, pRB induced BAX-dependent pore formation and release of the fluorescent dye (Figure 5.3, *B*). Neither BAX nor pRB alone at concentrations up to 250 nM were capable of permeabilizing the liposomes.

Upon activation, BAX undergoes a conformational change, which allows the use of a conformation-specific antibody (6A7) to immunoprecipitate activated BAX. I performed an *in vitro* binding experiment in which pRB was incubated with recominbant BAX protein, and BAX activation was monitored by 6A7 immunoprecipitation followed by western blot analysis (Figure 5.3, *C*). These results clearly demonstrated that pRB promoted BAX activation and its associated conformational change. I also confirmed the direct interaction between pRB and BAX in the context of BAX activation. Using the same 6A7 immunoprecipitation conditions to isolate activated BAX species, I documented that pRB protein co-immunoprecipitated with recombinant BAX *in vitro* (Figure 5.3, *D*). Thus, pRB can associate with BAX and triggers its conformational activation, which leads to membrane permeabilization. These results suggest that alternate paradigms for direct BAX and BAK activation may exist, and participate in the regulation of mitochondrial apoptosis.

By appyling our interactome analyses, as described above, we aim to systematically examine the BCL-2 family interactome and how non-canonical interaction partners may contribute to regulating key signaling pathways during health and disease.

References

1. Wei, M.C. et al. Proapoptotic BAX and BAK: a requisite gateway to mitochondrial dysfunction and death. *Science* **292**, 727-30 (2001).

2. Muchmore, S.W. et al. X-ray and NMR structure of human Bcl-xL, an inhibitor of programmed cell death. *Nature* **381**, 335-41 (1996).

3. Sattler, M. et al. Structure of Bcl-xL-Bak Peptide Complex: Recognition Between Regulators of Apoptosis. *Science* **275**, 983-986 (1997).

4. Oltersdorf, T. et al. An inhibitor of Bcl-2 family proteins induces regression of solid tumours. *Nature* **435**, 677-81 (2005).

5. Park, C.M. et al. Discovery of an orally bioavailable small molecule inhibitor of prosurvival B-cell lymphoma 2 proteins. *J Med Chem* **51**, 6902-15 (2008).

6. Wilson, W.H. et al. Navitoclax, a targeted high-affinity inhibitor of BCL-2, in lymphoid malignancies: a phase 1 dose-escalation study of safety, pharmacokinetics, pharmacodynamics, and antitumour activity. *Lancet Oncol* **11**, 1149-59 (2010).

7. Ferrer, P.E., Frederick, P., Gulbis, J.M., Dewson, G. & Kluck, R.M. Translocation of a bak C-terminus mutant from cytosol to mitochondria to mediate cytochrome C release: implications for bak and bax apoptotic function. *PLoS One* **7**, e31510 (2012).

8. Gavathiotis, E., Reyna, D.E., Davis, M.L., Bird, G.H. & Walensky, L.D. BH3-triggered structural reorganization drives the activation of proapoptotic BAX. *Mol Cell* **40**, 481-92 (2010).

9. Nechushtan, A., Smith, C.L., Hsu, Y.T. & Youle, R.J. Conformation of the Bax C-terminus regulates subcellular location and cell death. *EMBO J* **18**, 2330-41 (1999).

10. Suzuki, M., Youle, R.J. & Tjandra, N. Structure of Bax: Coregulation of Dimer Formation and Intracellular Localization. *Cell* **103**, 645-654 (2000).

11. Hinds, M.G. et al. The structure of Bcl-w reveals a role for the C-terminal residues in modulating biological activity. *EMBO J* **22**, 1497-507 (2003).

12. Lovell, J.F. et al. Membrane binding by tBid initiates an ordered series of events culminating in membrane permeabilization by Bax. *Cell* **135**, 1074-84 (2008).

13. Wilson-Annan, J. et al. Proapoptotic BH3-only proteins trigger membrane integration of prosurvival Bcl-w and neutralize its activity. *J Cell Biol* **162**, 877-87 (2003).

14. Leshchiner, E.S., Braun, C.R., Bird, G.H. & Walensky, L.D. Direct activation of full-length proapoptotic BAK. *Proc Natl Acad Sci U S A* (2013).

15. Braun, C.R. et al. Photoreactive stapled BH3 peptides to dissect the BCL-2 family interactome. *Chem Biol* **17**, 1325-33 (2010).

16. Gavathiotis, E. et al. BAX activation is initiated at a novel interaction site. *Nature* **455**, 1076-81 (2008).

17. Llambi, F. et al. A unified model of mammalian BCL-2 protein family interactions at the mitochondria. *Mol Cell* **44**, 517-31 (2011).

18. Walensky, L.D. et al. A stapled BID BH3 helix directly binds and activates BAX. *Mol Cell* **24**, 199-210 (2006).

19. Kim, H. et al. Stepwise Activation of BAX and BAK by tBID, BIM, and PUMA Initiates Mitochondrial Apoptosis. *Molecular Cell* **36**, 487-499 (2009).

20. Edlich, F. et al. Bcl-x(L) retrotranslocates Bax from the mitochondria into the cytosol. *Cell* **145**, 104-16 (2011).

21. Basanez, G. et al. Bax-type apoptotic proteins porate pure lipid bilayers through a mechanism sensitive to intrinsic monolayer curvature. *J Biol Chem* **277**, 49360-5 (2002).

22. Annis, M.G. et al. Bax forms multispanning monomers that oligomerize to permeabilize membranes during apoptosis. *EMBO J* **24**, 2096-103 (2005).

23. Dewson, G. et al. To trigger apoptosis, Bak exposes its BH3 domain and homodimerizes via BH3:groove interactions. *Mol Cell* **30**, 369-80 (2008).

24. Dewson, G. et al. Bak activation for apoptosis involves oligomerization of dimers via their alpha6 helices. *Mol Cell* **36**, 696-703 (2009).

25. Dewson, G. et al. Bax dimerizes via a symmetric BH3:groove interface during apoptosis. *Cell Death Differ* (2011).

26. Czabotar, P.E. et al. Bax Crystal Structures Reveal How BH3 Domains Activate Bax and Nucleate Its Oligomerization to Induce Apoptosis. *Cell* **152**, 519-31 (2013).

27. Pang, Y.P. et al. Bak Conformational Changes Induced by Ligand Binding: Insight into BH3 Domain Binding and Bak Homo-Oligomerization. *Sci Rep* **2**, 257 (2012).

28. Terrones, O. et al. Lipidic pore formation by the concerted action of proapoptotic BAX and tBID. *J Biol Chem* **279**, 30081-91 (2004).

29. LaBelle, J.L. et al. A stapled BIM peptide overcomes apoptotic resistance in hematologic cancers. *J Clin Invest* **122**, 2018-31 (2012).

30. Walensky, L.D. et al. Activation of apoptosis in vivo by a hydrocarbon-stapled BH3 helix. *Science* **305**, 1466-70 (2004).

31. Gavathiotis, E., Reyna, D.E., Bellairs, J.A., Leshchiner, E.S. & Walensky, L.D. Direct and selective small-molecule activation of proapoptotic BAX. *Nat Chem Biol* **8**, 639-45 (2012).

32. Whelan, R.S. et al. Bax regulates primary necrosis through mitochondrial dynamics. *Proc Natl Acad Sci U S A* **109**, 6566-71 (2012).

33. Hetz, C. et al. Bax channel inhibitors prevent mitochondrion-mediated apoptosis and protect neurons in a model of global brain ischemia. *J Biol Chem* **280**, 42960-70 (2005).

34. Bombrun, A. et al. 3,6-dibromocarbazole piperazine derivatives of 2-propanol as first inhibitors of cytochrome c release via Bax channel modulation. *J Med Chem* **46**, 4365-8 (2003).

35. Ku, B. et al. An insight into the mechanistic role of Beclin 1 and its inhibition by prosurvival Bcl-2 family proteins. *Autophagy* **4**, 519-20 (2008).

36. Kamer, I. et al. Proapoptotic BID is an ATM effector in the DNA-damage response. *Cell* **122**, 593-603 (2005).

37. Zinkel, S.S. et al. A role for proapoptotic BID in the DNA-damage response. *Cell* **122**, 579-91 (2005).

38. Danial, N.N. et al. BAD and glucokinase reside in a mitochondrial complex that integrates glycolysis and apoptosis. *Nature* **424**, 952-6 (2003).

39. Danial, N.N. et al. Dual role of proapoptotic BAD in insulin secretion and beta cell survival. *Nat Med* **14**, 144-53 (2008).

40. Craxton, A., Draves, K.E. & Clark, E.A. Bim regulates BCR-induced entry of B cells into the cell cycle. *Eur J Immunol* **37**, 2715-22 (2007).

41. Roy, S.S. et al. Bad targets the permeability transition pore independent of Bax or Bak to switch between Ca2+-dependent cell survival and death. *Mol Cell* **33**, 377-88 (2009).

42. Heath-Engel, H.M., Chang, N.C. & Shore, G.C. The endoplasmic reticulum in apoptosis and autophagy: role of the BCL-2 protein family. *Oncogene* **27**, 6419-33 (2008).

43. Billen, L.P., Shamas-Din, A. & Andrews, D.W. Bid: a Bax-like BH3 protein. *Oncogene* **27 Suppl 1**, S93-104 (2008).

44. Kaufmann, T. et al. The BH3-only protein bid is dispensable for DNA damage- and replicative stress-induced apoptosis or cell-cycle arrest. *Cell* **129**, 423-33 (2007).

45. Yeretssian, G. et al. Non-apoptotic role of BID in inflammation and innate immunity. *Nature* **474**, 96-9 (2011).

46. Desagher, S. et al. Phosphorylation of bid by casein kinases I and II regulates its cleavage by caspase 8. *Mol Cell* **8**, 601-11 (2001).

47. Chipuk, J.E. et al. Direct activation of Bax by p53 mediates mitochondrial membrane permeabilization and apoptosis. *Science* **303**, 1010-4 (2004).

48. Leu, J.I., Dumont, P., Hafey, M., Murphy, M.E. & George, D.L. Mitochondrial p53 activates Bak and causes disruption of a Bak-Mcl1 complex. *Nat Cell Biol* **6**, 443-50 (2004).

49. Vousden, K.H. & Prives, C. Blinded by the Light: The Growing Complexity of p53. *Cell* **137**, 413-31 (2009).

50. Fulcher, A.J., Dias, M.M. & Jans, D.A. Binding of p110 retinoblastoma protein inhibits nuclear import of simian virus SV40 large tumor antigen. *J Biol Chem* **285**, 17744-53 (2010).

51. Jiao, W., Datta, J., Lin, H.M., Dundr, M. & Rane, S.G. Nucleocytoplasmic shuttling of the retinoblastoma tumor suppressor protein via Cdk phosphorylation-dependent nuclear export. *J Biol Chem* **281**, 38098-108 (2006).

52. Ferecatu, I. et al. Evidence for a mitochondrial localization of the retinoblastoma protein. *BMC Cell Biol* **10**, 50 (2009).